

Magical Allotropes of Carbon: Prospects and Applications

Santosh K. Tiwari, Vijay Kumar, Andrzej Huczko, R. Oraon, A. De Adhikari & G. C. Nayak

To cite this article: Santosh K. Tiwari, Vijay Kumar, Andrzej Huczko, R. Oraon, A. De Adhikari & G. C. Nayak (2016): Magical Allotropes of Carbon: Prospects and Applications, Critical Reviews in Solid State and Materials Sciences, DOI: [10.1080/10408436.2015.1127206](https://doi.org/10.1080/10408436.2015.1127206)

To link to this article: <http://dx.doi.org/10.1080/10408436.2015.1127206>

 View supplementary material 

 Published online: 09 May 2016.

 Submit your article to this journal 

 View related articles 

 View Crossmark data 
CrossMark

Full Terms & Conditions of access and use can be found at
<http://www.tandfonline.com/action/journalInformation?journalCode=bsms20>

Magical Allotropes of Carbon: Prospects and Applications

Santosh K. Tiwari^a, Vijay Kumar^b, Andrzej Huczko^c, R. Oraon^a, A. De Adhikari^a, and G. C. Nayak^a

^aDepartment of Applied Chemistry, Indian School of Mines, Dhanbad, Jharkhand, India; ^bDepartment of Physics, University of Free State, Bloemfontein, South Africa; ^cLaboratory of Nanomaterials Physics and Chemistry, Department of Chemistry, Warsaw University, Warsaw, Poland

ABSTRACT

The invention of carbon and its allotropes have transformed the electronic and optoelectronic industry due to their encouraging properties in a large spectrum of applications. The interesting characteristic of carbon is its ability to form many allotropes due to its valency. In recent decades, various allotropes and forms of carbon have been invented, including fullerenes, carbon nanotubes (CNTs), and graphene (GR). Since the inception of nanotechnology, carbon allotropes-based nanocomposites have become a leading sector of research and advancement due to their unique bonding properties. Fullerenes and CNTs-based polymer nanocomposites have attracted significant research interest due to their vast applications in every sphere of science and technology. Current research impetus reveals that carbon and its allotropes have revolutionized the industry and academia due to their fascinated properties. Recent advances in various aspects of graphene, CNTs, graphene nanoribbons, fullerenes, carbon encapsulates, and their nanocomposites with polymeric materials and their different applications are reported in this review article. Also, current status and future prospects of graphene-based polymer nanocomposites are presented in common along with proper citations extracted from the scientific literature. Moreover, this article is a unique collection of vital information about GR, CNTs, fullerenes, and graphene-based polymer nanocomposites in a single platform.

KEYWORDS

Carbon allotropes; graphene; carbon nanotube; fullerene and polymer nanocomposites

Table of Contents

1. Introduction	2
2. Fullerenes	3
2.1. Discovery and properties	3
2.2. Structure and symmetry.....	4
2.3. Pyramidalization in fullerene	5
2.4. Aromaticity and electronegativity of fullerene C ₆₀	6
2.5. Higher fullerenes.....	6
3. Carbon nanotubes.....	7
3.1. Discovery	7
3.2. Structure and symmetry.....	8
3.3. Unique properties of CNTs	10
3.4. Synthesis and growth of CNTs	10
3.4.1. Grow-in-place of CNTs	11
3.4.2. Grow-then-place of CNTs.....	11
3.4.3. Arc-discharge.....	12
3.4.4. Laser ablation.....	12
3.4.5. Chemical vapor deposition (CVD)	14
3.5. Some potential applications of CNTs.....	15
3.5.1. Sensors and nanoprobes	16
3.5.2. Transistors.....	17

3.5.3. Field-emitting devices	17
3.5.4. Supercapacitors	18
3.5.5. Lithium intercalation	19
3.5.6. Hydrogen storage.....	19
3.5.7. Energy storage	20
3.5.8. Composite material	21
4. Graphene (GR): A sensational material for materials scientist	22
4.1. Structural properties and band structure of graphene	24
4.2. Quantum hall effect in GR.....	26
4.2.1. Integer quantum hall effect in graphene	27
4.2.2. Fractional quantum hall effect in graphene.....	28
4.3. Graphene nanoribbons (GNRs)	28
4.4. Electronic properties of GR	29
4.5. Mechanical strength of GR.....	30
4.6. Optical properties of GR	30
4.7. Thermal properties of GR.....	30
4.8. Synthesis methods of GR	30
4.9. Applications of GR.....	31
4.9.1. Nanoelectronics.....	31
5. Polymer nanocomposites (PNCs)	35
5.1. Brief history of nanocomposites.....	35
5.2. Types of PNCs.....	37
5.2.1. Ceramic-matrix nanocomposites	37
5.2.2. Metal-matrix nanocomposites	37
5.2.3. Polymer-matrix nanocomposites	38
5.3. Graphene-based PNCs: Status and prospects	38
5.3.1. Methods for GR-based nanocomposites ppreparation	39
5.3.2. Some examples of recently reported GR-based PNCs.....	39
5.3.3. GR-CNTs hybrid PNCs.....	41
5.3.4. Distribution, dispersion, and interaction between GR derivatives and polymer	42
5.3.5. Other GR-based polymer composites.....	43
5.4. Applications and importance of GR-based polymer nanocomposites	44
5.5. Ceramic-GR nanocomposites	46
5.6. Biological applications of GR and GR-based nanocomposite	46
5.7. In field of sustainable energy	46
6. Conclusions and future prospects	48
Acknowledgments	49
Funding.....	49
References.....	49

1. Introduction

Nobel Laureate Dr. Richard Smalley stated that the discovery of carbon atom has revolutionized the science and technology to a great extent and now it is reality that carbon has the potential of making a chemically stable, two-dimensional, one-atom-thick membranes in three-dimensional world.^{1–3} It is believed that the discovery of carbon-related materials and their development will be crucial for the future of chemistry and technology.³ The existing works of literature reflected that carbon is the most studied element of the nano era.^{3–5} The fate of nanotechnology and nanoscience is also connected to

the diamond age owing to the broad utility of carbon as an essential element for all fabricated components.^{5,6} For the last few decades, different allotropes of carbon have been explored and used for many applications.

The 2010 Nobel Prize was awarded jointly to Andre Geim and Konstantin Novoselov (University of Manchester, UK) for their outstanding discovery regarding the two-dimensional material graphene.³ GR is resembled atomic scale hexagonal pattern that is tightly packed in a regular way. The bond length of the C-C bond in GR is around 0.142 nm. GR is the fundamental structural unit of various carbon allotropes (the physical arrangement of atoms)

covering carbon nanotubes, graphite, and fullerenes.^{3–8} It is now treated as the most striking material of the universe.³

Carbon nanotubes (CNTs) are also designated as buckytubes and refer to a cylindrical molecular form of graphene with numerous exceptional and unique features.^{4,7,8} CNTs are probably valuable in an extensive range of applications including nanoelectronics, materials applications, optics, and so on.^{4,7} CNTs show remarkable tensile strength, better electrical properties, and efficient thermal conductivity.^{7,8} They can be classified into two forms single-walled nanotubes (SWCNTs) and multi-walled nanotubes (MWCNTs). Most of the SWNTs are close to one nm in diameter, with a tube length that can vary up to millions of times longer.^{7,8} However, different suppliers give as-synthesized arc discharge SWNTs. If two or more GR sheets are rolled up suitably, then they form MWCNTs.^{7,8} The interlayer distance in MWCNTs is defined as the distance between GR layers in graphite, i.e., approximately 330 pm. Fullerenes are the allotrope of carbon distinct from both graphite and diamond, football shaped single layer of graphene (with 12 pentagons).¹ Fullerenes are mostly spherical, cylindrical or ellipsoid in shapes consisting of many carbon atoms.^{1,2,5} The name “fullerenes” came into existence after the developmental author, Richard Buckminster Fuller, for their similarity to the geodesic dome.^{1,2} The spherical fullerene consists sixty carbon atoms and is termed as buckminsterfullerene (C_{60}).^{1,2} It also looks similar to a soccer ball and is often regarded to a “Buckyballs.” Cylindrical fullerenes are acknowledged as “buckytubes” or usually “nanotubes. They have tremendous potential to be employed in superconductors, catalysts, drug delivery devices, scanning tunneling microscope tips, or even as a nano ball-bearing lubricant.^{4,5,9} Graphene nanoribbons (GNRs) are a structurally deformed graphene and initially its existence was doubtful but at present is a reality.¹⁰ Graphene has brought the interest of both academia and industry due to its astounding properties.^{1,2} Besides, the numerous applications of GR, functions of graphene and its derivatives as nano filler have matured a most striking field of modern research for materials and polymer chemists.^{11–15} And it has been experimentally proved that graphene-based polymer nanocomposites possess tunable properties and easy accessibility.^{16,17}

So far, many excellent review articles have been published on CNTs, GR, fullerenes, and graphene-based polymer nanocomposites individually which reflects the high interest in academic and industrial research in these materials.^{4,5,9,18,19} This review article covers broad information related to GR, CNTs, GNRs, fullerenes, and polymer nanocomposite in a single platform. Although, various authors published a few review articles which summarize fundamental information of fullerene, CNTs, and GR.^{20–24} An attempt has been made to crush out the juice of excellent scientific literature of the subject matter. Additionally, the

recent applications of GR, CNTs, and graphene-based PNCs in the many disciplines such as in large-scale assembly and field effect devices, transparent electrodes, sensors, photo detectors, energy storage devices, solar cells, and PNCs have been reviewed in detail.

In this article, we give a detailed discussion of the progresses made in the carbon-based materials such as graphene, GNRs, CNTs, fullerenes, and graphene-based polymer nanocomposite (PNCs). We also summarized some of the properties of these materials that have particular relevance in the performance of these materials in the various areas of science and technology. The purpose of the introductory section is to provide enough information to understand the origin of carbon materials-based research and how these magical materials utilized for various technological applications. **Section 2** describes the discovery and properties of fullerene. The goal of this section is not to cover all the existing literature, but rather to present some of the most relevant achievements and a brief information in this direction. In **Section 3**, we include the discovery, structure, synthesis, properties, and some potential applications of CNTs. **Section 4** includes the invention of graphene and its properties and applications. In **Section 5**, polymer nanocomposites (PNCs) based on different carbon nanomaterials are discussed. Finally, we end the article with conclusion and prospects for future development of carbon and its allotropes based materials. With this, we hope that the reader will get updated information on the carbon-based materials that have arrived for plenty of applications and also new insights on this topic.

2. Fullerenes

2.1. Discovery and properties

Graphite and diamond are the most common allotropes of carbon and the third magical allotrope of carbon atom was discovered by Kroto et al. of UK in 1985 as C_{60} and later on was named Buckminsterfullerene or simply fullerene.^{1,2,4} First of all, Kroto studied some organic molecule in space by a telescope with exactly 60 carbon atoms found near various red giant stars. For this, Kroto collaborated with Smalley and Curl to recreate conditions in the lab and form C_{60} molecules by laser vaporization of graphite.^{1,2,4,9} After the laser vaporization experiment they analyzed that C_{60} molecules were made of pentagonal and hexagonal rings that are similar in structure to graphite.^{1,2} Thus, fullerenes can be made by vaporizing carbon/graphite within a gas medium. The schematic drawing of the supersonic laser-vaporization nozzle used in the discovery of fullerenes is shown in **Figure 1**.¹

Thus, fullerene may be defined as a molecule entirely made of carbon in the form of a hollow sphere, ellipsoid,

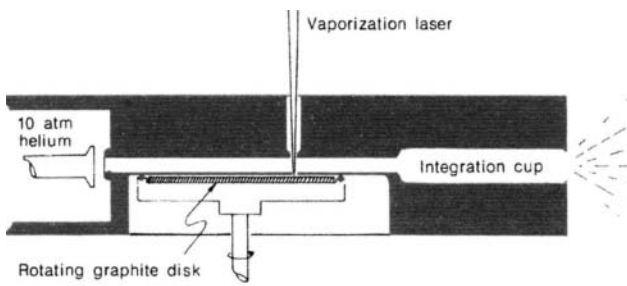


Figure 1. Schematic diagram of apparatus used to generate and analyze carbon-cluster and in the discovery of fullerenes. (© American Physical Society. Reproduced with permission from R. E. Smalley.¹ Permission to reuse must be obtained from the rightsholder.)

and various other configurations. The spherical fullerenes are commonly called Buckyballs, because of their shape resemble with the balls used in footballs. The mass spectrum of C₆₀ first gives milestone experimental evidence to Kroto et al. for the existence of C₆₀, C₇₀ clusters shown in the Figure 2. It was landmark experiment because Kroto et al.^{1,2} has taken some the mass spectrum of laser-sublimated graphite, and they interestingly noticed that a peak at 720 always appeared in the mass spectra. Since the atomic mass of carbon atom is 12, then the peak at 720 must relate to a type holding 60 carbon atoms ($720/12 = 60$), i.e., C₆₀ molecule. Sometimes the peak was very sharp, at other times it was relatively small but still there, as displayed in Figure. 2.

Later, tiny amounts of the fullerenes, in the form of C₆₀, C₇₀, C₇₆, C₈₂, and C₈₄ also have been discovered in soot and some of them were synthesized by electricity flows in the environment.^{25,26,9} In 1992, some fullerenes and their derivatives were detected in a species of minerals identified as Shungites in Karelia, Russia.²⁵ According

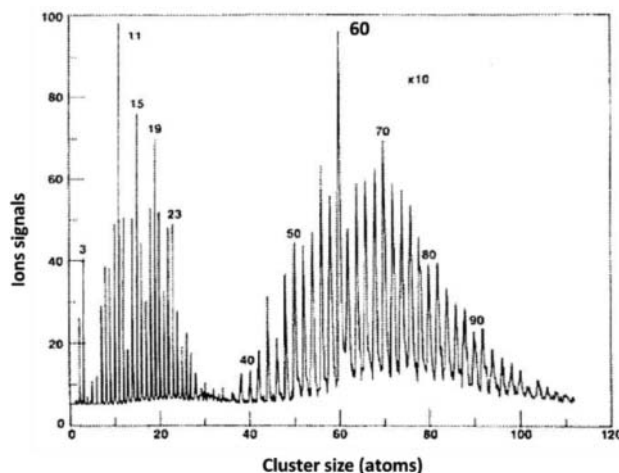


Figure 2. Mass spectrum and the preponderance of C₆₀. (© American Physical Society. Reproduced with permission from R. E. Smalley.¹ Permission to reuse must be obtained from the rightsholder.)

to NASA in 2010 some fullerene were exposed in a cloud of cosmic dust resembling a distant star of 6,500 light years away and it is suspected that fullerenes exist in the space since the primeval time in the dark holes of our galaxies.^{27,28} Finally, existence the fullerenes in Space was unambiguously confirmed a couple of years ago by Canadian scientists.²⁸ Molecular structure and SEM image of fullerene C₆₀ are shown in Figure 3.

2.2. Structure and symmetry

The fullerenes are closed-caged, symmetrical molecules and exhibits 5-fold symmetry that closely resembles the head of the numerous biological organisms for instance bacteriophage, as shown in Figure 4.

All fullerenes so far discovered have an even number of carbon atoms without any exceptions and ordered in a convex-shaped cage structure.^{30,31} The fullerene C₆₀ and C₇₀ has well-defined spheroid geodesic geometry with an approximate diameter of 0.7 nm. It consists of 12 pentagons and 20 hexagons rings (Figure 5). Fullerene C₆₀ has 60 vertices covered by a single carbon atom each in trimmed icosahedral geometry.^{30–32} The Buckyballs (C₆₀) obey Euler's Theorem, which defines that each closed-caged geometry can be built up of a vast number of hexagons but must hold exactly 12 pentagons in order to implement suitable curvature essential to lock the cage.³⁰ Thus, mathematically according to the Euler's theorem, the smallest fullerene that can exist is C₂₀.^{30–32} Although C₂₀ is probably possible, it is highly unstable because two pentagons do not go well together structurally and because of a lot of strain.^{30–33} Almost all fullerenes and derivative obeys the pentagonal rule (pentagons not existing well in pairs are known as the Isolated Pentagon Rule). Thus, the smallest fullerene that obeys Isolated Pentagon rule exactly is C₆₀. Therefore, the fullerenes with less than 60 carbon atoms are quite a few and very unstable.^{30,31} The C₇₀ is the next well-known fullerene that resembles a rugby ball-shaped molecule and detected in the soot.³¹ The pentagonal and hexagonal rings were clearly shown in the C₆₀ in Figure 5. The carbon atoms in the buckminsterfullerene molecule are covalently linked to three others by sharing three of its four outer electrons thus it seems that it involves conventional sp² hybridization.^{33,34} However, physical measurement can't be explained on the basis of standard sp² hybridization.^{33–35} For example, two types of exceptional bonds present in the C₆₀ molecule.³² First, the shorter bonds that are not pure C=C bonds but just have a double bond character than the longer ones. Second, the longer bonds that are not purely single bonds but they just have a single bond character than the shorter ones. In other words, we can say that in benzene (hexagonal ring) C=C bond length is

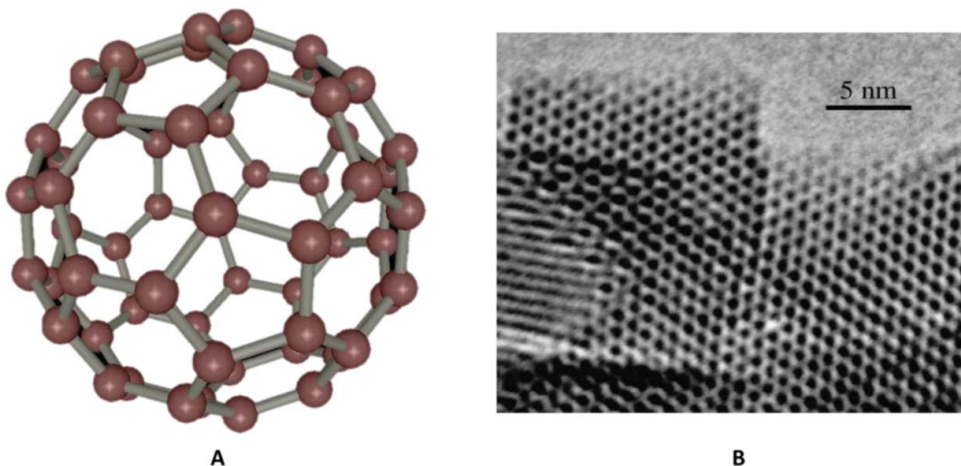


Figure 3. (A) Molecular structure of fullerene (C_{60}) designed by using Niniti software and (B) HRTEM image of pure C_{60} . (© Elsevier. Reproduced with permission from A. Goel et al.²⁹ Permission to reuse must be obtained from the rightholder.)

1.39 Å and in pentagonal rings having double bonds is 1.337 Å but the case of fullerene is different.^{32–34}

2.3. Pyramidalization in fullerene

Since this molecule is spherical the carbon atoms are very much pyramidalized (i.e., distortion of the molecular geometry towards a tetrahedral geometry); this pyramidalization is responsible for unique chemical reactivity of fullerene in contrast to the standard alkenes.³⁴ The process of pyramidalization in fullerene molecules is schematically shown, as in Figure 6, with simple mathematical description using pyramidalization angle (θ_p):^{34,35}

$$\theta_p = (\theta_{\sigma x} - 90)$$

This pyramidalization in the fullerene molecule creates an additional strain, and it has been experimentally

observed that strain energy constitutes about 80% of its heat of formation.²⁴ Theoretical data indicates that in a fullerene molecule the orbital rehybridization process is involved which is also ultimately due to the pyramidalization, thus fullerene (C_{60}) contains two types of hybridized carbon atoms, as shown in Figure 7.^{32–34} Therefore, it is clear that conversion of sp^2 hybridization to sp ^{2,27} involves a gain of p-orbital character this phenomenon in C_{60} result in a measurable deviation from ideal trigonal planarity.^{31–33} The double bonds in fullerene are not altogether the equal; it is mainly because of two types of rings present in the C_{60} molecules. The p lobes spread extra on the exterior than they do into the interior of the sphere, and this is one of the reasons that fullerene is electronegative.^{31,34,35} The other reason is that the empty low-lying π^* orbitals also have a high s orbital character.^{31,33,34} The x-ray diffraction bond length of fullerene is 1.355 Å for the hexagonal rings bond and 1.467 Å for

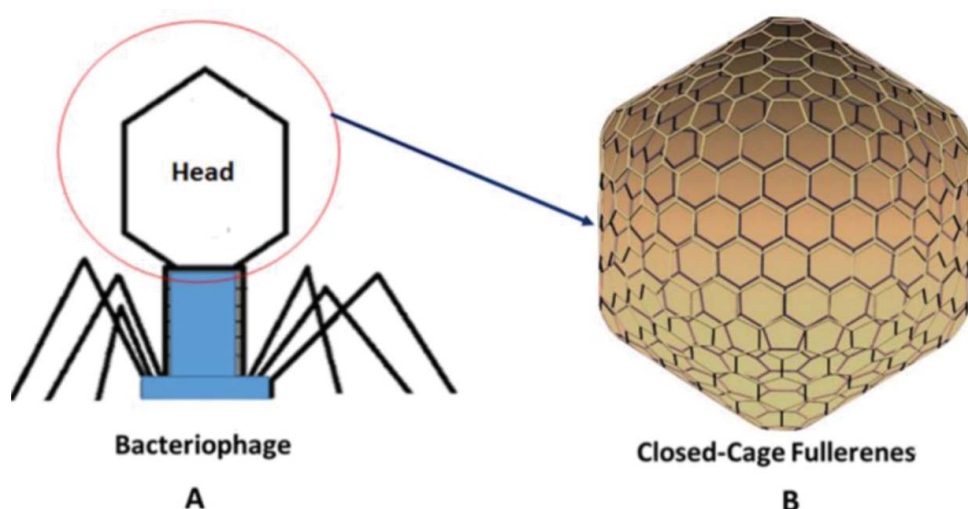


Figure 4. Similarity in symmetry of bacteriophage (A) and higher fullerene molecule (B).

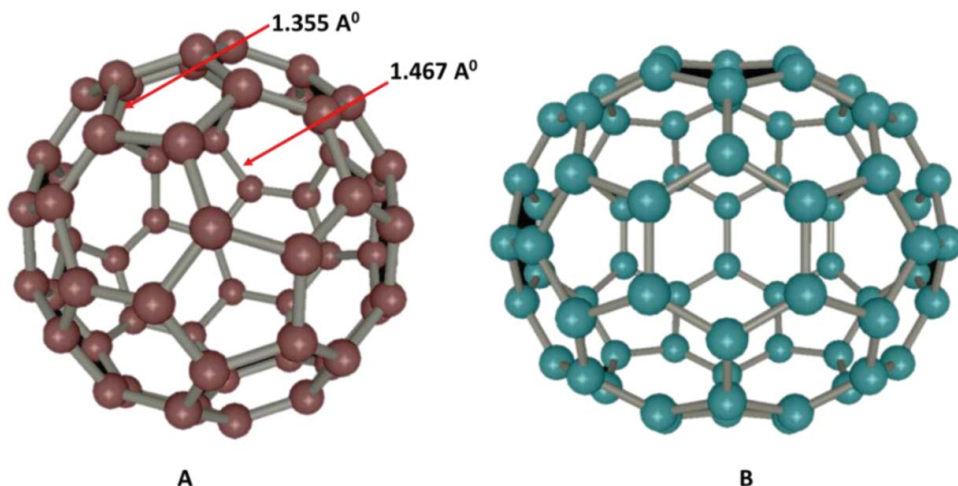


Figure 5. (A) C_{60} showing different bond lengths in the molecule and the colored area in (B) indicate five hexagons rings additionally to the C_{60} molecule (molecular structure of fullerenes designed by using Niniithi software).

the pentagonal rings.^{33,34} Thus, in the hexagonal rings double bond character is more than in pentagonal double bonds of fullerene C_{60} . This fullerene has 60π electrons, but a closed shell configuration requires 72 electrons, and this is one of the reasons why fullerene has a high affinity for nucleophiles.³⁷

2.4. Aromaticity and electronegativity of fullerene C_{60}

The Hückel's theory [$4(N + 2)\pi$] is one of the best method for the determination of substantiate aromaticity and orbital symmetry arguments in the molecule, but it is insignificant to fullerene and derivatives for aromaticity determination.^{31,38,39} For such a molecular system another rule commonly called "fullerene rule" is used which is very similar to Hückel's rule. This rule assumes that D_{nh} symmetry molecules have a strong diamagnetic ring current and zero or very small paramagnetic current.^{39,40} When

these concepts applied on the Buckminsterfullerene C_{60} , then both diamagnetic and paramagnetic effects direct a slight modification in the chemical shift displaying no considerable aromatic contribution. In other words, we can say that fullerene is neither aromatic nor antiaromatic.^{38–40} However, many fullerene ions show aromaticity when charge is located on the suitable orbital of fullerene systems.^{31,38–40} In other parts of the fullerene, the rule depends on the availability of the electrons in the valence shell.^{38–40} These π electrons can be expressed by the wave functions in which the electron gas has different angular quantum values ($l = 0, 1, 2, 3, 4, 5 \dots$). The $l = 0$ shell is similar to the s atomic orbital in its structure.^{31,38–39} The main contrast between this electron is that the center of the $l = 0$ shell should be approaching zero density of particles. This method can be also applied to the other shells with their analog atomic orbital. It is notable that there is still no any universal rule for determination of aromaticity in almost all fullerene systems, mainly due to complicated structure and exceptional bonding that is a matter of profound attention.^{37–39}

2.5. Higher fullerenes

Higher fullerenes molecules contain more than 70 carbon atoms.^{40,41} They are represented by a cage-like fused ring that is made up of pentagonal and hexagonal rings with a carbon atom situated at each polygon. Most of the higher fullerene falls in the D_{nh} , D_n , D_{nd} , and C_{nv} point group categories.⁴⁰ The most common and stable higher fullerene is given in Table 1 with their point groups that play an imperative role in the study of physical properties of such molecular systems.^{40,41}

In 1993, R.C. Haddon developed an easy and very efficient method that was considered a milestone step in fullerene chemistry research. In this process, carbon smoke is

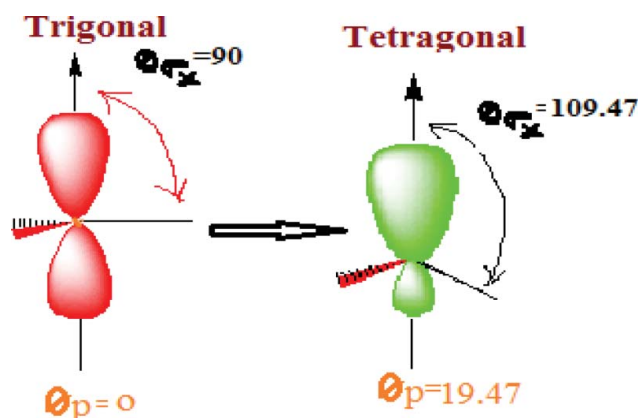


Figure 6. The Process of pyramidalization in the fullerene molecules and its effect on bond angle.

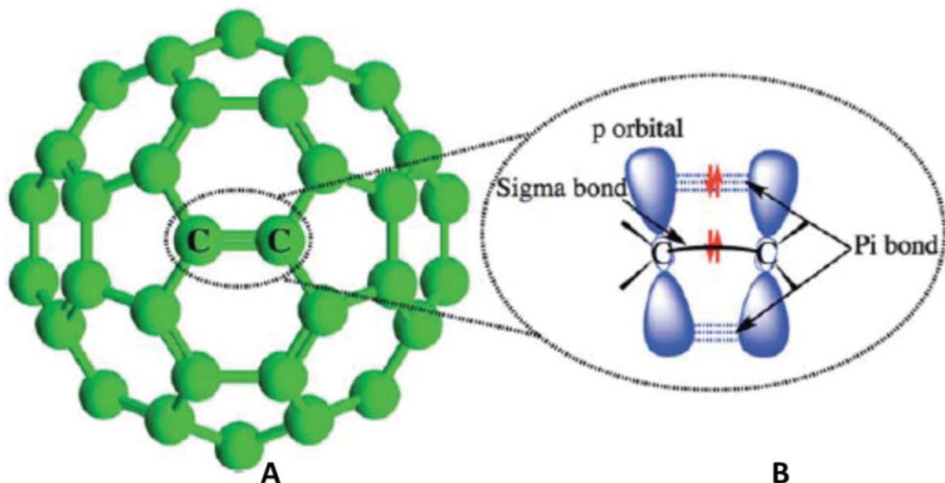


Figure 7. A typical mixing of orbitals (schematic) in the fullerene molecule (A) and orbital overlapping of fullerene (B). (© Royal Society of Chemistry. Reproduced with permission from S. Muhammad et al.³⁶ Permission to reuse must be obtained from the rightsholder.)

synthesized from two very high-purity graphite electrodes by lighting an arc discharge in a vacuum (He or N₂ gas, etc.).^{40–44} A better yield alternatively can be obtained by the laser ablation of graphite or by pyrolysis of suitable aromatic hydrocarbons.^{44,45} Excellent qualities of fullerenes like C₇₆, C₇₈, C₈₄, etc., are currently obtainable in the laboratory as well industrial scale, by dissolving soot in suitable organic solvents.^{40,41,45} In recent years, many fullerenes have been isolated and characterized, for instance C₃₉₉, C₉₆₀, C₅₄₀, etc. Different forms of C₉₆₀ obtained on the basis of DFT analysis are shown in Figure 8. These giant molecular systems have different structural orientation, calculated on the basis of DFT. However, the properties and structure of such molecular systems are still a point of profound study.^{43,44,47}

3. Carbon nanotubes

3.1. Discovery

The history of CNTs discovery is still fully understood. Therefore, it is necessary to acknowledge the efforts of a person who invented the CNTs and nowadays it is a

cause for various scientific discussions and controversy among material scientists.^{4,7–9,48} The preliminary history of nanotubes began in the 1970s.^{4,7–9,48} The synthesis of the proposed carbon filaments was made by Morino Endo, who obtained his Ph.D at the University of Orleans, France.^{47,48} The production of these carbon filaments was originally believed to be the invention of the first CNTs.⁴⁸ Nevertheless, they failed to satisfy the measurement conditions for width and thus were assumed, ultimately, barrelenes. It was considered as an important discovery in the synthesis of CNTs, but they did not receive much attention at that time.³⁸ Even the inventor did not get full credit for another 20 years.^{48,49} The remarkable discovery of the CNTs came into existence in 1991, and it was deemed as an actual invention of the nanotube. It seems that there was a competition between the Russian nano scientists and Sumio Iijima of IBM.^{49,50} The initial sight of the multi-walled CNTs was attributed to S. Iijima.^{49–50} Some researchers think that the primary invention of CNTs came into existence in the 1950s when Roger Bacon viewed the first CNT with a high-powered electron microscope.^{7,49,50} He was recognized as the premier visual response of the tubes of atoms that rolled up and were covered up with fullerene molecules by various investigators in the area. Some researchers say that his development was not considered very thoughtfully at that time as science was ignorant of how this development could influence science and technology. Therefore, it is pretty fair that it was Iijima who first witnessed the multi-walled CNTs (MWCNTs) using HRTEM (see Figure 9).^{49,52}

In 1993, Iijima and Donald Bethune conformed single-walled nanotubes (SWCNTs) and they named this new material “Buckytubes.”^{49,52} The discovery of SWCNTs encouraged the whole scientific organization

Table 1. Point group table of some higher fullerenes collected from Tohji et al.,²⁶ Choudhary,³⁰ Diederich and Whetten,⁴¹ Diederich et al.,⁴² and Reddy.⁴³

S. No.	Higher fullerenes	Point groups	Possible no. of isomers obeying isolated pentagonal rule (N _i)
1	84	D ₂ , D _{2d} , D _{6h}	24
2	82	3C ₂ , C _{2v} , 2C _{3v} , 3C _s	9
3	80	D ₂ , 2D _{3h} , 2C _{2v} , D _{5h} , D _{5d} , I _h	7
4	78	D ₃ , 2D _{3h} , 2C _{2v}	5
5	76	D ₂	1
6	74	D _{3h}	1
7	72	D _{6h}	1
8	70	D _{5h}	1
9	60	I _h	1
10	20	—	Only theoretically possible

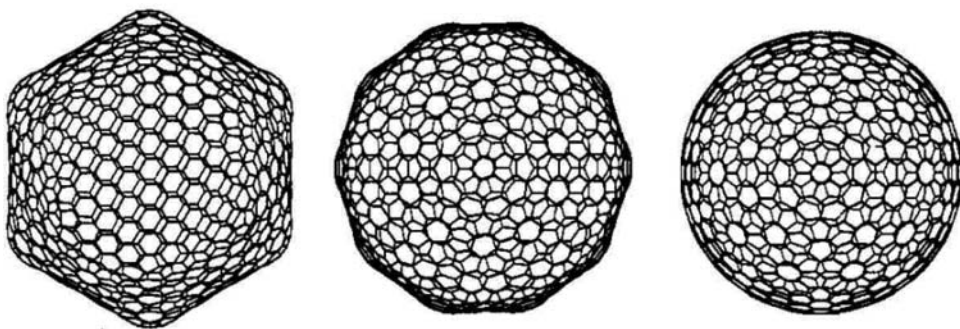


Figure 8. Different forms of C_{960} obtained on the basis of DFT analysis. (© Bakowies et al. Reproduced with permission from Bakowies et al.⁴⁷ Permission to reuse must be obtained from the rightsholder.)

to get more understanding out of not only the capability for CNTs study but also the applicability and occurrence of fullerenes. With this groundbreaking discovery, the full development of CNTs was achieved, and Iijima and Bethune were finally appreciated for their development worldwide.^{49–52}

3.2. Structure and symmetry

It is well known that graphite is planar and involves sp^2 hybridization. If a single layer of graphite is rolled up in such a way that it becomes a one-dimensional cylindrical tube then it will be single-walled carbon nanotube; on the other hand, if more than two layers of graphite are rolled up in such a way that they become a one-dimensional cylindrical tube then it will be multi-walled carbon nanotube (MWCNT).^{4,7–9} The carbon fibers that are visible one-dimensional materials are intimately linked to CNTs owing to their unique high length to diameter ratio (aspect ratio). A carbon fiber is made up of a large number of graphite planes and microscopically shows electronic properties comparable to MWCNTs.^{53,54}

Figure 10 indicates why CNTs have long been defined as rolled-up graphene sheet.^{53,54}

CNT is a tube-shaped material that is made up of carbon atoms whose diameter falls in the nanometer range.⁴⁴ The word nanometer is referred to one-billionth of a meter.^{44,50–53} The graphite layer in the form of CNTs looks similar to a rolled-up-chicken wire with a regular array in the form of hexagonal geometry in which carbon molecules present at the top of the hexagons. CNTs exist in the variety of structures that differed in terms of their thickness, type of helicity, and number of layers.^{44,52–55} Even though they are produced originally from the same graphite sheet their electrical properties vary due to the variation in their shapes and, as a result, they act as metals or semiconductors.^{50,52–55} The diameter of CNTs ranging from <1 nm up to 70 nm, whereas their lengths are in order of several microns.^{44,52–55} The recent progress in this direction produced CNTs of quite longer length. Thus, it is possible to say that CNTs are unique nanostructures that can be deemed a prototype one-dimensional quantum wire conceptually.⁵⁶ The basic architecture of CNTs is long enough.^{44,50–53} Originally,

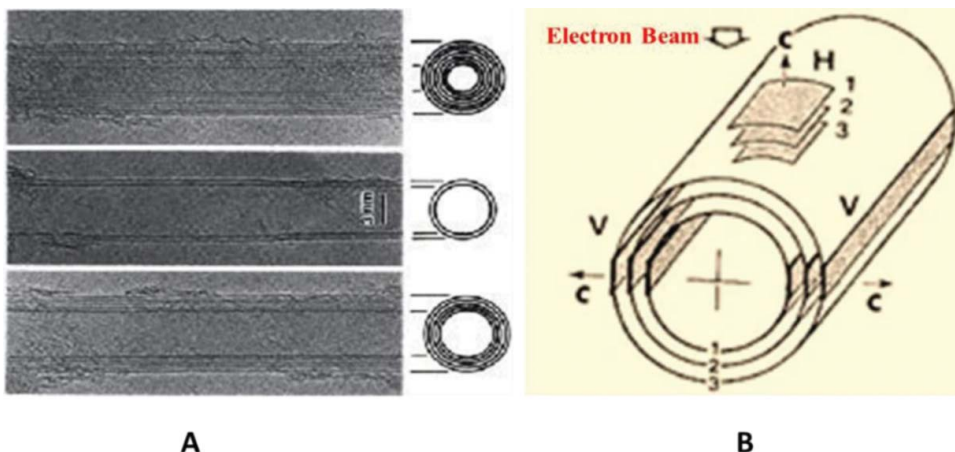


Figure 9. Observation of coaxial MWCNTs by Iijima in 1991: SEM image of microtubules of graphitic carbon (A); parallel dark lines (B) correspond to the (002) lattice images of graphite. (© Nature Publishing Group. Reproduced with permission from S. Iijima.⁵² Permission to reuse must be obtained from the rightsholder.)

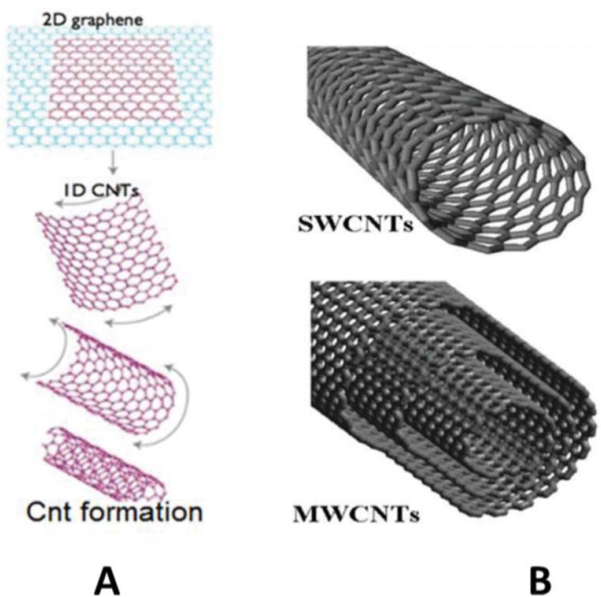


Figure 10. Formation of CNTs from single layer of graphite (A) (© Elsevier. Reproduced with permission from T. Kulia et al. Permission to reuse must be obtained from the rights holder.) and its derivatives (B) (© Royal Society of Chemistry. Reproduced with permission from J. L. Delgado et al.⁵⁴ Permission to reuse must be obtained from the rightsholder.)

CNTs got tremendous attention among the researchers due to their fascinating electronic properties.^{56,57} This interest remained as other extraordinary characteristics were also found, and the hope of possible applications was received.^{44,50–53,56,57} As mentioned previously, structure of CNTs was examined in the beginning by HRTEM (Figure 11), which reflects the evidence that the CNTs are seamless cylinders resembling the honeycomb lattice describing a single atomic layer of crystalline graphite.

Recently, Kosynkin and co-worker reported that longitudinal splitting of CNTs chemically, catalytically, and electrically may lead to the formation of unzipped thin graphene strips of various widths and

shape.⁵⁹ These unzipped CNTs are often called graphene nanoribbon (see Figure 12).⁵⁹ It is notable that opening of rolled up CNTs flimsy ribbons into the tubes in a real experiment has not been possible but according to Kit and coworker theoretically it is possible.^{50–60–62} However, Omachi and coworker reported a very good strategy for CNT growth using a carbon nanoring as a template (see Figure 12).⁶¹ It is also notable that the properties of CNTs, GR, and GNRs are entirely different which is due to different shape, size, surface area, etc.^{59–60,62}

The unique structural feature of SWCNTs/MWCNTs can be explained in the terms of its one-dimensional unit cell defined by vectors C_h and T , shown below diagrammatically in Figure 13.

The fundamental properties of CNTs mostly depend on the circumference and are expressed in terms of chiral vectors $C_h = n_{a1} + m_{a2}$ which connects two cryptographically equivalent sites on the 2D graphene sheet.^{54–60} The formation of CNTs totally depends on pairs of the integers "m" and "n" which explicitly represents the chiral vectors.^{55,58–60} The chiral angle (θ) is the angle between chiral vector C_h and zig-zag direction. On the basis of their value, three different types of CNTs can be constructed suitably by rolling up of graphene sheet into a cylinder.^{60–62} In the case of zig-zag and armchair, CNTs resemble chiral angles of $\theta = 0$ and $\theta = 30^\circ$, respectively, and chiral CNTs correspond to $0 < \theta < 30^\circ$. The complete crossing of the vector C_h with the first lattice point defines the fundamental one-dimensional translation vector T .^{60–62,63} The unit cell of the one-dimensional lattice is the rectangle which correctly represented by the vectors C_h and T , as shown in Figure 13. The container that connects the two semi-circular caps of the CNTs, which is made by overlaying the two ends of the vector C_h , whereas the

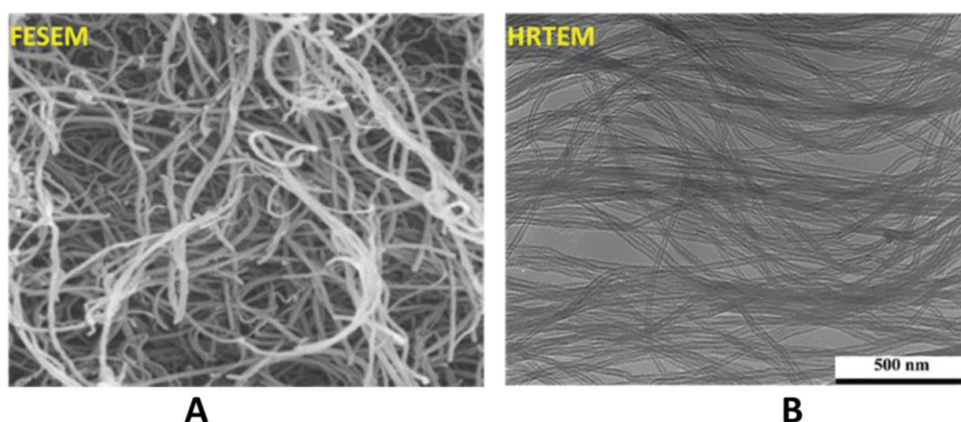


Figure 11. FESEM (A) images of MWCNTs and HRTEM (B) image showing good graphitization within the nanotubes. (© Nature Publishing Group. Reproduced with permission from M. Terrones et al.⁵⁸ Permission to reuse must be obtained from the rightsholder.)

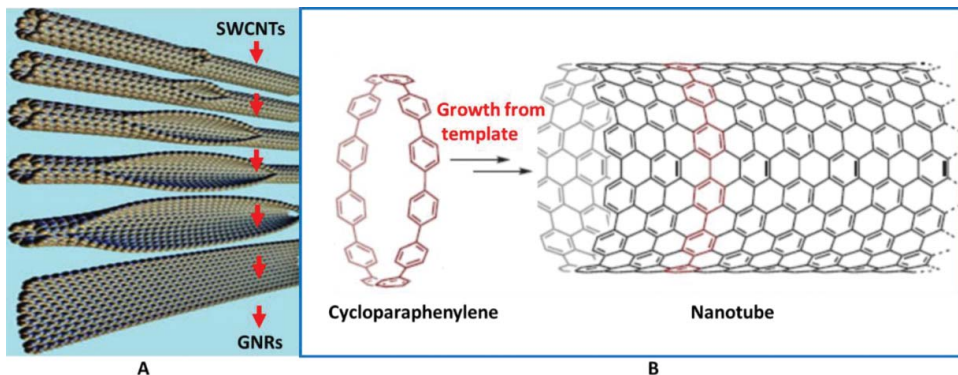


Figure 12. Formation of GNRs from SWCNTs, its different structural forms (A) (© Nature Publishing Group. Reproduced with permission from D. V. Kosynkin et al.⁵⁹ Permission to reuse must be obtained from the rightsholder.) and a strategy for CNT growth using a carbon nanoring (Cycloparaphenylenne) as a template (B) (© Nature Publishing Group. Reproduced with permission from H. Omachi et al.⁶¹ Permission to reuse must be obtained from the rightsholder.)

cylinder joint is completed along the two lines 5 and 6 in Figure 13.⁶⁴ These two lines treated as two different vectors, and both are completely perpendicular to vector C_h at each end of this vector. The simple equation given below is very informative ($C_h = n_{a_1} + m_{a_2}$) because vectors (0 n) (or 0 m) denotes zig-zag CNTs, whereas vectors (n, m) correspond to the chiral CNTs. The diameter of various CNTs can be obtained by the empirical formula given as follows:^{63,64}

$$dcnt = \frac{|Ch|}{\Pi} = \frac{\sqrt{3ac - c} \cdot \sqrt{m^2 + mn + n^2}}{\Pi},$$

where the term dr = d if (n - m) is not a manifold of

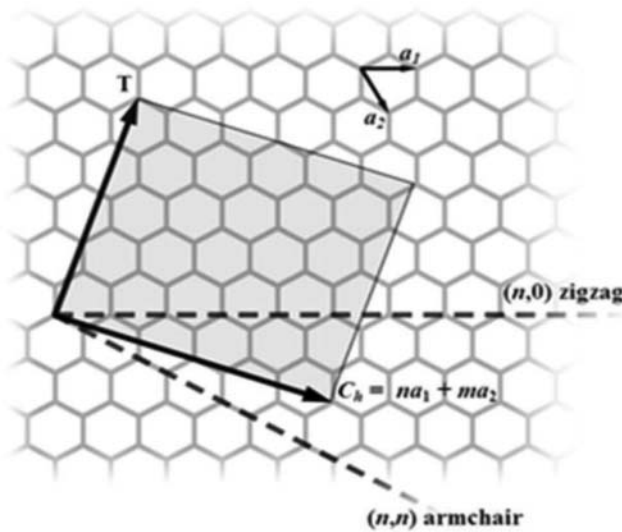


Figure 13. Schematic representation of Ch to describe how to "roll up" the graphene sheet to make a nanotube. Where T tube axis, and a_1 and a_2 are the unit vectors of 2D graphene sheet. (© Springer-Verlag. Reproduced with the permission from permission from M. S. Dresselhaus et al.⁶⁰ Permission to reuse must be obtained from the rightsholder.)

3d and dr = 3d if (n-m) is a multiple of 3d and is defined by as the greatest common divisor (GCD) of the (n m). Each hexagon of CNTs in the honeycomb lattice contains two carbon atoms.^{58–60} The unit cell region of the CNT is N times greater than that for a graphene layer, and, as a result, the unit cell area for the CNT in reciprocal space is correspondingly 1/N times smaller. The very vital information regarding SWCNTs is given below on the basis of group theory symmetry properties showing the construction of SWCNT (see Figure 14).⁶⁴

3.3. Unique properties of CNTs

CNTs are regarded as the second hardest material known in the universe after graphene. An SWCNT can hold pressure up to 24 GPa.^{60–64} It can withstand such enormous pressure without any significant defects. The thermal properties and electrical properties of CNTs are unique and brilliant, and will play a vital role in the fields of superconductivity and telecopy.^{60–65} Ballistic conduction is a property that is shown by the CNTs as they go about their thermal conduction. The important information about unique physical properties of SWCNTs and comparison with MWCNTs are given in Tables 2–5.

3.4. Synthesis and growth of CNTs

CNTs have been widely studied in the past two decades because of their amazing physical properties that can be utilized in a significant number of applications.^{7,8,50–52,60–68}

It is reported that hundreds of tons of CNTs are generated annually, and most of them are completely substrate-free CNTs.⁶⁹ The most prominent application of such CNTs is their mechanical reinforcement where the CNTs are dispersed into polymeric matrices.^{69,70} In other words, CNTs acts as nano filler and polymer as matrix.^{70,72} However, scalable CNTs production is still a

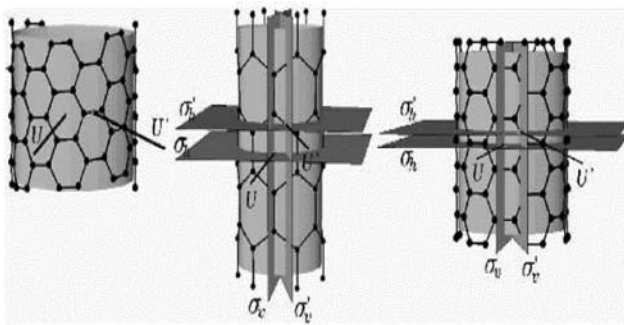


Figure 14. Carbon nano (A) tube showing mirror and glide planes and the two-fold rotational axes (U and U' axes). From the diagram, it is very clear that CNT (A) as a chiral tube and it does not have mirror symmetries. On another hand, Middle (B) tube (zig-zag) and Right (C) tube (armchair). The chiral tubes occupy the horizontal rotational axes (U and U'), the flat (σ_h) and the vertical (σ_v) mirror planes (σ_x is in the figure designated as σ_v), the glide plane σ_x' (σ_v'), and the roto-reflection plane. (© American Physical Society. Reproduced with the permission from M. Damnjanovic et al.⁵⁷ Permission to reuse must be obtained from the rightsholder.)

matter of further consideration, because of the fabrication challenges.^{70–72} This section provides a far-sighted view of various critical methods and technique that have been developed for CNTs production technologies. And we will illustrate their significant technical advantages and shortcomings. CVD is considered as the best method for the synthesis of pure CNTs, and this is why it receives particular recognition from the scientific community.⁷¹ This method allows CNTs to be developed in predefined areas, offers some degree of control of the types of CNTs produced, and may have the greatest probability to obtain commercially.^{71,72} This section is mainly based on the CNTs synthesis on the substrates, which can be assumed to be the best approach for electronic applications. In this regard, CVD is crucial for regulating the characteristics of the CNTs produced and continues the main obstacle to overcome.^{71,73} A large number of parameters affects the growth of CNTs such as substrate materials, choice of catalyst, process parameters, and source gasses.^{71–73} Keeping these specialties of CVD technique in mind we will pay descriptive attention to various aspects of CVD method for CNTs. All the prominent methods of carbon nanotube synthesis are shown in Figure 15.^{70–75} To employ carbon nanotubes on substrates for manufacturing applications, two foremost strategies have been developed: (1) grow-in-place and (2) grow-then-place. A very short comparison between both is given in the following subsections.

3.4.1. Grow-in-place of CNTs

This approach mostly consists of making the sample with a catalyst available in the neighborhoods where the CNTs will be synthesized.^{74,75} For example, a fragile catalyst film can be deposited using e-beam evaporation or

sputtering, or nanoparticles can be deposited on a substrate. The synthesis is typically conducted using thermal or assisted CVD approaches. CVD technique is one of the best method to produce CNTs with controlled shape, size and desired physical properties.⁷³ The main disadvantage of the grow-in-place approach is the chance of breaking peculiar structures during the synthesis. For example, a very high degree of distortion in the structure of carbon nanotubes has been observed which may be due to the effects of temperature.^{73,75}

3.4.2. Grow-then-place of CNTs

This technique involves the first synthesis of carbon nanotubes and then shifting them to the target system.

Table 2. Physical properties of SWCNT. (Data collected from Dreselhaus et al.,^{60,64} Saito et al.,⁵⁷ Barros et al.,⁶⁵ Zheng et al.,⁶⁶ Zhao et al.,⁶⁷ and Baughman et al.).⁶⁸

Equilibrium structure		
Average diameter of SWNTs	1.2–1.4 nm	
Distance from opposite carbon atoms	2.83 Å	
Analogous carbon atom separation	2.456 Å	
Parallel carbon bond separation	2.45 Å	
Carbon bond length	1.42 Å	
C-C tight bonding overlap energy	~ 2.5 eV	
Group symmetry	C_{SV}	
Lattice: Bundles of ropes of nanotubes	Triangular Lattice (2D)	
Lattice constant	17 Å	
Lattice parameter	Armchair	16.78 Å
	Zigzag	16.52 Å
	Chiral	16.52 Å
Density	Armchair	1.33 g/cm ³
	Zigzag	1.34 g/cm ³
	Chiral	1.40 g/cm ³
Interlayer spacing	Armchair	3.38 Å
	Zigzag	3.41 Å
	Chiral	3.39 Å
Fundamental gap	For (n, m); n-m is divisible by 3 [metallic]	0 eV
	For (n, m); n-m is not divisible by 3 [semi-conducting]	~ 0.5 eV
Fundamental electrical properties	Conductance quantization	(12.9 k) ⁻¹
	Resistivity	10 ⁻⁴ cm
	Maximum current density	10 ¹³ A/m ²
Thermal transport	Thermal conductivity	~ 2000 W/m/K
	Phonon mean free path	~ 100 nm
	Relaxation time	~ 10 ⁻¹¹ s
Elastic Behavior	Young's modulus (SWNT)	~ 1 TPa
	Young's modulus (MWNT)	1.28 TPa
	Maximum tensile strength	~ 100 GPa

Table 3. CNT sheet properties compared to copper and aluminum. (Data collected from Dresselhaus et al.,^{60,64} Saito et al.,⁵⁷ Barros et al.,⁶⁵ Zheng et al.,⁶⁶ Zhao et al.,⁶⁷ and Baughman et al.⁶⁸).

Property	CNT sheet	Copper	Aluminum
Thermal conductivity (W/m-K)	22 random/100 aligned	395	237
Coefficient of thermal expansion	2	17	23.6
DC resistivity (Ohm-cm)	2×10^{-4}	1.56×10^{-6}	2.45×10^{-6}

Laser ablation and arc discharge were historically the two primary approaches applied to manufacture substrate-free nanotubes.^{76,77} The CNTs may be afterward chosen and purified prior to applications.⁷⁶ Later on, the nanotubes transfer to the pre-selected regions of the target substrate.^{76,77} Only a few systems, such as deposition from solution using alternating electric fields, lithographic techniques, and more specifically di-electrophoresis, have shown outstanding results.^{76–78} The primary benefits of this approach comprise (1) no constraints on the process or temperature used for CNTs synthesis (2) ability to pretreat CNTs (viz. selection, purification and functionalization). The main problem of the grow-then-place method is the lack of repeatability, reproducibility, and so command to transfer the CNTs to particular regions of a target substrate, which makes it a weak competitor for the substrate-based applications.^{76–78}

3.4.3. Arc-discharge

This method is used to generate CNTs through arc vaporization of two carbon rods positioned end to end, detached by roughly 1 mm in an arena which is usually packed with inert gas (helium, argon) at a low pressure (between 50 and 700 mbar).^{79–80} Recently, it has been investigated that it is also feasible to produce CNTs with the arc method in liquid nitrogen in place of He or Ar.^{79,80} The carbon arc discharge technique was initially employed for the synthesis of C₆₀ and other fullerenes,⁸¹

however since the last decade it is treated as the easiest method to produce CNTs.⁸⁰ But in this process the product obtained as a mixture of SWCNT and MWCNT along with other components.⁸⁰ Moreover, carbon arc does not operate in a continuous mode of operation. Thus, separation of CNTs from the soot and the catalyst present in the crude product in a tedious step. In the arc discharge method, the carbon atoms are vaporized by helium plasma originated by high currents delivered over a divergent carbon anode and cathode.^{79–81} Arc-discharge has been generated in an attractive approach for fabricating both high-quality MWCNTs and SWCNTs. For the growth of SWCNTs, a metal catalyst is required in the arc discharge system.⁸² The first success in producing a scalable amount of SWCNTs by arc discharge was achieved by Bethune et al. in 1993, by using a carbon anode containing a small percentage of cobalt metal as impurity in the discharge experiment.⁸² Depending on the different experimental conditions in arc discharge method, it is feasible to selectively and precisely grow SWCNTs or MWCNTs, shown in Figure 16.^{79–82} The two separate methods of synthesis can be conducted with the same arc discharge setup.

3.4.4. Laser ablation

Arc discharge and laser ablation methods for the growth of CNTs have been actively attempted in the past decade.^{73–75} These methods comprise the com-

Table 4. Comparison of properties of SWCNT, DWCNT, and MWCNT. (Data collected from Salvetat et al.,⁵³ Dresselhaus et al.,^{60,64} Saito et al.,⁵⁷ Barros et al.,⁶⁵ Zheng et al.,⁶⁶ Zhao et al.,⁶⁷ and Baughman et al.⁶⁸).

Properties	SWCNTs	DWCNTs	MWCNTs
Surface area (m ² /g)	300–600	300–400	40–300
Geometric aspect ratio (length/diameter)	~10,000	~5,000	100~1,000
DC resistivity (Ohm-cm)	2×10^{-4}	1.56×10^{-6}	2.45×10^{-6}

Table 5. Some important theoretical and experimental data for SWCNT and MWCNT^{50–52, 60–68}.

Properties	SWNTs	MWNTs
Specific gravity	0.8 g/cm ³	1.8 g/cm ³
Elastic modulus	~1 TPa	~0.3–1 TPa
Strength	50–500 GPa	10–60 GPa
Resistivity	5–50 $\mu\Omega$ cm	5–50 $\mu\Omega$ cm
Thermal conductivity	3000 W m ⁻¹ K ⁻¹	3000 W m ⁻¹ K ⁻¹
Thermal stability	> 700°C (in air).	> 700°C (in air);
Specific Surface Area	2800°C (in vacuum) ~400–900 m ² /g	2800°C (in vacuum) ~200–400 m ² /g

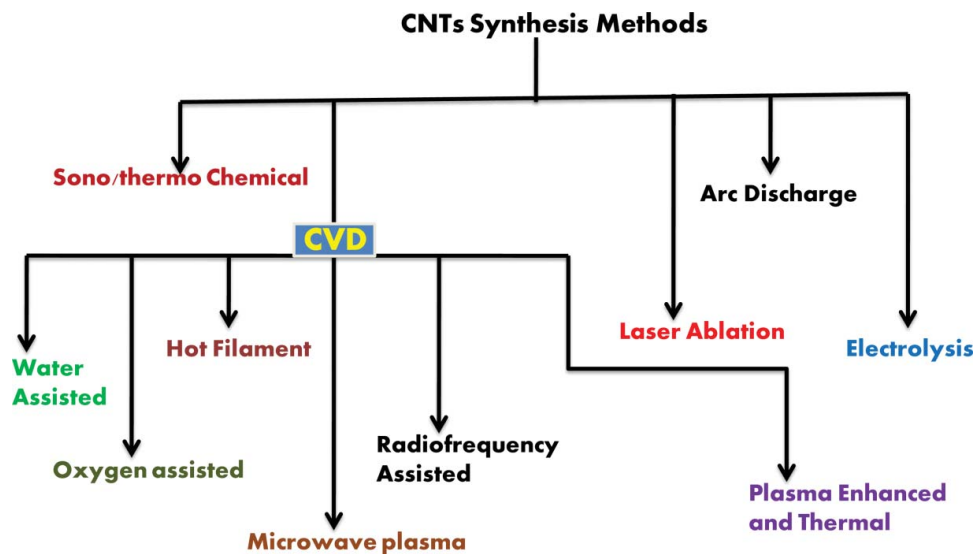


Figure 15. Different approaches of CNTs synthesis.

pression of carbon atoms produced by the departure of solid carbon sources. The temperature required in this experiment was 3000–4000°C which is quite near to the melting temperature of graphite.^{73–75,79} As mentioned previously, in 1995 American scientist Smalley, and co-workers, first precisely reported the synthesis of CNTs by lasers vaporization technology.^{1,83} The apparatus employed by Smalley's group for the synthesis of CNTs is shown in Figure 17.⁸³ In this mode, a pulsed or continuous laser is utilized to vaporize a graphite powder target in a programmable temperature oven at 1200°C.^{73,83} The fundamental

difference between continuous and pulsed laser is the pulsed laser needs a very higher light intensity (100–150 kW/cm² compared with 12 kW/cm²). The oven is filled with inert gas viz. He or Ar gas to keep the pressure at 500 Torr results in a scorching vapor plume forms then expands and cools rapidly.^{83,84} As soon as the evaporated species cool, small carbon molecules and atoms immediately compress and form bigger clusters, possibly including various kinds of CNTs and fullerenes.⁸⁵ The catalysts also start to condense, slowly at first, and then connect to carbon clusters and stop their closing into cage

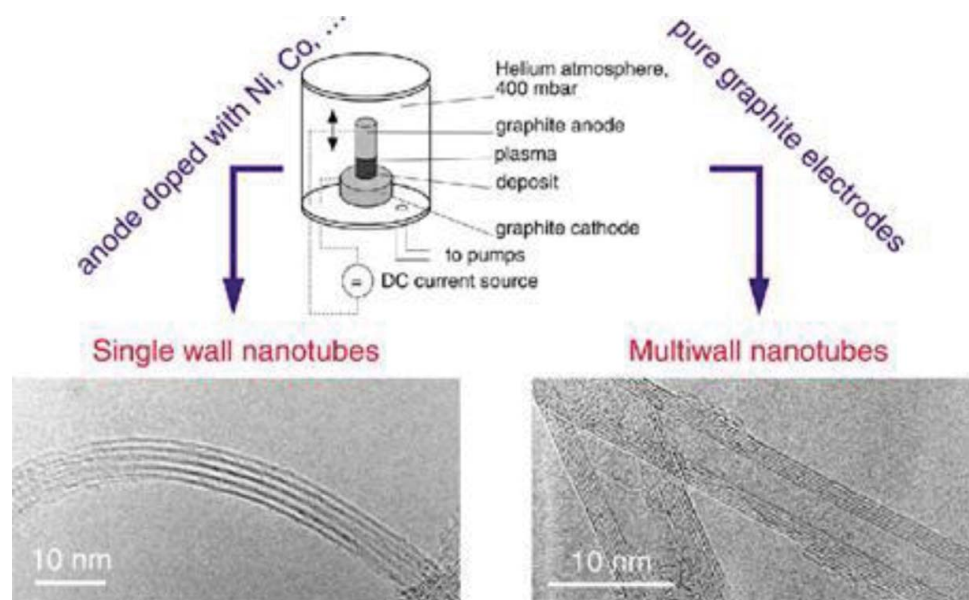


Figure 16. Schematic representation of an arc discharge apparatus, along with SEM images of the products obtained with doped and pure anodes. (© Royal Society of Chemistry. Reproduced with permission from G. D. Nessim.⁷³ Permission to reuse must be obtained from the rightsholder.)

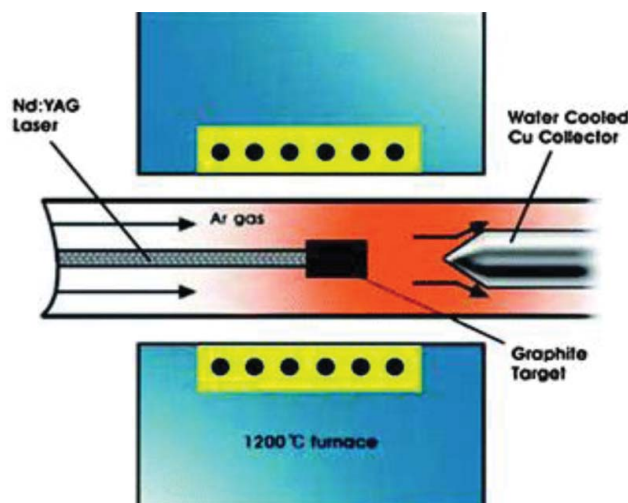


Figure 17. Apparatus used by Smalley's group for synthesis of CNTs by laser. (© Royal Society of Chemistry. Reproduced with permission from G. D. Nessim.⁷³ Permission to reuse must be obtained from the rightsholder.)

structures.^{85,86} The catalysts may point to the creation of cage structure when they bind together. The tubular molecules cultivate into SWCNTs until the catalyst elements come to be large enough or until the processes have ventilated adequately and inhibit the diffusion of carbon across the surface of the catalyst particles. During this process, the particles are coated so much with a carbon layer so that they cannot grasp more particulate matter and, as a result, the growth of nanotubes ends.^{87–89} The SWCNTs so formed are joined to each other by van der Waals force of interactions.⁸⁹

3.4.5. Chemical vapor deposition (CVD)

The CVD method enables grow-in-place synthesis of various carbon nanotubes at lower temperatures in comparison to arc discharge and laser ablation.⁷³ Hence, it is one of the best methods for CNT synthesis in the electronics and CMOS industry.^{73,91} CVD is employed in nanoelectronics fabrication, which allows growth

relatively at lower temperatures and undoubtedly provides the grow-in-place path for direct CNT growth on a substrate. Moreover, CVD can be combined as a step in chip fabrication using suitable conditions.^{90,91} Thus, it is one of the most frequently used methods to create high-purity, high-performance solid state materials.^{91,92} This method is usually employed in the semiconductor manufacturing to produce thin films.^{93,94} In typical CVD, the substrate (called as a wafer) is exposed to one or more volatile precursors, which decompose or react on the substrate surface to deliver the wanted deposit.⁹⁵ Volatile by-products are also produced during this process which can be separated by gas flow through the reaction chamber.^{96,97} Nowadays, CVD process is one the commonly used method for the synthesis of CNTs. Overall CVD process is diagrammatically shown in Figure 18.

The first catalytic vapor phase deposition of carbon was reported from 1952–1959, but it was not until 1993 that CNTs were formed by this method.^{97,98} In 2007, a material scientist at the University of Cincinnati developed a particular technique to grow aligned CNTs arrays of 18–20 mm length on a First Nano ET3000 CNT growth system.^{97–99} For this method of CNTs, the substrate is prepared with a layer of transition metal catalyst particles.^{73–75,79} The most frequently used transition metal catalysts in CVD process are Ni, Co, Fe, or utilized in an alloy form.^{97,100} The diameters and length of the CNTs that are to be grown mainly depend on the size of the transition metal catalyst particles.^{100,103,106} The size of catalyst particle can be triggered by the patterned deposition of the metal, by plasma etching of a metal layer, “hot filament,” or annealing.^{96,97} The wafer is heated up to a high temperature to at least 600–700°C.^{103,104} To start the growth of carbon nanotubes, two gases are bled into the reactor: (1) a process gas (such as NH₃, N₂, or H₂) and a (2) carbon-containing gas (such as acetylene (C₂H₂), ethylene (C₂H₄), ethanol (C₂H₅OH or other alcohols), carbon oxides or methane

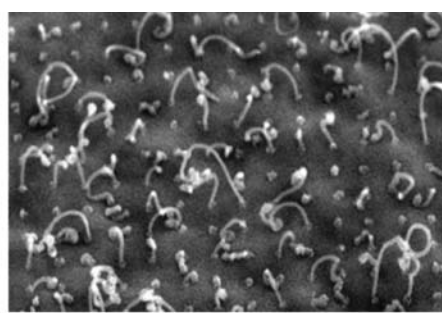
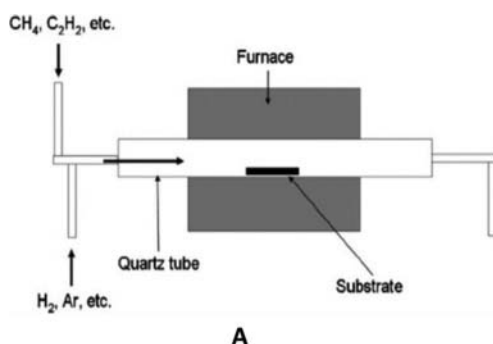


Figure 18. Schematic representation of high temperature CVD technique (A) and nonaligned growth of CNTs using CVD process (B). (© IOP Science. Reproduced with permission from A. V. Melechko et al.¹⁰¹ Permission to reuse must be obtained from the rightsholder.)

CH_4).^{73,105,106} The nanotubes develop at the sites of the transition metal catalyst, the carbon-containing gas is impoverished separate from the surface of transition metal catalyst particle, and the carbon is transferred to the boundaries of the particle, where it generates the nanotubes.^{105,106} The above mechanism is still being investigated and is also a matter of further consideration and deeper understanding.¹⁰⁶ The catalyst activity of the particles can stay at the tip of the growing CNTs during development, or rest at the carbon nanotubes base, depending on the complete or partial adhesiveness among the catalyst particle and the substrate.^{106,107} The thermal catalytic decay of hydrocarbon has become a very attractive area of research in material science and may be a ravishing route for the bulk production of CNTs and derivatives in the future. Nowadays, CVD is a most commonly used method for the industrial production of CNTs.^{73,107} For the commercial production of CNTs, transition metal catalysts used along with the some other catalyst support such as MgO or alumina, CaO , and ZrO .^{106–108} This additional catalyst support increases the surface area of catalyst resulting in higher yield of CNTs.^{106–109} The most significant drawbacks of this route is the removal of the catalyst support which requires an acid treatment for purification. Due to this, sometimes structural distortion is introduced in CNTs.^{73,105,106} However, alternatively, some excellent catalysts supports have been developed and utilized which are completely soluble in water have proven useful for nanotubes growth according to need.^{105–107} For the CNTs synthesis, the CVD approaches are mainly of three types:

1. APCVD (Atmospheric pressure chemical vapor deposition)^{110,111}
2. PECVD (Plasma enhanced chemical vapor deposition)¹¹¹
3. LPCVD (low pressure chemical vapor deposition)^{111,112}

The most prominent CVD technique is plasma-enhanced CVD. In this method, plasma is generated using very high electric field and results in the CNTs growth will follow the identical direction of the electric field.^{111,112} It is possible to synthesize vertically aligned CNTs by simply adjusting the geometrical position of the reactor.^{111,113} Among the various methods of CNTs synthesis, the CVD is one of the most promising route for industrial-scale CNTs production due to its low fabrication cost. Moreover, CVD is capable of growing CNTs directly on a desired substrate in the single step.^{111,112} In this technique, the growth sites are controllable by careful deposition of the transition metal catalysts as ‘islands.’^{104,108,113,114} In 2007, a research group from Meijo University Japan developed a very efficient CVD technique for growing

CNTs using camphor.^{114,115} In a similar fashion, Smalley and co-workers at Rice University have developed a unique approach for the synthesis of large-scale and pure amounts of particular types of CNTs.^{110,116–119} The studied methods produce long fibers from several small seeds cut from an SWCNT and, as a result, the fabricating fibers were found to be of the similar diameter as the original nanotube.¹¹⁶ Interestingly tubular-shaped nanostructure formation is favored over other forms of carbon such as graphitic sheets, open edges, and GNRs.^{117,118} The tube does not contain any dangling bonds which reflects a system with lower energy and, as a consequence, leads to the generation of a stable system. At present, the CVD route of CNT synthesis has attracted much more attention than another synthetic route due to the formation of ordered CNT structures and can be grown on a surface in a very precise way that is not achievable with other methods.¹¹⁹ The number of methods has been developed to obtain MWCNTs via CVD growth of tubes in the pores of mesoporous silica substrate.¹²⁰ Dai and coworker developed a growth approaches for ordered SWCNTs and MWCNTs by CVD on a suitably patterned wafer with the help of particular metal catalyst.^{120–122,124} They reported that MWCNTs can self-assemble into aligned structures as they grow, and the driving force for self-alignment is the week molecular interaction such as Van Der Waal forces between CNTs.^{122,123} The SEM images of regularly positioned arrays of CNTs towers grown from patterned iron squares on a mesoporous silicon substrate are shown in Figure 19. A comparative study of CVD, laser ablation and arch discharge method for CNTs synthesis is given in Table 6.

3.5. Some potential applications of CNTs

As illustrated previously, the CNTs are cylinders of one or more layers of graphene (mother of all graphitic forms) and the diameters of SWNTs and MWNTs are typically ranging from 0.8–2 nm and 5–20 nm, respectively.^{50–52,73} The diameter of MWNTs can exceed up to 100 nm.^{73,58} The CNT lengths range from less than 100 nm to several centimeters.¹²⁸ The CNTs possess many unique properties along with above physical properties. Statistical data very clearly indicates that in the year 2012–2013 commercial production of CNTs exceeded several thousand tons per year because of its extensive applications in energy storage, automotive parts, boat hulls, sporting goods, water filters, thin-film electronics, coatings, actuators, and electromagnetic shields.^{128,129} At present, CNTs are mostly utilized for the structural composite materials, flat-panel displays (FPD), gas and energy storage, antifouling paint, micro- and nanoelectronics,

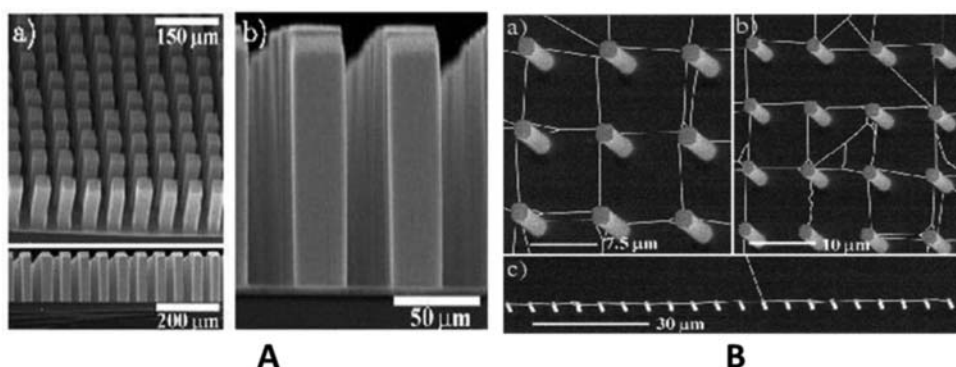


Figure 19. (A) Self-aligned MWCNTs arrays grown by CVD on a catalytically patterned mesoporous silicon substrate: (a) SEM image of tower structures consisting of aligned CNTs and (b). (© Wiley. Reproduced with permission from H. J. Dai et al.¹²⁴ Permission to reuse must be obtained from the rightsholder.) (B) SEM image of the side view of the towers and directed growth of suspended SWCNTs (a) and (b) square of CNTs and c) CNT power-line structure. (© ACS Publications. Reproduced with permission from N. Franklin et al.¹¹⁷ Permission to reuse must be obtained from the rightsholder.)

radar-absorbing coating technical textile, ultra-capacitors, atomic force microscope (AFM) tip, batteries with enhanced lifetime, biosensors, and so on. Some of them are discussed in details.^{73,117–123,128–130}

3.5.1. Sensors and nanoprobe

As we know that CNTs are mono- or diatomically thick carbon layers, and possess very high flexibility, so the nanotubes could be used in scanning probe instruments.^{126,131} Because of significant conductivity of MWNT-tips they can be employed in STM and AFM instruments as shown in Figure 20.^{132,133} The main advantages of using CNTs in the place of conventional Si or metal tips^{122,123} are the highly improved resolution in

comparison with the standard tip. Moreover, such a tip does not suffer from crashes with the surfaces because of their high elasticity.¹³³ But the main drawback with CNTs is the nanotube vibration due to the considerable length; however, this problem may be resolved in future by the controlled growth of CNTs.^{133,134}

At present, sensors continuously play a significant role in our daily life and has been a high market for generating highly sensitive, responsive, and cheaper sensors.^{133,134} Therefore, the demand for fabricating new sensing materials and technologies increase day by day.¹³⁵ CNTs have many distinct characteristics that can be employed to assemble next generation of sensors and some very high-quality CNTs based sensors have already

Table 6. A comparative study of CVD, laser ablation, and arc discharge method for CNTs synthesis.^{50–52, 73,117–123,124–127}

Method	Arc discharge method	Chemical vapor deposition	Laser ablation
Who	Ebbesen and Ajayan, Japan 1992 ¹²⁵	Endo, Shinshu University, Nagano, Japan ¹²⁶	Smalley, USA, 1995 ¹²⁷
How	Connect two graphite rods to a power supply, place them a few millimeters apart, and throw the switch. At 100 amps, carbon vaporizes and forms a hot plasma	Place substrate in oven, heat to 600°C, and slowly add a carbon-bearing gas such as methane. As gas decomposes it frees up carbon atoms, which recombine in the form of NTs	Blast graphite with intense laser pulses, use the laser pulses rather than electricity to generate carbon gas from which the NTs form, try various conditions until hit on one that produces prodigious amounts of SWNTs
Typical yield SWCNT	30–90% Short tubes with diameters of 0.6–1.4 nm	20–100% Long tubes with diameters ranging from 0.6–4 nm	Up to 70% Long bundles of tubes (5–20 microns), with individual diameter from 1–2 nm.
MWCNT	Short tubes with inner diameter of 1–3 nm and outer diameter of approximately 10 nm.	Long tubes with diameter ranging from 10–240 nm	Not very much interest in this technique, as it is too expensive, but MWCNT synthesis is possible
Pro	Can easily produce SWCNT, MWCNTs. SWNTs have few structural defects, MWCNTs without catalyst, not too expensive, open air synthesis possible	Easiest to scale up to industrial production; long length, simple process, SWNT diameter controllable, quite pure	Primarily SWCNTs, with good diameter control and few defects. The reaction product is quite pure.
Con	Tubes tend to be short with random sizes and directions, often needs a lot of purification	CNTs are usually MWCNTs and often riddled with defects	Costly technique, because it requires expensive lasers and high power requirement, but is improving

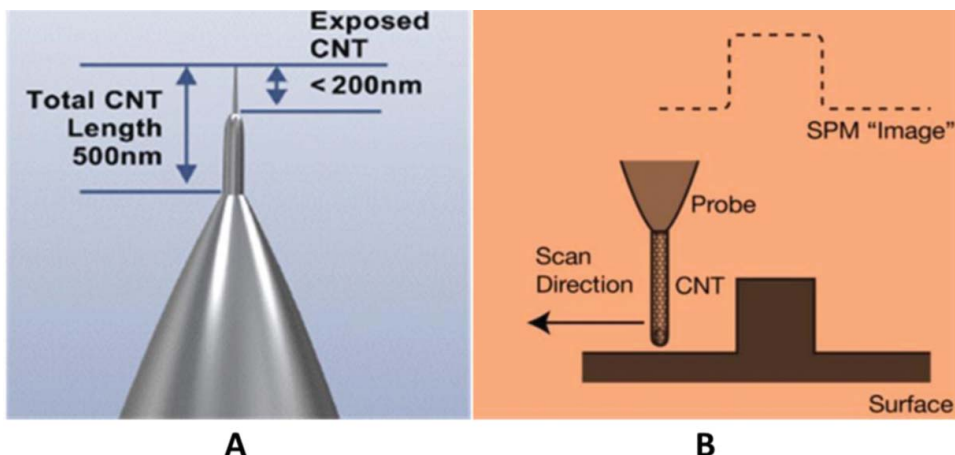


Figure 20. (A) The very high-quality CNT AFM probes for detailed imaging in metrology and materials science applications. The standard CNT probe length is 500 nm, with the exposed CNT tip <200 nm. (B) Schematic diagram for the application of CNTs in AFM instrument as sensing tip. (© Prof. P.M Ajaya Group. Reproduced with permission P. M. Ajayan et al.¹³³ Permission to reuse must be obtained from the rightsholder.)

been developed.^{135,136} Also to this it is believed that SWCNTs may be employed as electromechanical actuators, simulating the actuator mechanism present in natural muscles.¹³⁶ Similarly, SWCNTs may be used as miniaturized chemical sensors.^{136,137} A schematic diagram of SWNTs-TFT based sensor showing ultra-high response is shown in Figure 21. The reason for the ultra-high response of CNTs for sensing purposes is its unique solubilization. It is reported that CNTs can be combined via solubilization into different forms to perform electrochemical detection, and this is the reason it plays a very crucial role in sensing technologies. Solubilization process of CNT with various moieties is schematically shown in Figure 22. For more detailed about solubilization of CNT and its importance, please see the very interesting article published by Merkoçi et al.¹³⁵

3.5.2. Transistors

The field-effect transistor is an important three-terminal switching device consisting of only one semiconducting

SWNTs.^{139,140} The nanotubes can be converted from a conducting state to a non-conducting state when a voltage is applied to the gate electrode.^{139,140} A diagrammatic representation of such a transistor is displayed Figure 23. CNTs transistors can be joined and, as a result, they are working as a logical switch of the fundamental part of computers.^{138,139,142} Franklin et al. fabricated a new generation transistor consists of a 9-nm-long channel constructed of SWCNT.^{117,140–142} When a voltage is employed to the transistor's gate electrode, electric current passes from the source electrode to the drain electrode. A 3-nm-thick layer of hafnium oxide provides enough electrostatic interaction between the gate and the SWCNTs.^{142,143}

3.5.3. Field-emitting devices

It is an experimental and theoretical fact of physics that if a solid is fixed to a very high electric field, electrons close to the Fermi level can be removed from the solid by drifting through the potential surface bar.¹⁴³ This emission

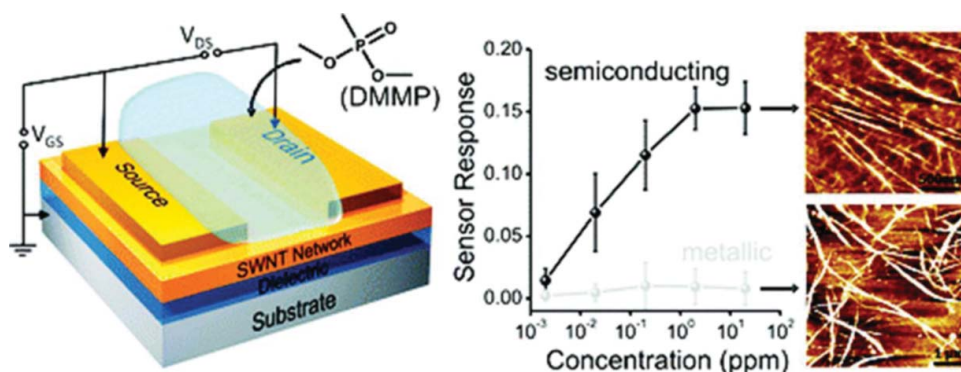


Figure 21. Schematic diagram of SWNTs-TFT based sensor showing ultrahigh response. (© ACS Publications. Reproduced with permission from M. E. Roberts et al.¹³⁶ Permission to reuse must be obtained from the rightsholder.)

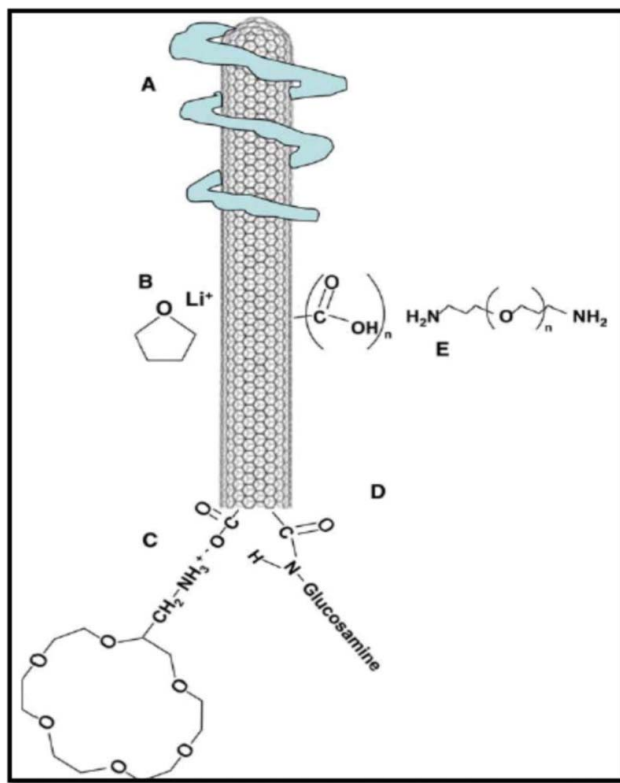


Figure 22. Diagrammatic representation of CNT solubilization alternatives: (A) supramolecular wrapping with polymer; (B) CNT-Li⁺ conducting polyelectrolyte; (C) with amino group of 2-aminoethyl-18-crown-6 ether; (D) by amide bonds with glucosamine; and (E) by diamine-terminated oligomeric poly(ethylene glycol). (© Elsevier. Reproduced with permission from A. Merkoçi et al.¹³⁵ Permission to reuse must be obtained from the rightsholder.)

current directly related to the intensity of the local electric field at the emission surface and its work function (commonly denoted by (ϕ)) which indicates the minimum energy required to remove an electron from its top-bounded state into the vacuum level.^{144,145} A very high electric field is needed to remove an electron from

the highest adjacent state to ground state.¹⁴⁵ The above-required condition is mostly fulfilled by CNTs because their sufficiently elongated shape ascertains vast field amplification.¹⁴⁵ A very low threshold emission area and a very high stability at high current density are needed for emissive materials to be utilized in technological applications.^{144,146} In addition to above characteristics a perfect emitter should also have a high surface area, a nanometer size diameter, a structural integrity, a high electrical conductivity, a small energy spread, and a very high chemical stability.¹⁴⁵ The CNTs hold all these peculiar characteristics. Owing to such unique properties, it is a superb candidate for the fabrication of next-generation field-emitting devices. The principle of field emission with CNTs is diagrammatically shown in Figure 24.

3.5.4. Supercapacitors

Supercapacitors (SCs, also known as ultracapacitors) are high-capacity electrochemical device with capacitance values much higher than other conventional capacitors and it bridge the gap between electrolytic capacitors and rechargeable batteries.^{148–150} This unique feature makes it beneficial for devices that need a small quantity of current and low voltage.^{148,189} Sometimes, supercapacitors can hold the position of a rechargeable low-voltage electrochemical battery that has a very high capacitance and is probably suitable for the various electronic devices.¹⁵⁰ They consist of two electrodes spaced by some non-conducting material that is ionically conducting in electrochemical devices. The range of SCs is inversely proportional to the separation between the charge on the electrode and the counter charge in the electrolyte.^{150,151} It means smaller the separation greater will be efficiency of the SCs.¹⁴⁹ The separation in CNTs is found to be in the nanometer range and, as a result, an enormous amount of capacitance is created from the high CNTs surface area to the electrolyte.^{149,150} A lot of charge

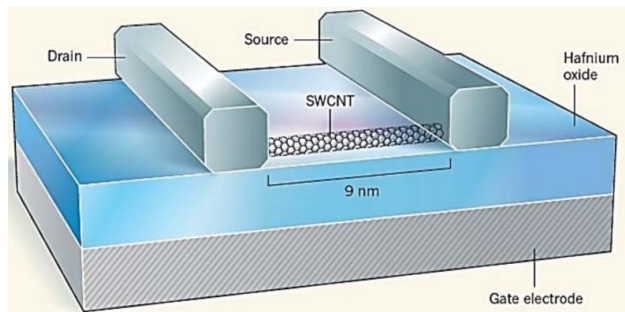


Figure 23. Schematic diagram of CNT based transistor; containing 9 nm long channel made of SWCNT 3-nm-thick layer of hafnium oxide. (© Nature Publishing Group. Reproduced with permission from F. Krepl.¹³⁸ Permission to reuse must be obtained from the rightsholder.)

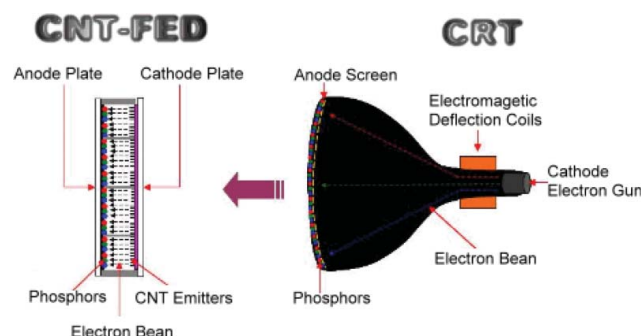


Figure 24. Principle of field emission display and application of CNTs. (© B. Thanveer. Reproduced with permission from B. Thanveer.¹⁴⁷ Permission to reuse must be obtained from the rightsholder.)

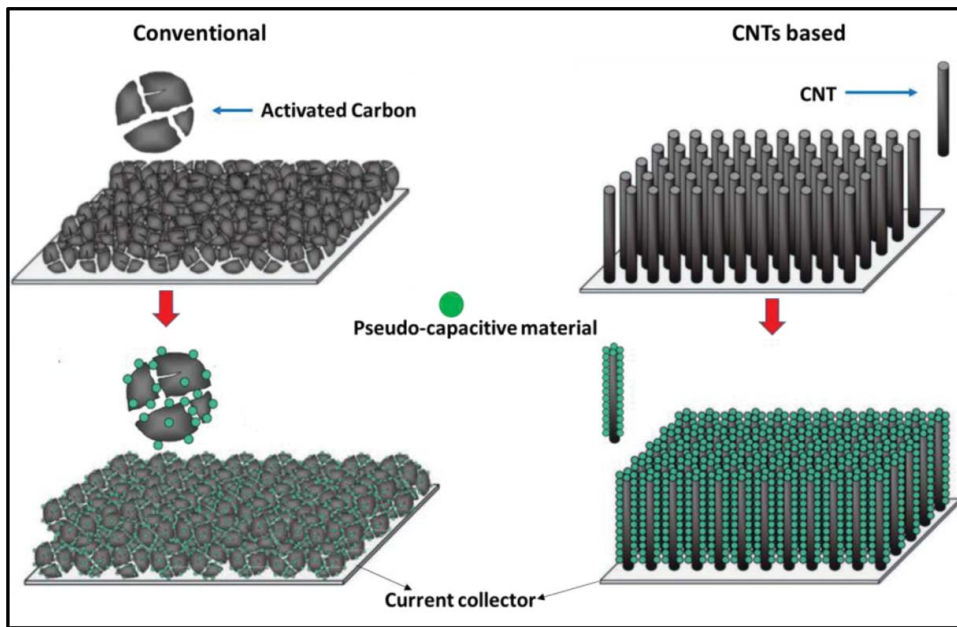


Figure 25. An ultracapacitor can store more charge than a capacitor can, because the activated carbon has a pocked interior, much like a sponge. This means that ions in the electrolyte can adhere to more surface area. With finer dimensions and more uniform distribution, CNTs enable greater energy storage in SCs than activated carbon does. (© Nature Publishing Group. Reproduced with permission from P. Simon and Y. Gogotsi.¹⁵¹ Permission to reuse must be obtained from the rightsholder.)

injection occurs only if an insignificant power is implemented.¹⁵⁰ This charge injection can be utilized for energy storage in CNT based SCs. Recently, CNT-fiber based stretchable wire-shaped SCs with very high efficiency have been elaborated, schematically shown in Figure 25. It is reported that CNT materials preserve the intrinsic features of individual SWNTs, such as large surface area, flexibility, and electrical conductivity.^{150–152} So by controlling the fabrication process, it is possible to fabricate a wide range of products such as flexible heaters, as well as SCs electrodes for compact energy-storage devices.¹⁵¹

3.5.5. Lithium intercalation

The CNTs, discovered by Iijima, are of particular concern since they initiate many ways of synergy with various molecules or atoms specifically.^{153,154} It was found that the nanotubes could offer Li intercalation between pseudo-graphitic layers or insertion of the central tube.^{153–156} The intercalation of donor or acceptor species between the carbon shells could provide direction of the electronic properties of nanotubes, and allow the transfer of atoms through redox process.¹⁵⁵ More recently, nanotubes have also been investigated for the storage of adsorbed molecules.^{156,157} The fundamental principle of rechargeable lithium ions batteries are electrochemical intercalation and de-intercalation of lithium ion in both electrodes. The perfect battery has a high-energy capability, quick charging time, and extended rotation time.¹⁵⁶ The storage space of the battery is calculated by the

lithium-ion saturation concentration of the electrode materials. For Li-ion battery, this is the largest in nanotubes if all the interstitial sites are available for Li-ion intercalation.^{155–157} SWNTs exhibited extremely reversible and invariable capabilities.¹⁵⁸ Due to the primarily perceived voltage hysteresis, however, Li-ion intercalation in nanotubes is yet inappropriate for battery utilization.¹⁵⁷ This issue can be overcome or removed by a process called “cutting” the nanotubes to a smaller parts. A schematic diagram showing the fabrication of MnO₂/CNTs electrodes for CNTs based battery is shown in Figure 26.^{157,158}

3.5.6. Hydrogen storage

Nowadays, hydrogen is treated as an alternative source of energy for the future. The principal use of hydrogen as a power source is that its combustion output is water. Also, hydrogen can be readily restored.¹⁶⁰ Hydrogen is considered as a potential agent to the challenges produced by fossil fuel insufficiency and the alarming rate of environmental inspection on prevailing energy sources such as coal, petroleum, and nuclear substances.^{160,161} First, hydrogen is a completely clean and endlessly renewable fuel because water is the only by-product and hydrogen is prepared sufficiently. Second, its gravimetric energy density is approximately three times than that of petrol, and hydrogen fuel cells are supposed to be at least twice as productive as internal combustion motors.^{160,161} So, the invention of an extremely proficient hydrogen storage system is very necessary. At present, the most

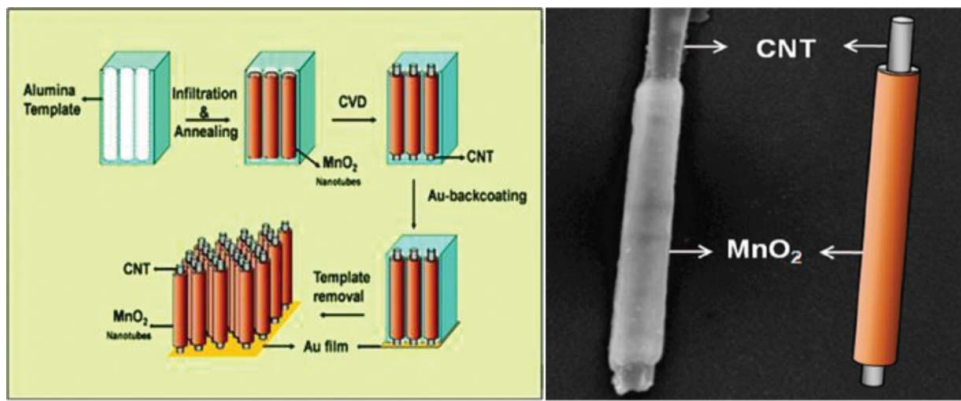


Figure 26. Schematic diagram showing the fabrication of MnO₂/CNTs electrodes for CNTs-based battery. And SEM image and a schematic representation of a single coaxial nanotube. The MnO₂ shell and carbon nanotube core are clearly seen. (© ACS Publications. Reproduced with permission from A. L. M. Reddy et al.¹⁵⁹ Permission to reuse must be obtained from the rightsholder.)

frequently used sources to collect hydrogen are a gas phase and electrochemical adsorption. The main reason for their utilization is their proper cylindrical and hollow geometry and having a diameter in the nanometer range. Thus, it is quite possible that CNTs can store liquid or gas in the internal cores by a capillary phenomenon.^{160,162,163} Therefore, CNTs can perform a very vital part in the construction of perfect hydrogen storage device.^{164–166} The general setup for hydrogen storage using SWCNTs is displayed in Figure 27.

3.5.7. Energy storage

Energy conservation is an important part of energy planning and its management. At present efficient energy storage is a common problem all over the world. So, that production of highly efficient, low cost energy storage devices is a front line research field. Especially, electrochemical capacitors and rechargeable batteries are recognized as the primary power

sources for applications for portable electronic appliance.^{152,154} For these devices, flexible power sources can be developed by using CNTs and its nanocomposites because CNTs are able to accommodate very high levels of deformation and stretch.^{160–165} Moreover, CNT-based electrode materials and devices can have high power density, excellent specific capacitance, be lightweight, miniaturization in size, safe, and have other significant properties. The potential applications of CNTs-based devices directly depends on its purity and type of CNTs which in turn controlled by its synthesis route. A comparative study of CVD, laser ablation, and arch discharge method for CNTs synthesis has been given in Table 6.

CNTs produced by the above methods (Table 6) have tremendous potential in the electrochemical applications due to their high surface area, remarkable tensile strength, outstanding flexibility, and very high electrical conductivity.^{155,157,162–165}

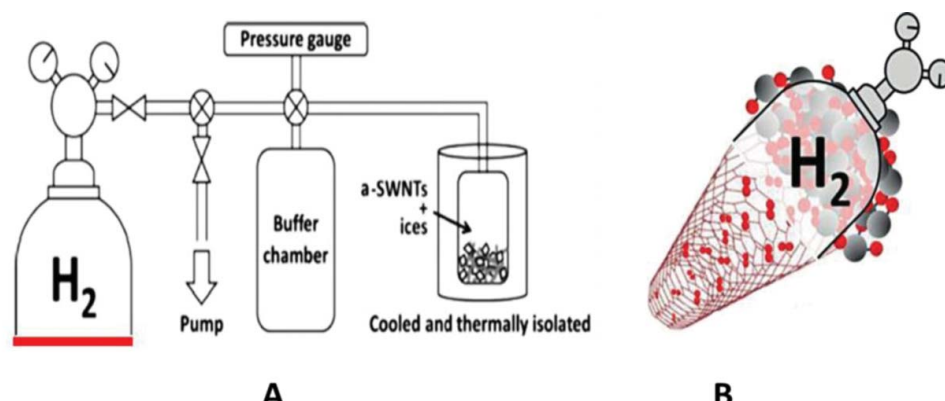


Figure 27. (A) Schematic setup for the hydrogen storage using SWCNTs and diagram for realizing the storage for pressurized hydrogen in the SWCNTs sealed with (B) aqueous valves. (© Wiley Online Library. Reproduced with permission from C. Tang et al.¹⁶⁵ Permission to reuse must be obtained from the rightsholder.)

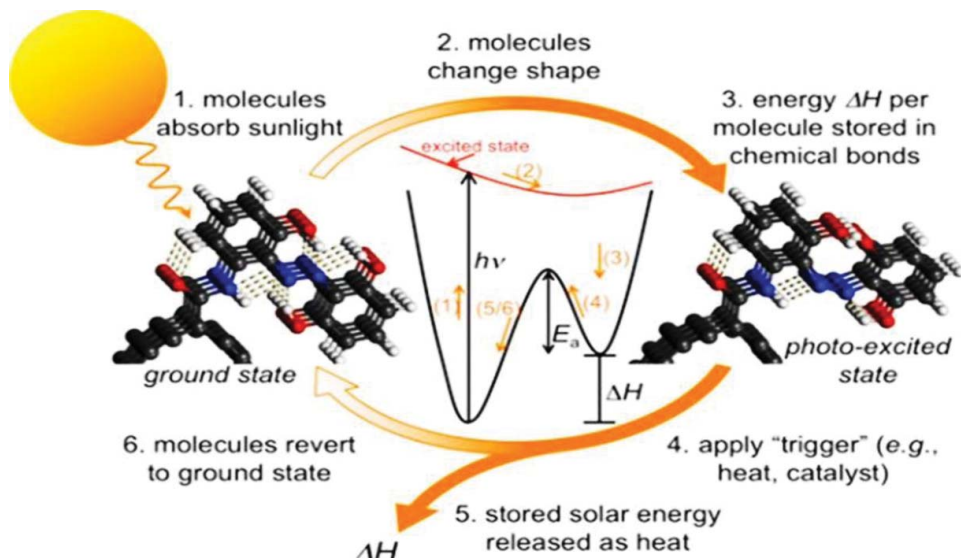


Figure 28. Solar thermal energy storage 2, 2' 5 -trihydroxy diazobenzene molecules covalently attached to CNTs undergo a photo induced trans-to-cis isomerization, storing $\Delta H = 1.55$ eV per azobenzene. (© ACS Publications. Reproduced with permission from A. M. Kolpak and J. C. Grossman¹⁶⁹ Permission to reuse must be obtained from the rightsholder.)

The use of various carbonaceous materials including graphite and carbon fiber electrodes are well known in the fuel cells, batteries, and other electrochemical purposes.¹⁵⁴

¹⁵⁶ The electron transfer rate determines the performance of fuel cells at the carbon electrodes and this efficiency ultimately depends on the dimensions, size, flat surface topology, and perfect surface specificity of the carbon electrode. Keeping all such specifications in mind, CNTs may be one of the best candidates for an ideal carbon electrode material.^{157–160} The solar panels are quite helpful for turning the sunlight into electricity for various applications.¹⁵⁸ This energy can be applied to charge batteries, for example, modern CNTs based solar panels for the domestic use. So, the investigators around the whole world have been watching at thermo-chemical storage of solar energy.^{150,151,153,154} From 2010–11 researchers at MIT found that the chemical fulvalene diruthenium was a very beneficial storage tool. Unfortunately, the ruthenium element is very toxic, expensive, and rare. As an alternative to this problem, some of the researchers have designed a new storage material that is cost-efficient and capable of storing more energy on the basis of thermo-chemical storage concept (Figure 28). Dr. Jeffrey Grossman (Associate Professor at MIT) started the research and his postdoc student Alexie Kolpak coupled CNTs with the compound azobenzene. They obtained a final product that is quite cheaper than fulvalene diruthenium and has more than 10^3 times as high volumetric energy density. As a result, it can save more than enough energy in less space.^{153,154} They further stated that the energy density of this product is comparable to that of a lithium-ion battery. One can control both how much energy

can be stored and for how long a period it can be saved by employing various methods of nanofabrications.^{150,152–154}

3.5.8. Composite material

CNTs have been considered as one of the most prominent candidates in the field of polymer blends nanocomposites as reinforcing nanofiller.¹⁷⁰ It is because nanotube is the quintessential tough material for the structural applications.¹⁷⁰ Owing to Young's modulus of 1TPa of SWNTs, it can be used as reinforcements for high strength, low weight, and high-performance composites.^{170,171} The nanotubes are highly flexible.¹⁷¹ The support increases by absorbing energy during their high flexible elastic behavior.^{171–172} The low density is an added advantage to its high electrical conductivity.¹⁷³ Such CNTs composites are much stronger and so much more mechanically advanced than pure polymer or conventional composites, as shown in Figure 29. These composites also have shown much importance in other fields including biochemical fields, nanoelectronic fields, nano-sensor, etc.^{170–173} The composites made out of nanotubes show an enormous enhancement in conductivity with little loss in photoluminescence and electroluminescence yields.^{174–176} The small channels in the nanotubes exert a strong capillary force that holds gasses and liquids in the nanotubes.^{173–175} In this way, the cavities in the nanotubes are filled up and hence we can easily prepare nano-wires. Because of the small pore size the filling of SWNTs is much harder than MWNTs.^{175,176}

The CNT arrays can be directly grown on a solid surface can be well fitted with the non-natural material

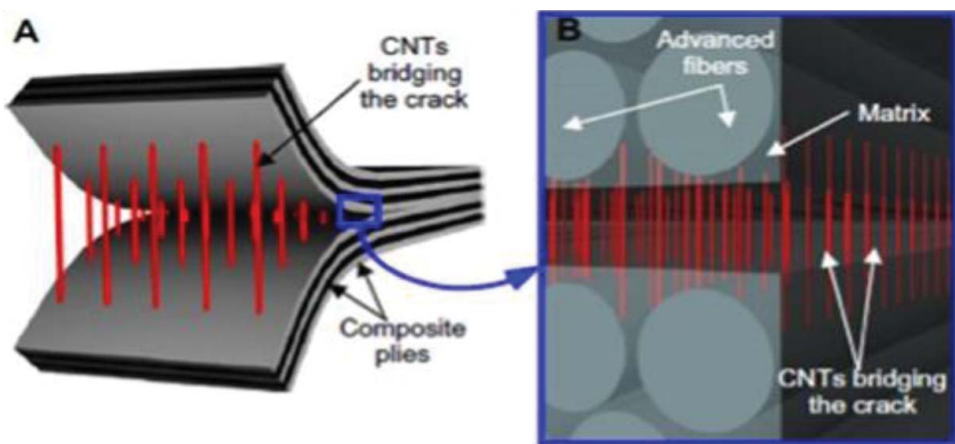


Figure 29. CNTs-based polymer blend nanocomposite showing interfacial strengthening. (© Springer. Reproduced with the permission from D. Bello et al.¹⁷⁷ Permission to reuse must be obtained from the rightsholder.)

representing a gecko foot structure.¹⁷⁷ When CNT array comes into the contact with a target surface with the absolute roughness, then the fine structure of CNTs ensure their capability of filling in the cavities at interface and make active links with the coupling surface.^{178,179} The difference between conventional polymer composites and CNTs-based polymer composites is shown in Figure 30.¹⁷⁸

4. Graphene (GR): A sensational material for materials scientist

Materials science continues to occupy a distinguished and significant place in our lives and without

advancement in material science we cannot imagine modern civilization in the world. The materials are fundamental to the technology that make our lives comfortable and great convenience, for instance, various electronic gazettes viz. laptop, cell phones, etc.^{180,181} The invention of novel materials always comes with the most thrilling and rewarding periods of scientific research in both theoretical and experimental fields.^{181,182} With the advent of new material, it often comes with new opportunities to reexamine old problems, as well as very new issues are generated which is one of the greatest gifts to the scientific community.^{3,180–182} In this tradition, we had known that carbon is a unique element in the periodic table and possesses many exceptional properties.^{3,182}

Graphene (GR) is newly discovered carbon allotrope.³ It is magical: the mother of all graphitic carbon, one atom thick, two-dimensional carbon material.^{3,11,61} Graphene has emerged as a new hope for the entire scientific fraternity.^{3,61} It has ultra-high intrinsic carrier mobility ($200,000 \text{ cm}^2/\text{V}^{-1}\text{s}^{-1}$) and exhibits thermal conductivity of several times greater than that of Cu metal. It also has the vast surface area that is even much higher than SWCNTs ($2630 \text{ m}^2\text{g}^{-1}$), excellent thermal, mechanical elastic properties, etc. In the whole scientific community initially the uniqueness of GR created hype due to the following unbelievable properties:^{3,11,61,183,184}

- i. it is the purest form of carbon;
- ii. it has very large theoretical specific area which is about $2630 \text{ m}^2/\text{g}$;
- iii. its highest intrinsic mobility is $200,000 \text{ cm}^2\text{V}^{-1}\text{s}^{-1}$;
- iv. it has extremely high Young's modulus of about 1.0 TPA;
- v. it has exceptionally high thermal conductivity of about $5000 \text{ Wm}^{-1}\text{K}^{-1}$;

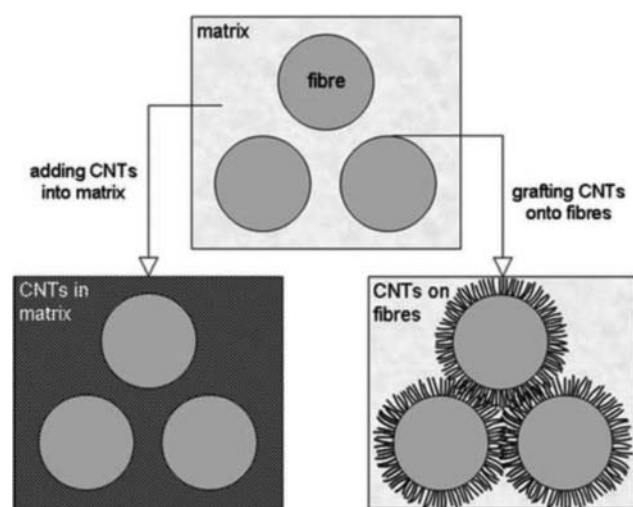


Figure 30. Schematic diagrams of conventional fiber-reinforced polymer composites and CNTs-based hierarchical polymer composites. (© Royal Society of Chemistry. Reproduced with permission from H. Qian et al.¹⁷⁸ Permission to reuse must be obtained from the rightsholder.)

- vi. it has optical transmittance of more than 98%;
- vii. it is the lightest and thinnest known material in the universe;
- viii. it has zero band gaps; and
- ix. it has outstanding elasticity.

This is why, nowadays, GR is treated as a rising star in the field of technological applications particularly in the areas of high-efficiency sensor, fuel cells, renewable energy sources, electrochemical capacitors, transparent electrodes, and nanocomposite materials.^{11–13,183–186} GR and GR-based material are being very rapidly studied, nearly in every field of science and technology worldwide, because of their exceptional charge transfer, thermal, mechanical, optical, and band structure properties.^{185,186} The latest scientific advancement has shown that GR-based material has a great impact on electronic devices, photo-electronic device, biochemical sensor, chemical sensor, blend nanocomposite, and energy storage devices in solar system.^{186–188} Due to such wonderful and luminous properties of GR, it is also known as the “Wonder Material” or miracle material. In 2008, James Hone and coworkers of Columbia University stated that: “Our investigation confirms that GR is the strongest material till now measured. It is approximately 200 times stronger than structural steel. It would need an elephant, adjusted on a pencil, to cut into a sheet of GR the width of Saran Wrap.”¹⁸⁹ Prof. Jiri Minaret of Chalmers University in Sweden stated that “Graphene can explore many novel uses in a variety of fields including transparent and flexible electronics, and electronics that are greatly quicker than existing one, and even beyond its digital applications, for example the addition of graphene powder in tires make them stronger.”^{189,190} Professor A. Geim stated about GR “It is not even one material; rather it is an enormous range of materials.”^{3,11,186} It can be added to all kinds of plastic to make hybrid materials due to which a large number of people in the scientific community have been interested in working on projects

related to GR. Around 300 organizations are now involved in research related to graphene and, interestingly, the number of research papers published on this wonder material have increased tremendously from around 3500, in 2010, to 14,000, in 2014, and already crossed 11,000 in 2015 (according to scopus database).¹⁹⁰ These research efforts obviously benefit both business and the consumers due to the availability of faster and more affordable devices. Some very important information and recent trends in GR based nanocomposites has greatly been explored by Mukhopadhyay et al.¹⁸⁶ CNT and fullerenes are also the allotropes of carbon and possess much specificity but they do not receive a lot of attention in scientific communities nowadays like GR, because mechanical, electronic magnetic, and optical properties of these allotropes are not similar to GR and functionalization of CNT and fullerene are also not easy as GR.^{190–194} The fundamental structure and properties of all the carbon allotropes are summarized in Figure 31 and Table 7, respectively.

The discovery of GR has entirely changed the face of material science.^{3,11,63} Discovery of GR started when Kaleb, a six-year-old child, look out his pencil and started writing letters on a piece of paper. He did not know that he was just going to open an outstanding research topic that caught the great attention of the entire scientific community that same day. For outstanding contribution to the field of GR, Andre Geim and Konstantin Novoselov of Manchester University, UK were awarded the Nobel Prize in Physics in 2010 (Figure 32).^{3,186} After the year 2010, many famous multi-national companies (MNCs), and even governments of different countries, allocated money for GR research which consequently helped in the commercialization of GR-based material, specifically GR-based polymer nanocomposites (PNCs).^{186,190–193} Such development and research in materials science certainly generate many opportunity and applications,

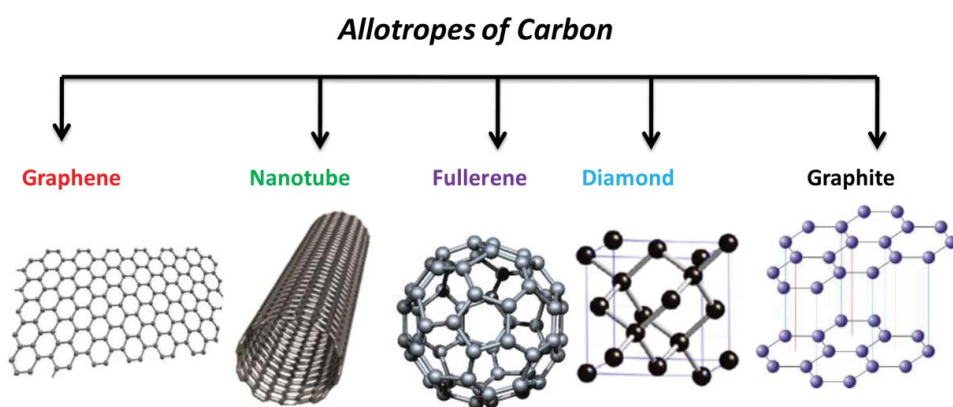


Figure 31. Allotropes of carbon and their crystal structure.^{3,194}

Table 7. A brief information about fullerene, CNT, graphite, and diamond.^{3,11–13,61,186–194}

Dimension	0D	1D	2D	3D
Allotropes	Fullerene	CNTs	graphite	Diamonds
Hybridization	Sp ²	Sp ²	Sp ²	Sp ³
Density g/cm ³	1.72	1.2–2.0	2.6	3.5
Bond length (Å)	1.40 C=C	1.42 C=C	1.42 C=C	1.54 C-C
Electronic properties	semiconductor	semiconductor	semi metal	Insulator

but challenges still need to be overcome to bring about the synergy between GR-research and its myriad anticipated application.^{186,190} The main problem that remains is the production of scalable amount of ultrapure GR, safely, and cheaply.^{186,190} The complete attention of the scientific community on GR came when Prof. A. Geim and K. Novoselov managed to extract pure single atomic thick crystal lattice from bulk graphite in 2004.^{3,193} They mechanically pulled out a GR layer from graphite and transferred them into thin SiO₂ on silicon wafer, an experimental process commonly known as the scotch tape method, as shown in Figure 32. Since then, it has established itself as one of the most remarkable materials available to condensed matter scientists. Before that, graphene had been investigated theoretically for over 60 years, although its existence as 2D crystals in free space was thought impossible, and separation of a single layer of graphite considered as beyond the possibilities.^{3,186} This was also a matter of debate.^{186,193} Before GR quantum physicist had no actual 2-D system for the physical manifestation of quantum mechanics, and they always used artificial 2-D system on the basis of 3-D system quantum mechanical properties.^{3,194} In this way, the discovery of GR opened a new branch of quantum physics and in the last ten years GR had been the most studied material in the world.^{3,194,195} However, this 2-D system is presently suffering from a number of experimental challenges and it is a matter of further experimental and theoretical study.^{3,194,195}

4.1. Structural properties and band structure of graphene

An atomically thick single layer of GR is similar to a single page of the notebook. And carbon atoms are bonded together in a hexagonal honeycomb lattice via sp² hybridization.^{3,11,63,183} This lattice consists of two equivalent sub lattices of carbon atoms bonded to one another.^{3,11,63} In this way, graphite is made up of many layers of GR and each layer interconnected to each other by Van Der Waal forces (see Figure 33).¹⁹⁷ Using the local orbital occupancy approach and second-order perturbation theory, Dappe and coworkers reported that the binding energy between the each sheet of graphite is approximately 60–72 meV.^{197,198}

Theoretical hypothesis of tight bonding mode (TBM) is frequently used to explain bonding and structural characteristics of GR because of its quantum mechanical ground.^{198,199} This theory gives a lucid and clear explanation about exceptional behaviors of graphene and derivatives.¹⁹⁸ According to this theory, in all carbon allotropes, except diamond, the π valance electron and its nature handles electronic, transport, magnetic, and other physical properties.^{198,200} However, unique band structure and 2D lattice of GR makes it particular and different from other materials.^{198,201} The ground state electronic configuration of the carbon atom is $1s^2\ 2s^2\ 2p^2$, so the number of valence electrons in graphene is four.^{201,202} For each carbon atom in dense honeycomb lattice crystal of graphene, three of four valence



Figure 32. Scotch tape experiment of Prof. Andre Geim and coworker for GR separation from graphite. Photograph of Prof. Andre Geim and Prof. Konstantin Novoselov of University of Manchester, UK, discoverers of GR. (© Nobel Academy. Nobel Laureate 2010: Physics, Image credit to Nobelprize.org.¹⁹⁶ Permission to reuse must be obtained from the rightsholder.)

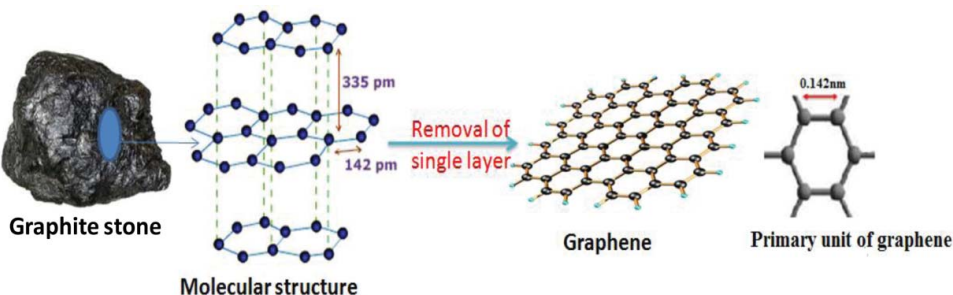


Figure 33. Schematic representation; graphene is the mother of all graphitic carbon allotropes.

electrons get very effective σ overlap with the neighboring carbon atom within the sheet, resulting in very strong sigma bond formation.^{198,202,203} This sigma bonds is responsible for exceptional flexibility and robustness to the lattice structure of GR.^{202–205} On another hand, the fourth remaining electrons in the p_z orbital overlap to each other with neighboring orbitals (identical symmetry) and formed π bonds (Figure 34). Thus, each π bond contributes the half-filled electrons of p orbitals to tunnel from a carbon atom to the nearest one in the honeycomb lattice of graphene.^{206,207} Therefore, graphene can be treated as a many-body system on which electrons can get correlated from one site to another of graphene, resulting in a rich collective behavior.²⁰⁷ The associated performance can be characterized by quantum mechanical effect, which may consequently affect intrinsic electronic properties of a graphene system.^{207,208} So, the chemical bonds in GR is sp^2 hybridization which is due to mixing of $2s$ with $2p_x$ and $2p_y$ all three localized sigma bond formed by overlapping with three nearest neighbor carbon atom in the honeycomb lattice, and they are responsible for most of binding energy and for elastic properties of GR sheet.^{207,208} The unused p_z orbital of GR skeleton is shown in Figure 34. It takes part in pi bonding due to suitable symmetry conditions. Thus, p_z orbital plays very

crucial in delocalization and determines electronic properties of GR^{197,208} The delocalization is depicted in the fundamental unit of GR.¹⁹⁷ Therefore, we can say these π bonds gives intrinsic electronic properties of GR.^{197,208} Theoretically exact electronic state of GR and theoretically energy dispersion relation can be obtained using linear combination of $2p_z$ orbitals and by solving the Schrodinger wave equation on the basis of orthogonal nearest-neighbor tight bonding approximation.^{197,205–207}

These three π bonds consequently decoupled from sigma bonds because of the inversion symmetry and gives exceptional Fermi energy for GR.^{203,205} Due to such Fermi energy conduction and valence bands have negligible band gap.^{205,209} However, in the case of neutral graphene sheet (a graphene sheet which have an insulating ground state in the presence of an external magnetic field) this energy is equal to the zero; this reason graphene is a material with zero band gaps.²⁰⁹ In this line, Jung and coworker reported that due to abnormal Fermi energy condition graphene sheets on substrates the ground state is most likely a field-induced spin-density wave and that a charge-density-wave state is possible for suspended samples representing characteristics of GR's band structure (see Figure 35).^{205,209} The band structure consist two groups of conical valleys (conduction and valance band) and these conical valleys touch at two points, which make graphene

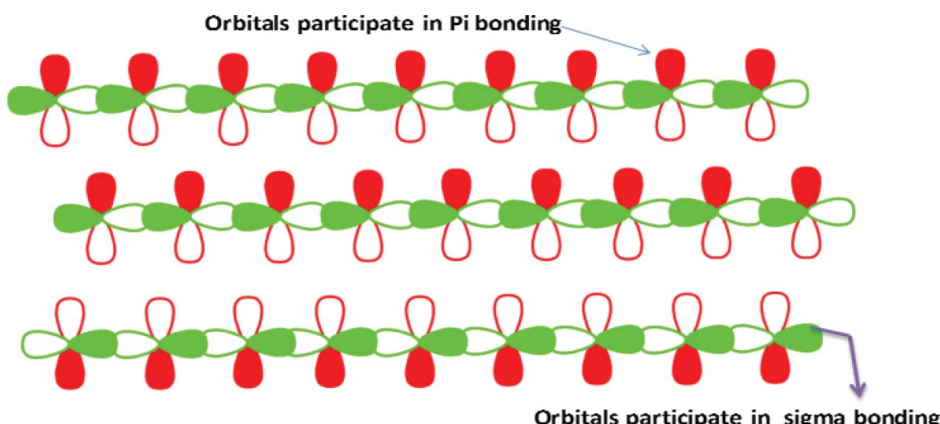


Figure 34. Position of Pi and sigma bonds in the honeycomb lattice of graphene and orbitals responsible for bonding.

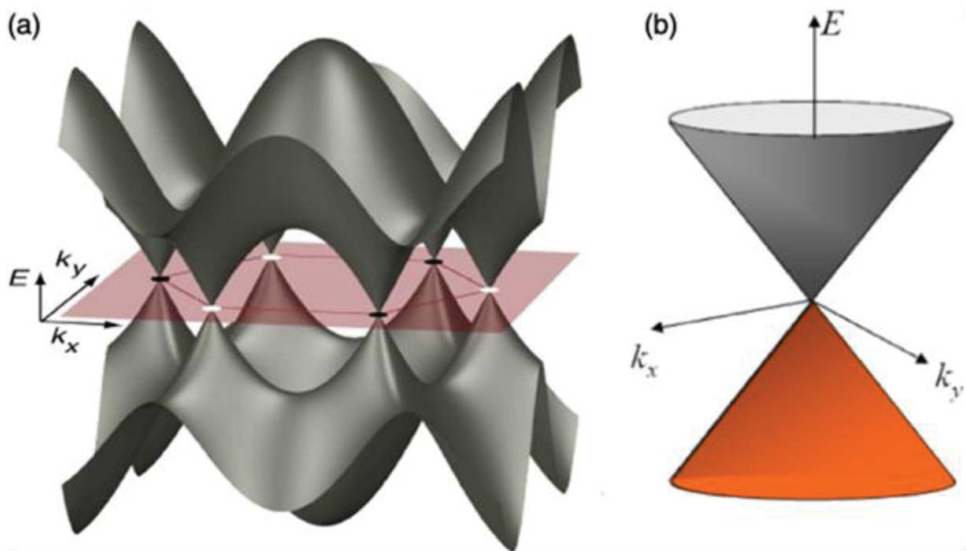


Figure 35. Schematic representation of Dirac point (a) and band structure of graphene (b). (© IOP Publishing. Reproduced with permission from E. Andrei et al.²⁰⁸ and S. Sahoo et al.²⁰⁹ Permission to reuse must be obtained from the rightsholder.)

a gapless semiconductor.^{205,209} These two touching points in the graphene are known as Dirac point.²⁰⁹

It is well established that in GR conduction bands and valance bands are completely degenerate at six points located on the corner of the Brillouin Zone also called K and K' valleys, as shown in Figure 35. This Brillouin zone (i.e., hexagonal region) in GR has a side length $4\pi/3a$ and delineates the Fermi surface of GR shown in Figure 35.^{208,209} The Fermi surface of GR is completed to a zero ($E_f = 0$) dimension zone that is composed of finite sets of six points in the Brillouin Zone, this is why GR also called a Semimetal material with no overlap or zero-gap semiconductor (ZGS).²¹⁰ Very interesting information can very easily drawn from the above diagrams that electronic properties of GR are fully invariant by interchanging K and K' states, meaning that the two valleys are related by time reversal symmetry, and this exceptional quantum-mechanical property of GR is only due to the phase reversal symmetry.^{211,212} And due to this time-phase reversal symmetry GR charge carriers behave as Dirac Fermions with an effective Fermi velocity that is around 300 times smaller than speed of light, it makes GR a very reliable two-dimensional system to study of Quantum Electrodynamics properties, an area of impressive research previously limited to Particle Physics and Cosmology.^{209,212} Dirac fermions can elaborated as the “energy-momentum relation” for GR (2D system) is always linear at the near to six corners of two-dimensional hexagonal Brillouin zone. Figure 35 gives zero effective mass for electrons and holes due to this linear or conical momentum relation (dispersion relation) at low energies electrons and holes near the six points, two of which become equivalent and behaves like a

relativistic particle that only be explained by “Dirac equation” spin $\frac{1}{2}$ particles hence the electrons and holes are commonly called “Dirac fermions.”^{209,213}

4.2. Quantum hall effect in GR

The conventional Hall Effect is “production of a voltage difference across an electric conductor, transverse to an electric current in the conductor and a magnetic field perpendicular to the current.”²⁰⁹ The values of Hall voltage can be obtained by following equation:²⁰⁹

$$R_H = \frac{E_y}{j_x B} = \frac{V_H t}{IB} = -\frac{1}{ne},$$

where R_H is called the Hall voltage, “e” is the charge of electron or hole, and “n” is the charge carrier density; other physical parameters have its usual meaning.^{209,210}

The Hall Effect raised in two-dimensional semiconducting systems like metal oxide semiconductor and field effect transistor (MOSFET) is called Quantum Hall Effect (QHE). Thus, Quantum Hall effect is a quantum-mechanical phenomena of the Hall effect, observed in 2D electronic systems, when subjected to low temperatures and high magnetic fields, in which the Hall field measures on the quantized values.²⁰⁹ This quantum mechanical phenomenon is somewhat different in the case of graphene because of its single atomic thickness and unique crystal lattice. The electrons in the honeycomb crystal lattice of graphene obey a linear dispersion relation^{191,192} given Equation (1):

$$E = \hbar v_F k = p v_F F \quad (1)$$

where $p = \hbar k$ momentum and vF is the velocity of the electrons in the graphene system.²¹⁰ This velocity is commonly known as Fermi velocity, and it is equal to the 10^6 ms^{-1} .²¹⁴ So in the case of graphene energy is directly proportional to momentum, which implies that the charge carriers in the graphene have zero effective mass and move with the constant velocity.^{209,210,214} It is interesting to note that the electrons are not completely massless in the graphene, but it is infinitesimal so that it may be neglected.^{215,216} This is because of the effective mass is a parameter that describes how an electron at a particular wave vector responds to the applied forces.²¹⁶ Since the velocity of electrons confined to honeycomb lattice of graphene remains constant, the result mathematically effective mass can be neglected.²⁰⁹ However, it is a matter of debate to decide that whether graphene is semimetal or semiconductor or a metal.^{213–216} Thus, there are different views regarding this ambiguous nature of graphene. Some groups considered graphene as an individual semiconductor or semimetal because the band gap is zero.²¹⁶ On the other hand, it is theoretically reported that the conductivity in graphene is independent of Fermi energy so that the effective scattering of the electron can vanish so graphene is metal.^{215,216} In contrast, according to band theory metals and semiconductors possess one and two bands, respectively, but neutral graphene have two energy levels one for electrons and other for the holes. However, many workers treated graphene as a hybrid of metals and semiconductors, i.e., semimetal.²⁰⁹

4.2.1. Integer quantum hall effect in graphene

Dirac's theory is entirely not applicable to explain electrons' spin behavior in the case of graphene, because of the unique honeycomb crystal lattice of graphene and anomalous electron scattering behavior.^{209,217,218} But use of Dirac's theory on the graphene gives the concept of pseudospin which protects graphene electrons against backscattering off defects and various impurities.²¹⁷ It results in an enhancement in the conductivity and explains why charge carriers in graphene tend not to localize.^{209,217} Graphene shows a number of appealing behaviors in the presence of a high magnetic field (perpendicular) at low temperatures.²¹⁸ It is reported that in the presence of applied magnetic field B , the electrons or holes restricted in 2D which are forced to move near to the cyclotron orbits that are quantized.^{219,220} The quantization of the cyclotron orbits is revealed in the quantization of the energy levels.²²⁰ At a finite applied magnetic field (B) and $B = 0$, dispersion is displaced by a discrete set of energy levels, which generally identified as Landau levels (LLs) and corresponding quantization is called Landau quantization.²⁰⁹ Quantum mechanical study of graphene shows that as one Landau levels fills up, the

conductance is flat, and shows no increase in carrier density until the next Landau level is filled.²⁰⁹ The plateau appears at conductance values $\sigma_{xy} = ve^2/h$, where v is a Landau level filling factor which takes on integer values in the case of Integer Quantum Hall Effect (IQHE).²⁰⁹ The filling factor may be defined as the ratio of the total number of charges to the total number of magnetic flux lines. In the graphene, the Landau level spectrum is entirely different from the conventional because of the massless chiral Dirac fermions which give a new type of integer quantum Hall effect.^{209,218–220}

The Hall conductivity^{202,203,207} $\sigma_{xy} = \pm 4e^2/h(n+1/2)$ under an applied magnetic field of 10 T and a temperature 1.6 K, where 'n' is the Landau level index and the factor 4 accounts for the graphene's double valley degeneracy.^{209,218–220} This unconventional quantum Hall effect in graphene forms a series of filling factors $v = \pm 2, \pm 6, \pm 10, \pm 14\dots$. This is why, Hall effect in the case of graphene called as half-integer quantum Hall Effect.²⁰⁹ Moreover, $1/2$ is the trademark of the chiral nature of the Dirac fermions in the case of graphene. In the graphene first plateau found at the $2e^2/h$ [$= (1/2)(4e^2/h)$] which is not present in non-relativistic 2DES.^{209,218–221} This is a special case of $n = 0$ Landau level for the massless fermions.²²¹ This uniqueness in QHE is the direct evidence for Dirac fermions in the graphene.²²¹ The QHE in the case of two layers graphene is very fascinating.²¹⁹ Such a graphene system consists of two weakly, van der Waal coupled honeycomb graphene sheets and the Landau level spectrum is composed of eight-fold degenerate states at the zero energy and four-fold ones at finite energies under the high applied magnetic field.²¹⁰ It allows us to observe the quantum Hall plateaus at a series of $v = \pm 4, \pm 8, \pm 12, \pm 16\dots$ In this case, the first plateau at $n = 0$ is absent, and the first plateau appears as $4e^2/h$.^{220,221} This quantity is very much similar to the conventional QHE in semiconductor-based 2DES.^{209,219} Mostly, the quantized plateaus appear at the standard sequence $\sigma_{xy} = \pm 4e^2/h$ (it is identical to the non-relativistic electrons) with a missing plateau at zero energy.²⁰⁹ In this way, the step in the Hall conductance distributing electrons and holes like zones is double as large as the quantized levels on both sides of the charge-neutral state.^{209,220} This abnormality, i.e., $E = 0$, can be eliminated by field-effect doping.²²⁰ It has the impact of combining transports and breaking the layer degeneracy of the zero-energy Landau level creating two entirely extra levels in the Hall conductance, each of height $4e^2/h$.^{220,221} Such abnormal quantization in the bilayer graphene handles the typical excitation commonly known as massive Dirac fermions, and all these fermions have a quadratic distribution similar to the massive non-relativistic particles.^{209,221} It is evident from the previous

discussion that the exceptional IQHE in single layer graphene is due to the massless Dirac fermions and a zero energy mode ($E = 0$). The abnormal IQHE in bilayer graphene is because of the massive Dirac fermions and two zero energy modes.^{219–221} Also to this it is reported that room-temperature QHE can be observed in graphene under suitable condition. Such a brilliant remark of QHE in graphene at ambient temperature unlocks up a new door for graphene/graphene derivative-based quantum mechanical devices.^{209, 219–221}

4.2.2 Fractional quantum hall effect in graphene

A theoretical physicist expects that electrons in graphene are the strongly interacting result; graphene shows the Fractional Quantum Hall Effect (FQHE).²²² It may be defined as a physical event in which the Hall conductance of 2D electrons indicates accurately quantized plateaus at fractional values of e^2/h .²²³ It is considered a combined state in which electrons handle magnetic flux lines.^{222,223} As a result, new quasiparticles and excitation are generated that have a fractional elementary charge and statistics.²²³ However, it is notable that still there is no sophisticated instrument to obtain direct information about FQHE in graphene.^{222,223} The Integer Quantum Hall Effect in graphene can be explained in terms of single electrons in an applied magnetics; on another hand, the FQHE in graphene can be understood by the collective behavior of all the electrons.²²⁴ It is because FQHE requires a higher magnetic field, low temperature, and very instant mobility than the IQHE investigation, but the IQHE never depends on interactions between the electrons.^{224,225} The quantized Hall conductivity (σ_{xy}) in FQHE in graphene can be obtained by equation given below.^{209,224,225}

$$\sigma_{xy} = \pm \frac{2p+1}{2m(2p+1)+1} \frac{2e2}{h},$$

where $m, p = 0, 1, 2, 3, 4, \dots$

The localization of electrons and quasi-particles is believed to be responsible for the formation of the plateaus in the Hall conductivity.^{225–227} Due to the honeycomb crystal lattice of graphene and unique Dirac nature of carriers, the edge states play a crucial role in quantum Hall transport.^{225,226} Very recently, it has been reported that Dirac electrons exhibit high collective behavior that give rise to FQHE in graphene.²⁰⁹ Also, Du and coworker had suspended the ultrapure graphene between two supports and observed that the electrons in suspended sample possess much higher mobilities than the samples coated on the substrate.^{226–230} Du and coworker obtained such a unique hall effect with a two-probe method to get the better results than the classical four-probe method.^{226,230}

They observed plateau in transverse conductance at 1/3 of the conductance quantum e^2/h , and they find that the FQHE can be observed at low temperatures in the magnetic fields as small as 2 T.^{230–233} Lately, the FQHE has been reported by Dean and coworker in a monolayer graphene that fabricated on a hexagonal boron nitride substrate.^{334,335} This substrate is very suitable because it is an insulating isomorph of graphite.^{232–236}

4.3. Graphene nanoribbons (GNRs)

In the previous section we have discussed the unzipping technique of CNTs and formation of graphene nanoribbons. These nanoribbons are strips of graphene with an ultra-thin width (<50 nm).^{236,237} First, graphene ribbons were added to a theoretical model by Mitsutaka Fujita and co-workers to evaluate the edge and effect of nano-scale size in graphene.^{237–338} Kosynkin et al. reported that longitudinal cleavage of CNTs, using specific chemical, catalytical, and electrical ideas, successfully unzips them into thin graphene strips of various widths and shape. These unzipped CNTs are very similar with the graphene nanoribbon but smaller in size Figure 13.⁵⁹ When advanced lithographic technique is employed on GR for profound study of its nanoscale structure, it has been observed that a lateral confinement of charge carriers can work as an efficient energy gap having parameter, the possibility of such narrow non-ideal GR is commonly called as graphene nano ribbon (GNR) or nano graphene ribbon.^{59,336–339} The TEM images of such graphene are strictly looking like the defect-free graphene, so the TEM is unable to distinguish GR and GNRs. The TEM picture of a GNRs is shown in the Figure 36.⁵⁹

Existence of GNRs first of all reported by Mitsutaka Fujita and coworker.^{22,24} In most of cases width of GNRs varies between the 30–40 nm and this reason it is also called as narrow graphene strips.^{59,336} It has been found that Physical and chemical properties of GNRs quite different from GR.^{22,24} The actual existence of GNRs is still a point of debate, but the advanced lithographic experiment and Raman spectroscopy has confirmed that confined GR structures are experimentally feasible.^{240,241} At present, synthesis of specific GNR is beyond a possibility, however, a lot of widths-controlled GNRs can be produced via Graphite anatomy process.^{22,241} Very recently, GNRs have been grown into silicon carbide sheet using iron implantation technique followed by laser annealing.^{22,24} Nowadays, this technique is considered as a best method for the generation of GNRs.²⁴² The properties of GNRs mainly depend on the width and morphology of the edge structures and it is reported that

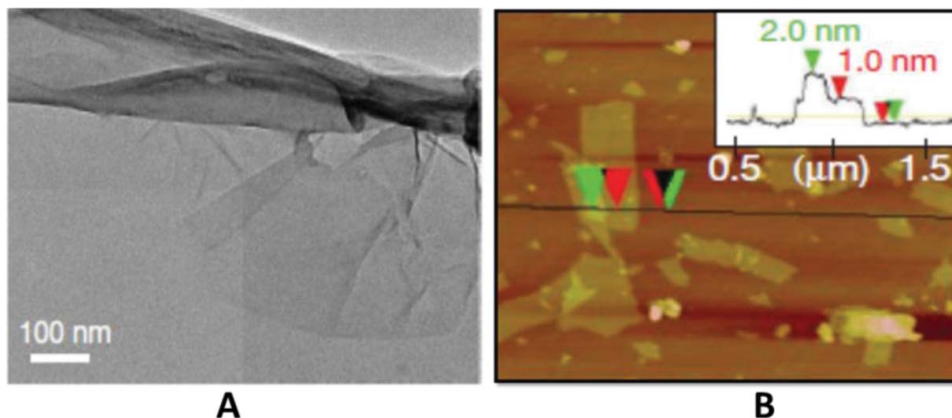


Figure 36. TEM (A) and AFM (B) micrograph of GNRs showing sheet and bent-like structures and surface morphology. (© Nature Publishing Group. Reproduced with permission from D. V. Kosynkin et al.⁵⁹ Permission to reuse must be obtained from the rightsholder.)

the zigzag edge provides edge localized state with nBMOs near the Fermi energy and, due to this, they have large changes in optical and electronic properties from quantization.^{242–245} It is notable that most of the known GNRs possess some defects in their lattice.²²⁹ The GR edges all the GNRs can be divided into two groups: (i) armchair graphene nanoribbon (AGNRs) and (ii) zigzag graphene nanoribbons (ZGNRs). The crystal lattice of AGNRs, ZGNRs, and defected GNRs is shown in Figure 37.²⁴³ The electronic properties of GNRs can be explained in terms of tight bonding theory (TBT) or by Dirac approach.^{245,246}

4.4. Electronic properties of GR

One of the most glamorous and charismatic properties of GR is its zero band gap with exceptionally high electrical conductivity.^{3,242} The four valence electrons in an individual carbon atom of the GR sheets are available for bond formation, but in GR, each atom is connected to three other carbon atoms in a 2D plane, leaving one electron free for π -bond formation that is ultimately responsible for the electronic conduction.^{242,247} These mobile

electrons are located above and below the GR sheet, and they also enhance the carbon to carbon bond strengths in GR. Therefore, the electronic properties of GR only depend on the BMOs and ABMOs of π electrons, as mentioned previously that the GR electrons and holes have zero effective mass.²⁴² It happened because of typical six individual corners of the Brillouin zone in the GR.²⁴⁸ Therefore, the electrons and holes of GR are called as Dirac fermions, whereas the six edges of the Brillouin zone are named as the Dirac points.^{248,249} Owing to their zero density at the Dirac points, the conductivity is comparable very less.²⁴⁹ However, the Fermi level can be adjusted by the process named as doping to produce a material that has probably superior conductivity as compared to the copper at standard temperature pressure (STP).²⁴⁸ It is reported that the electronic mobility in GR is very high, and theoretically potential limits of $200,000 \text{ cm}^2 \cdot \text{V}^{-1} \cdot \text{s}^{-1}$. It is said “GR electrons work similar to photons in terms of their movement due to their lack of mass.”²⁴⁸ Due to this the charge carriers can propagate within sub-micrometer distances without any scattering. This unique transport of electrons in the GR is quantum mechanically called “ballistic transport.”^{248,249}

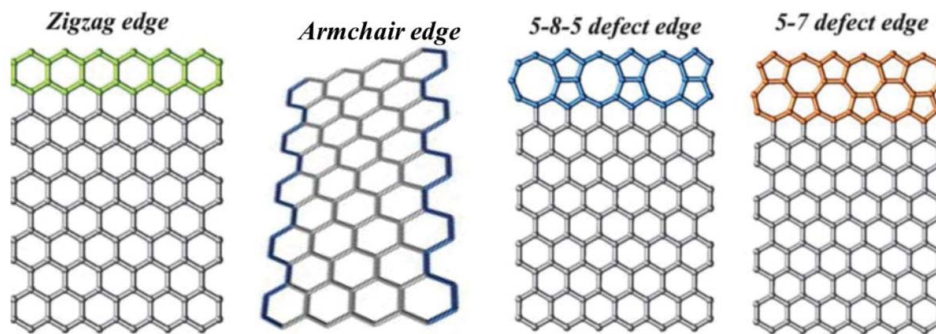


Figure 37. Lattice arrangement of various types of graphene nanoribbons. (© Royal Society of Chemistry. Reproduced with permission from X. Jia et al.²⁴³ Permission to reuse must be obtained from the rightsholder.)

4.5. Mechanical strength of GR

Graphene is the strongest material in the universe which is the second most unbelievable property of graphene, and this magical strength is ultimately due to the 1.42 Å very short C=C bond.^{250–252} Theoretically, the ultimate tensile strength of graphene is reported in Gigapascals.^{250,251} Interestingly, graphene is not only exceptionally strong, but also very light at 0.77 mg per square meter.²⁵² It is often said that a 1 g single sheet of graphene is more than enough in size to cover a whole football. In 2007, atomic force microscopic (AFM) tests were carried out on single sheeted graphene, and it is found that an ultra-pure single sheet of graphene is able to bear the load of an elephant (Figure 38). The test also showed that graphene sheets had a Young's modulus of 0.5 TPa, and spring constants in the region of 1–5 N/m.^{250–252} It is considered a miracle material owing to its power, lightness, elasticity, conductivity, and low price; it could now enter the market to improve telecommunications dramatically.^{247–249}

4.6. Optical properties of GR

The firm affinity of graphene to absorb a rather significant 2.3% of the white light is also an outstanding property.²⁵³ It is because of its outstanding electronic properties that the electrons act as massless charge carriers with a very high mobility.²⁵³ Recently, it was confirmed that the quantity of white light consumed is related to the fine structure constant, preferably than being managed by material particulars.²⁵⁴ The addition of an extra layer of graphene improves the amount of white light absorbed by about the same rate (2.3%). Graphene's opacity of $\pi\alpha \approx 2.3\%$ compares to a universal dynamic conductivity value of $G = e^2/4\hbar$ ($\pm 2\text{--}3\%$) over the visible frequency range.^{253–255} Because of these unusual features, it has been noted that once the optical intensity approaches a certain threshold saturable absorption takes place.²⁵⁵ It is considered as an

important property of graphene with regards to the mode-locking of fiber lasers.²⁵³ A full-band mode locking has been achieved using an erbium-doped dissipative solution fiber laser able of getting wavelength tuning as large as 30 nm due to the wavelength-insensitive ultrafast saturable absorption of graphene's.^{255,256}

4.7. Thermal properties of GR

It is an ideal thermal conductor with the conductivity value more than $5000 \text{ W}\cdot\text{m}^{-1}\cdot\text{K}^{-1}$, and it is found that the thermal conductivity of graphene is much higher than all other allotropes of carbon.^{257–258} The thermal conductivity of graphene is measured by a non-contact optical technique.²⁵⁸ The ballistic thermal conductance (when phonons in defect less structure propagate without scattering then thermal conduction is called ballistic) of graphene is identical in all directions, i.e. its ballistic thermal conductance is in nature isotropic.^{257–259} It was reported that the thermal conductivity of graphene is about five times more than graphite.²⁵⁸ This is due to the unique crystal lattice of graphene and anomalous propagation elastic waves in the graphene lattice commonly, called phonons.^{258,259} Theoretically, it is found that a graphene sheet is thermodynamically unstable if its size is less than 20 nm (about 6000 carbon atoms) and becomes highly stable fullerene.^{260–262}

4.8. Synthesis methods of GR

Several methods have been developed for the synthesis of graphene.^{191–193,263–275} Each method has their advantages and disadvantages among the various techniques; chemical exfoliation is most familiar, but it is tedious, time-consuming, and involves the use of highly hazardous chemicals which creates severe environmental problems.^{274,275} Also to this structural defect are always established in the graphene sheet, which directly related to the unique properties of this wonder material.²⁷⁵ The micromechanical cleavage, in this case, the quality of

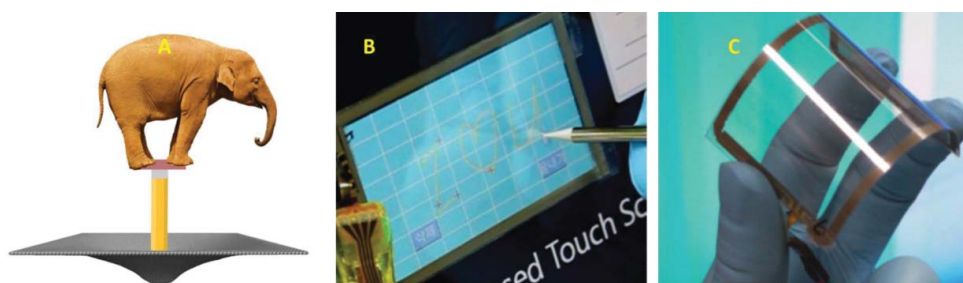


Figure 38. Schematic diagram (A) showing strength of a single sheet graphene, (B) an assembled graphene/PET touch panel showing outstanding flexibility, and (C) a graphene-based touch-screen panel connected to a computer. (© Wiley Online Library. Reproduced with permission from S. Bae et al.²⁴⁹ Permission to reuse must be obtained from the rightsholder.)

graphene is excellent, but the yield is indigent and highly time-consuming. Similarly, chemical vapor deposition of graphene synthesis (CVD) is one of the best technique for ultrapure graphene synthesis.^{191–193,275} But it is highly expensive and requires sophisticated instruments, so it is not feasible in ordinary labs. The electrochemical expansion (ECE) approach of graphene synthesis is cost effective, green, time efficient, and potentially useful for the bulk production of GR.” Due to the experimental simplicity and easy purification this method of GR synthesis have widely been accepted in scientific community.^{275,191–193} However, the challenge persists to identify a high-yield method that can exfoliate graphite efficiently into solution-dispersible graphene sheets without any significant chemical toxicity and structural damage to the graphene sheets.^{191–193,273,274} Thus, at present, the biggest challenge for a material scientist is to develop a cheaper and eco-friendly method for the production of pure single-layer graphene (SLGR) and few layers graphene (FLG) at industrial scale.^{192,275} An overview of GR synthesis techniques is depicted in the flow chart in Figure 39. The idea of synthesis of GR is not new, and many attempts have been done to synthesize a few layers of graphite. For instance, in 1975 a few layers of graphite was synthesized on a single crystal of Pt metal crystal via chemical decomposition method by Lang and coworker.^{191–193} However, it was not designated as GR due to lack of sophisticated characterization techniques and also due to its very limited possible application at that time.^{252,255} This is why it has not obtained a lot of attention in 2004 as synthesized by Andre Geim (Research Professor at the Manchester Centre for Meso-science and Nanotechnology).³ Many excellent articles and review papers are available for synthesis of GR via mechanical exfoliation, chemical exfoliation, chemical synthesis, CVD, ECE, and on other traditional GR

synthesis so there is no need to discuss it again in this article.^{191–193,263–275} The molecular structure of graphene is shown in Figure 40.

4.9. Applications of GR

Graphene, the extraordinary and wonder material, has a broad range of applications in diverse fields. Its outstanding applications have been found in areas like nanoelectronics, bioenergy, nanobiotechnology, nanosensors, nanocatalysis, and many more due its high working ability, cost effectiveness, and ease of availability.^{275–288} Since the discovery of GR, researcher’s curiosity has popped up and many multinational companies like Apple, Samsung, IBM, Lockheed Martin, and others use graphene and its derivatives to produce next-generation electronic gadgets.^{275–286} According to British patent consultancy Cambridge IP, China has registered for more than 2,200 patents on GR. The topmost country was followed by the U.S with around 1700 patents that are further accompanied by South Korea with around 1200 patents.^{275,280–283} Besides a lot work on GR, it still has to travel a long way before it approaches commercialization. Some of the GR’s contribution to various fields was summarized in Figure 41.^{285–288} A few very recent and advanced applications of graphene in science and technology are briefly described in the next sections.^{275,285–288}

4.9.1. Nanoelectronics

Nanoelectronics can be defined as the application of nanotechnology in the world of electronic systems. Nanoelectronics is a diverse and avast field that merges electronic devices with mechanical devices, bio-devices, chemical devices, and so on.^{288–290} Nanotechnology is used to build up new components by integrating with electronic components to design better electronic systems

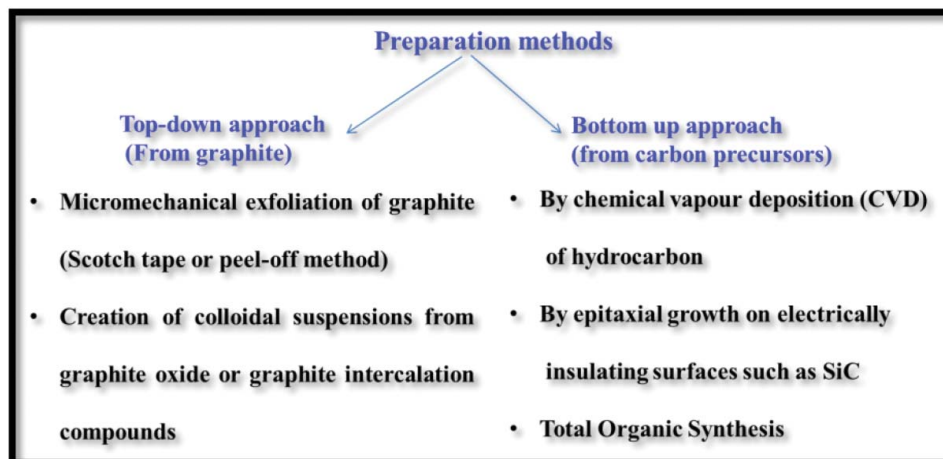


Figure 39. Two important paths for the graphene synthesis and derivatives.

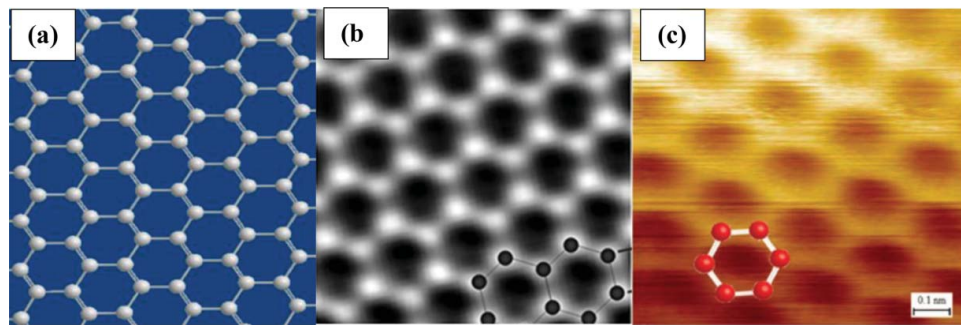


Figure 40. Molecular structure of graphene: (a) high-resolution transmission electron microscope images (HRTEM) of graphene showing its hexagonal honeycomb crystal lattice (© Springer. Reproduced with permission from A. Dato et al.²⁷⁷ Permission to reuse must be obtained from the rightsholder.), (b) and STM image single layers graphene, and (c). (© Royal Society of Chemistry. Reproduced with permission from E. Stolyarova et al.²⁷⁸)

with better work output.^{288–290} Nanoelectronic devices include computers, memory storage, novel optoelectronic devices, displays, quantum computers, radios, etc. GR has extremely high conductive properties and thus it has been exploited in the field of nanoelectronics.^{290,291} It has zero band gap, high surface area, high electron mobility, and many more essential features which contributes to this exclusive property.²⁹¹ In today's world of growing technologies, there is a production of every advanced microchip. Nanotechnology delivers to meet these manufacturing challenges.²⁹¹ Transistor chips, interconnects, and integrated circuits (IC) are some of the common areas where nanoscience have contributed well. Recent studies reveal that GR can serve its use in “interconnects in all computer chips.”^{290–292–294} Interconnects are the electrical pathways that connect transistors and

other circuit components to one another.^{292–294} Interconnects act as an umbilical cord which connects the constituents of IC to the outside world.^{291–294} The copper metal previously used as interconnects with many shortcomings that can be removed only by GR. In the small computer chips, the copper interconnects are also smaller but this increases the resistance of copper and thereby decreasing its conductivity.^{290–296} Whereas in case of GR, there is smooth electron transfer even at room temperature and below leading to less resistance and high conductivity due to its unique band structure.²⁹¹ Use of GR can increase the lifetime of silicon-based integrated circuit technologies.^{291,296} Apart from resistivity improvement in GR, interconnects also have higher electron transfer, greater thermal, mechanical strength, as well as better capacitance.²⁹⁶ Another broad application of GR is in the

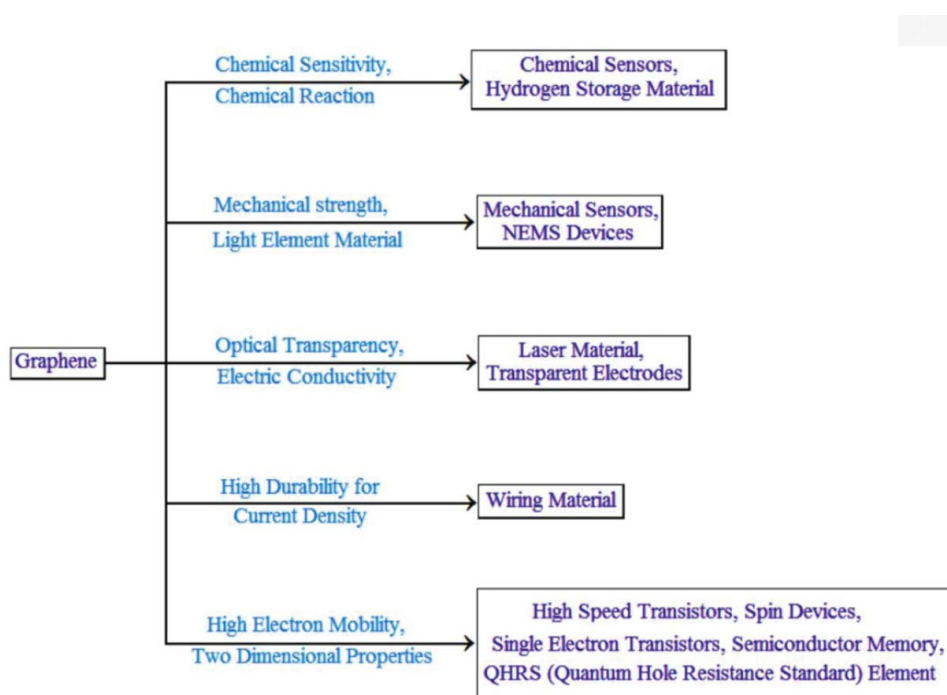


Figure 41. The chart shows a wide range of application of GR in various fields of science and technology.

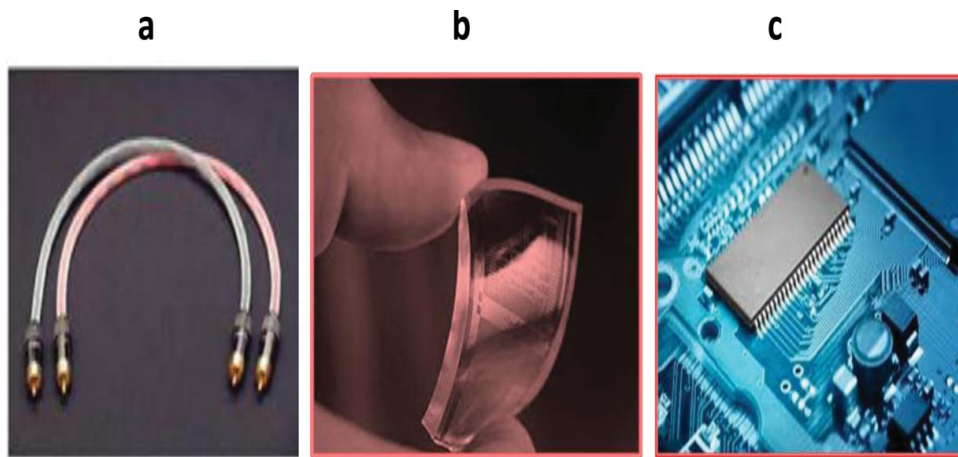


Figure 42. (a) Graphene-based interconnect for electric devices can replace gold and silver based interconnects (b) single sheet of GR used in transistors and, (c) graphene-based microchips in transistor.^{299–301}

transistors.²⁹⁶ It is well known that the transistor is a semiconductor device used in various electronic devices. This is used to amplify and switch electronic signals and electronic devices.^{296,297} The transistor transformed the field of integrated circuit technology, and paved the way for smaller calculators, cheaper radios, computers, among other things. And this the reason transistor is on the list of IEEE milestones in electronics. The huge focus has been made in preparing field-effect transistor (FET).^{297–98} Since the fabrication of IC is very complex, semiconductor plants are very expensive. Making of smaller silicon metal-oxide-semiconductor FETs have become a recent progress in digital logics.²⁹⁸ For high-speed applications, FETs requires short gates and fast carriers in the channel (Figure 42).^{297,298} Scaling theory predicts that FETs with a thin barrier and a small gate-controlled area will be sound toward short-channel impacts down to very short gate lengths.^{296–298} The probability of possessing channels that are just one atomic layer thick is conceivably the most charming characteristic of GR for use in transistors.²⁹⁸

BBC News Science and Environment wrote: “GR transistors in high-performance demonstrations.”²⁹¹ The hope for the “miracle material” GR to fulfill its promise in electronics has received a boost by changing the recipe when cooking it. Optoelectronic devices like touch screen, displays, solar cells, and LEDs all require materials with low sheet resistance and high transparency.^{250,251,264} New research areas now aim to use GR in display screens. The rising cost of indium tin oxide (ITO) used in displays brings GR in the limelight as its substitute.^{288,289} ITO has many disadvantages like it is rare and brittle and, as a result, there is often a risk of breakage, sensitive to the surrounding environment. GR, on the other hand, is very strong, highly transparent, and offers less resistance.^{297,298} Use of GR in photovoltaic

devices (a device that converts light into electricity; see Figure 43) is also a challenge in recent technology. Currently, photovoltaic technology is based on silicon cells with efficiency about 25%. GR can satisfy the various functions in photovoltaic cells like transparent voltage window, photoactive material, a channel for charge transport, and as a catalyst. Organic light-emitting diodes (OLED’s) have electroluminescent layers between charge injecting electrodes, at least one of which is transparent.^{305–307} OLED’s are used to create digital displays like television screens, computer monitors, mobile phones and so on.^{302–305} ITO can act as the transparent electrode having work function 4.4–4.5 eV. But because of various disadvantages of ITO, it is quickly replaced by GR which has a similar work function of 4.5 eV.^{306,307}

Many modifications were made in GR to increase the work function and to offer better results. Tae-Woo Lee and colleagues of the Pohang University of Science and Technology (POSTECH) in Korea developed a way to increase the work function of GR layers to around 6 eV.³⁰⁸ The team also suggested that by lowering the sheet resistance to $30\Omega / \text{sq}$ by doping with chemicals like HNO_3 and AuCl_3 .^{289,308,309} GR absorbs from ultraviolet to terahertz (THz) range.^{308,309} Therefore, GR may be very much useful in photodetectors. Photodetectors are sensors of light or other electromagnetic energy. GR-based photodetectors can work over a broader wavelength. Detection or sensing of light is based on solid state technology devices. The principle of operation of such photodetectors includes:^{289,308,309}

- carrier generation by absorption of an incident photon in a semiconducting layer;
- carrier transport and application if available; and
- extraction of photo-generated carriers as a junction or device current.

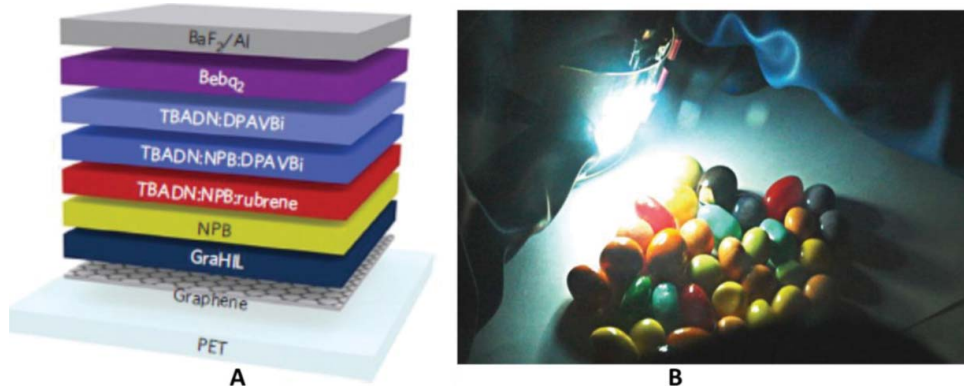


Figure 43. (A) Structure of OLED and (B) highly flexible OLED lighting device with a graphene anode on a 5 cm × 5 cm PET substrate. (© Nature Publishing Group. Reproduced with permission from T. H. Han et al.³⁰⁶ Permission to reuse must be obtained from the rightsholder.)

As GR has zero band gap, it can absorb photons of frequencies ranging from visible to infrared. It is demonstrated theoretically and experimentally that single layer GR absorbs 2.3% of incident light.^{289,308,309} By stacking a few layers, one could increase light absorption in GR. Strong coupling to plasmonic oscillations was also found to enhance the photo response of the GR metal junction detector. GR-based photodetectors offer excellent quantum efficiency fast response and broadband operation.^{302–305} The touchscreen is an electronic visual display that the user can control through simple or multi-touch gestures by touching the screen with one or more fingers.^{302–305} Touch panels are widely used in the smartphones, tablet computers, and in game consoles. GR can be a master material for being used on the touch

screen as it has large surface area, high transparency, and high conductivity.^{302–305} The use of GR can still improve performance and reduce cost. GR-based touch screen is shown in Figure 44.³⁰³

Another use of graphene sheet has been found in the field of ultrafast lasers. A laser is a machine that transmits light by a process of optical amplification based on the stimulated emission of electromagnetic radiation.^{309,303} The production of pulses of radiation in the femtoseconds range (one millionth of a nanosecond, i.e., 10^{-15} of a second) have conquered a new area of investigation.³⁰³ Ultrafast lasers offer pulses shorter than 5 fs that is equal to a couple of oscillations of light. Ultra-short laser pulses accelerate ions and electrons to higher energy for thermonuclear fusion and developing

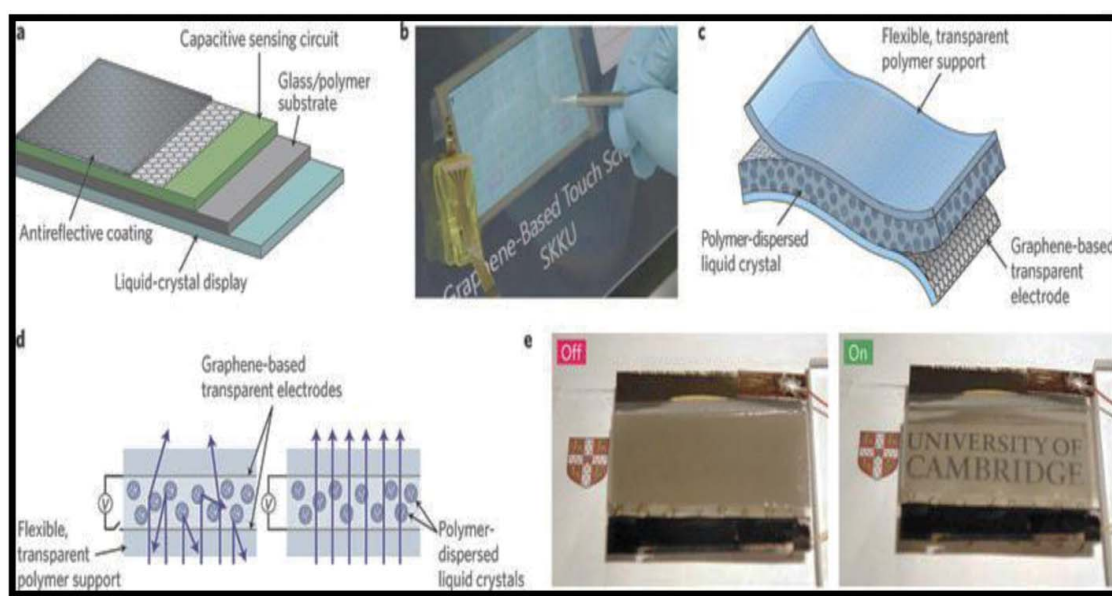


Figure 44. (a) Schematic of a capacitive touch screen; (b) resistive graphene-based touch screen; (c) schematic of a PDLC smart window using a GTCF; (d) with no voltage, the liquid-crystal molecules are not aligned, making the window opaque; and (e) graphene/nano-tube-based smart window in either an off (left) or on (right) state. (© Nature Publishing Group. Reproduced with permission from F. Bonaccorso et al.³⁰³ Permission to reuse must be obtained from the rightsholder.)



compact particle accelerators.^{303–308} Most of the ultra-short lasers works on a mode-locking technique in which a nonlinear optical element turns the continuous laser wave output into ultra-short optical pulses.^{303–308} The nonlinear optical element is known as saturable absorber. GR can be a splendid choice for the saturable absorbers. The gapless linear dispersion of Dirac electrons allows broadband saturable absorption in GR. The optical absorption, ultrafast carrier relaxation time, and controllable modulation depth of GR have been measured. Optical frequency converters are used to expand wavelength accessibilities of lasers.^{303–308} One of the recent and advanced challenges of GR is its use for radio frequency electronics. For radio frequency transistors, the cut-off frequency is the most widely used figure-of-merit to characterize the fundamental speed limit. The cut-off frequency is defined as the frequency at which point the magnitude of the small-signal current gain of the transistor is reduced to the unit.^{303–309}

5. Polymer nanocomposites (PNCs)

Materials always play a vital role fundamentally in our lives in the innovation, creation, and origination of various kinds of novel materials and as a result the quality of our life has greatly been improved over the time. Thus, we can say that without the improvement in the material science and technology, it is not possible to imagine our modern lives. All the most significant breakthroughs in the progression of our civilization are closely linked to the progress in the materials throughout history. For example, the stone age, bronze age, iron age, steel age (industrial revolution), silicon, and silica age (communication revolution), all these reflect that our modern society and everyday activity in the 21st century extensively depends upon the high number of materials to an extent of sophistication. Moreover, the whole world is governed by a customer market directing for development in our lifestyle without limits which finally depends on the creation of new materials. Thus, materials are essential for the technology that makes our lives full of convenience. For instance, the introduction of the laptop, digital cell phones, and touch screens. Hence, the difficulty of designing novel, more utilitarian and different materials increases with the requirements of civilization. The shortcomings for satisfying essential needs such as sustainable energy, affordable personal care, etc. are intimately associated with restrictions on the properties of materials.^{310–321} The most crucial perspective of achieving advanced material with desired and enhanced properties is the creative molecular design and synthesis of new material. This can be accomplished with a deep understanding of molecular physics and nano physics, quantum mechanics,

nanochemistry, and advanced computational techniques. Thus, material science involves the study of the structure and properties of well-known materials and the synthesis and characterization of new or improved and desired materials.^{310–321} The use of advanced computational methods to predict structures and properties of materials that have not still invented. By the existing knowledge of current materials and their modification leads to the formation of a new material with better properties.

Presently, in the verges of material science and technology, the concept of conflating different kinds of materials synergically in suitable experimental conditions is one of the most accessible ways to achieve specific goals with the highest performance in the properties and cost effectiveness. Since it is well known that polymers are used in innumerable applications and fields and are very familiar in tuning the properties or upgrading the performance of polymer systems to obtain an accurate processing and applications. Thus, specific additives are frequently used to alter the polymer properties or to improve the performance of polymer systems. Due to this is the reason the mixing of two or more different materials in a suitable manner leads to the creation of a new material with improved which is widely accepted by the scientific community. In this regard, polymers are one of the most affable and favorably used sources of materials due to their large number of chemical structures. They also have outstanding properties, along with their affordable cost, simple processing, and their utility as sustainable materials.^{270–273} The field of PNCs has expanded to serve one of the largest classes within the reach of materials science. Nowadays, the area of PNCs has grown so rapidly and attains highest position within the scope of material science and become a main branch of nanoscience and nanotechnology, which provides many new materials having numerous and diverse application area.^{260–270}

5.1. Brief history of nanocomposites

The field of composite materials and PNCs is not new;^{310–315} it has been known and utilized for decades, or even centuries.³¹⁰ Nanoparticles were used in the glazes on Ming Dynasty ceramics (1368–1644). Carbon black reinforced rubber is in use since the 1900s as a reinforcing agent in automobile tires which is also a form of nanocomposite.^{311,312} But all these early materials were produced and used without the ability to control their structural, morphological, and physical properties,³¹² and also without a full understanding of what gives nanoparticles their unique properties. But the dawning of modern nanotechnology can be traced to Richard Feynman's Caltech speech, "There's Plenty

of Room at the Bottom.” Feynman described how the laws of physics did not limit the ability to manipulate single atoms and molecules. Instead, it was a lack of the appropriate methods for doing so. Feynman predicted that the “time would come in which atomically precise manipulation of matter would inevitably arrive.” BCC Research Report publishes some milestones in the history of nanocomposites.^{312–318}

- The initial commercial nanocomposites were based on nylon. It was nylon filled with montmorillonite and used for automobile timing belts.
- 1988: Hitachi Metals develops the first nanomagnetic compound, Finemet, used to fabricate low-loss transformers.
- 1998: Inframat LLC patents Nanox 2613 thermal spray, the first commercial ceramic nanocomposite.
- 2005: U.S. National Academies Keck FUTURES initiative awards grant to Yale/University of Texas team to develop nanocomposite solar cells.
- Global uses of the nanocomposites were evaluated 118,768 metric tons with a value of over \$800 million in 2010. In 2011, the market reached 138,389 metric tons and \$920 million. By 2016, the market should amount to 333,043 metric tons and \$2.4 billion, a 5-year compound yearly growth rate (CAGR) of 19.2% in unit terms and 20.9% in value terms.
- Clay nanocomposites estimated for more than 50% of total nanocomposite utilization by value in 2010. Its market share is assumed to rise approximately by 58% in 2016.
- CNT composites deemed for 21% of total nanocomposite consumption in 2010, and this market share is presumed to decrease to 16% in 2016.
- Nylon nanocomposites comprising carbon nanotube fillers have come into frequent, widespread use since the 1990s, especially for applications such as dissipative static components in auto fuel systems as well as for computer read-write heads.
- At present, GR-based PNCs received the highest attention among all others due to the exceptional and excellent properties of GR.

A summary of global consumption of PNCs 2010–2016 [\$ millions] is graphically presented in Figure 45.

Before describing the PNCs in details, it will be more fruitful if we made a conclusive consideration on what is composite. Because PNCs are engineered form of composites. Therefore, a fundamental information about composite materials will be helpful for better understanding of PNCs science.^{312–318} In simple words, we can say that a naturally occurring or synthetic materials which constituent two or more components with significantly different but acclimate

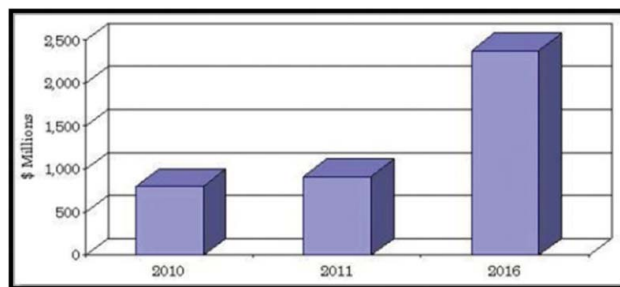


Figure 45. A graphical representation for global consumption of PNCs from 2010–2016. (Source: BCC Research.)³¹⁸

physical or chemical properties which remain separate and distinct from the macroscopic/microscopic scale within the finished material called composite (Figure 46).^{317,318}

PNCs belong to the class of multi-phase systems like foams blends composites, etc. and may be defined as the “combination of a polymer matrix and additives that have at least one dimension in the nanometer range.”^{317,318} The additives may be in 1D, 2D, or 3D forms such as CNTs, GR, or layered clay minerals sheets and various spherical particles. In other words, we can say that PNCs always consisting of two or more components and, generally, the component used in small amounts called filler and the elements that are relatively in larger number called matrix thus mixing of filler and matrix in a suitable manner gives a hybrid material which completely or partially distinct from parental components (Figure 47).^{320–323} In a better way we can say that an actual PNCs should be a new hybrid material in which the nanometer scale (up to 200 nm) component or structure gives rise to many new physical and chemical properties, which are not present in the pure elements (parental components).^{321,322}

In this way, area of PNCs is an exciting branch of Polymer nanoscience and material science which involves the study and application of nanoscience to polymer-nanoparticles matrices.³²¹ Previously, PNCs are associated with plastics and related material production, but at present the term PNCs is very much widely used to describe a very broad spectrum of materials.³²⁴ For example, it is well evident that polystyrene is potentially very useful in the various industries of all.^{324,325} Today, most common use of polyester is to make the plastic bottles that can store our much-beloved beverages, but it has been proved that CNTs-based polystyrene nanocomposite are much better than pure polystyrene fibers.^{321,324,325} This latter definition commands that the nanostructure has dimensions smaller than an average scale that holds a physical property of the material.^{324,325}

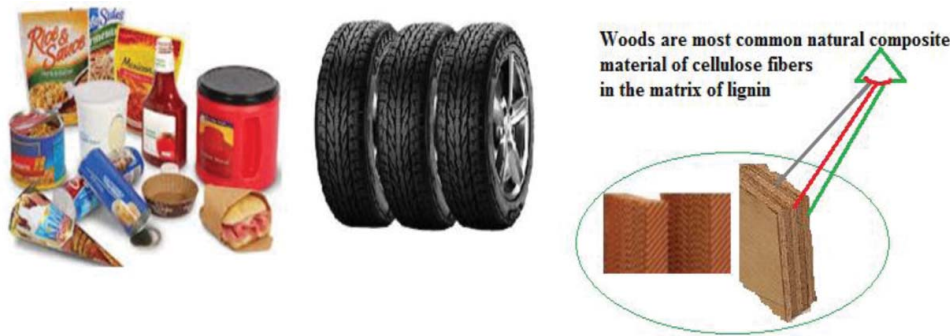


Figure 46. Conventional and modern composite materials.

5.2. Types of PNCs

PNCs have been classified into several categories on the basis of different parameters such as on the basis of the nature of fillers, matrix, preparation method, etc. The most common classification of PNCs based on the nature of forms is given below.³²¹

5.2.1. Ceramic-matrix nanocomposites

In this type of nanocomposite ceramic compounds (chemical compound from the group of oxides, nitrides, borides, silicides, etc.) function as matrix and various types of metals as fillers, fully dispersed each other in order to draw out the particular nanoscopic properties.³²⁶ Thus, a significant part of the total volume of such composites is occupied by ceramics and metals used in very minute amount.^{326,327} Nanocomposites from these groups were confirmed in promoting their magnetic,

electrical, mechanical, and optical properties as well as tribological corrosion-resistance and other protective characteristics. It is observed that in most of the ceramic matrix type nanocomposites, the property reinforcement mainly depends on the ratio of ceramic moiety and filler (mostly metals), nature of filler and matrix and also on path of synthesis.³²⁸

5.2.2. Metal-matrix nanocomposites

In this, metallic component behaves as a matrix and some nanomaterials such as CNTs, graphite or fullerene, etc. as the fillers. These kinds of nanocomposites are renowned for their mechanical reinforcements.^{173–175,329} For instance, CNTs metal matrix composites are emerged as exotic composite material because of its outstanding tensile strength and excellent electrical conductivity.^{173–175,330} This is mainly because of very high surface area, good conductivity, and mechanical

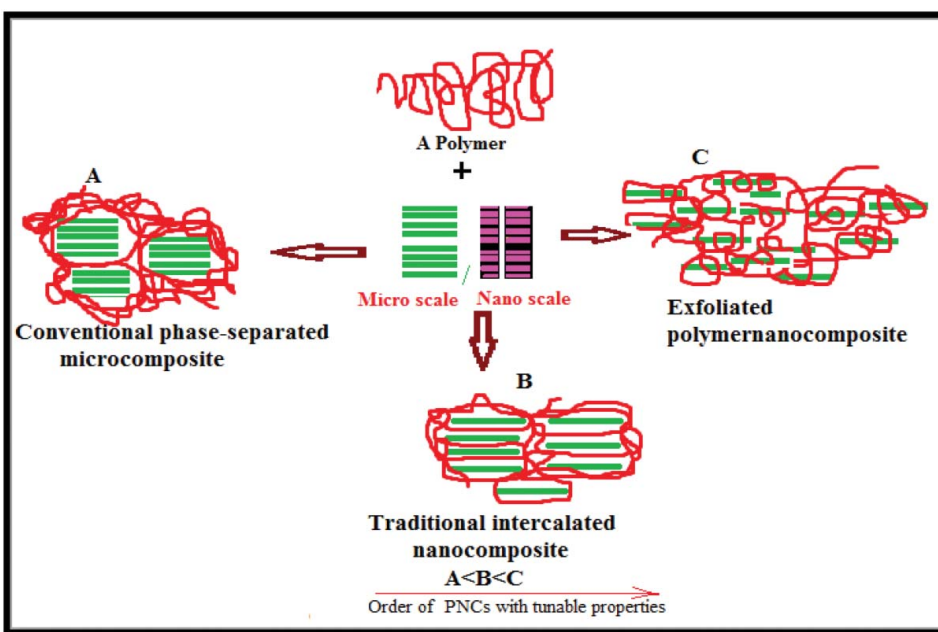


Figure 47. Schematic representation of extent of interaction of fillers with the matrix.

properties of nanotubes. One major issue commonly arises in the synthesis of such type of nanocomposites is the proper dispersion of CNTs and its desired functionalization.^{331,332,173–175}

5.2.3. Polymer-matrix nanocomposites

At present in the field of nanocomposite and materials science, PNCs have grown so rapidly and attained the highest position within the scope of material science and become a main branch of nanoscience and nanotechnology providing many new materials with numerous and diverse application area.^{312–318,335–337} Due to the addition of specific nano filler in the polymers, matrix gives polymer matrix nanocomposites. So category of PNCs is very common and widely accepted by material scientist because of the greatest tuning possibilities.^{318,335–337} The proper distribution of filler or regulated nanostructures in the composite can inject many outstanding physical properties and novel behaviors which are missing in the typical polymers.^{337,338} Thus, the nano-filters very effectively change the nature of the original matrix.^{338–340}

5.3. Graphene-based PNCs: Status and prospects

As previously mentioned, that GR is a mono atomically thick (2 nm) exotic material with sp^2 hybridized carbon atom and honeycombs lattice.^{3,191–193,361–362} Many methods have been developed after Andre Konstantin Geim's Scotch Tape method of GR synthesis with different properties according to need.^{3,191–193} Some of them are a lithographic method, CVD method, from graphite oxide, growth on crystalline silicon carbide, and highly oriented paralytic graphite process, and so on.^{3,11,63,183} It is notable that uniqueness and different application of GR only depend on the number of layers (i.e., the thickness).^{3,11} So, we can say that the main bottleneck in the desired

property of GR is the depth and extent of planarity of honeycombs lattice.^{3,11,63,183} Some very fine microscopic images of few layers GR (FLG) are shown in Figure 48.³⁴²

Many research groups extensively working on GR based PNCs and they have found GR as an outstanding nanofiller and much superior than the conventional nanofillers (including graphite, clay, CNTs, etc.). Polymer chemist and material scientists have a high expectation from GR for desired reinforcement in properties of PNCs.^{186,333–337} Such a huge interest in GR is due to its intrinsic properties, and they are only dependent on the nature of the material.¹⁸⁶ According to the theoretical prediction, ultra-pure single layer GR could have an intrinsic tensile strength higher than that of any other known material.¹⁸⁶ Some groundbreaking investigation have proved that single-layer GR membrane is impermeable to most of the standard gasses, including He.^{186,343} These extraordinary properties of GR provide many practical application opportunities for GR sealed micro-chambers.^{186,343,344} So there is much uniqueness in the GR, which makes it ultimate and shining candidate among the nano-filters that already have been mentioned in the previous section. In addition to original GR another twisted form of GR called GNRs produced via CVD, lithographic methods, by unzipping CNTs using plasma etching route in gas phase, have also been used as nano filler found to be superior than other various CNTs (SWCNTs or MWCNTs).^{186,345,346} Because of many superlative properties, just like easier functionalization, very high contact surface area, and geometrical properties, etc. These characteristics of GNRs are very useful which makes the maximum possible contact of fillers with the polymer matrix.^{186,345,346} Thus, many outstanding properties in a single nanomaterial have made the whole scientific community very curious about graphene. Even though commercial bulk production of

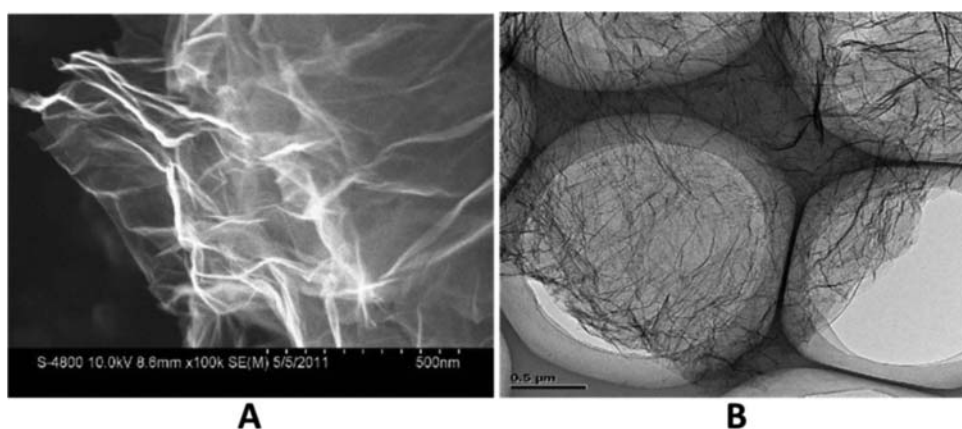


Figure 48. SEM (A) and TEM (B) image of ACS material-industrial-quality GR. (© Advanced Chemicals Suppliers. Reproduced with permission from ACS Material.³⁴² Permission to reuse must be obtained from the rightholder.)

graphene is still under investigation, its application in the field of polymer nanocomposite has been already explored for the fabrication of superior polymer nanocomposite.^{186,347–349} Numerous application of GR is well established among them use of GR as nanofiller in production of industrially important PNCs is now real time application. This is the main reason GR, and its derivatives production output has increased to 100 tons per annum.^{186,347–349} Based on our recent studies it seems the commercial production of GR nanoplatelet is expected to exceed 200 tons per year within the next two years, and reports also indicate that most of them will be used in polymer and material science.^{186,350}

5.3.1. Methods for GR-based nanocomposites preparation

Three synthetic route ways have mainly used for GR based PNCs preparation (Figure 49).^{16,186,330} All these methods had their advantage and disadvantage and employed according to a particular need. The utilization of these methods depends on the molecular weight, polarity, hydrophobicity, functional groups, and physical interaction and present in the GR, polymer, and solvent.^{16,186,330}

In-situ polymerization. Various *in-situ* reactions are well known in organic and inorganic chemistry, and such reactions are done because of the high reactivity of intermediate cannot be isolated, or simply due to convenience.^{16,186,330} In the case of GR-based PNCs, *in-situ* Intercalated Polymerization reveals polymerization of pure monomer along with the GR or GR derivatives in the solution phase.^{330,351} A suitable initiator is used, and the polymerization reaction is initiated either by radiation or heat.^{352–353} This method is very much useful and accessible for the two types of GR-based PNCs system exhibiting covalent bonding and system without any bonding.^{353,354} However, in the case of covalent interaction novel properties of the reinforcement is better. In this, a chemical encapsulation is involved which is very much similar to interfacial coating. The synthesis outline has been depicted in Figure 50. In an *in-situ* polymerization, no reactants are required in the core

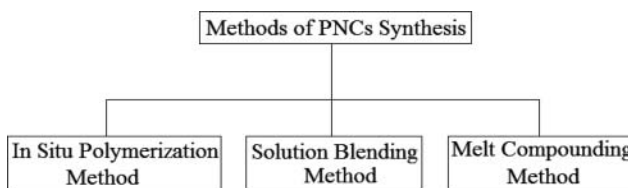


Figure 49. Common methods for GR-based PNCs preparation.

materials and, as a result, the polymerization process follows the constant phase on both sides of the interface.^{354,355} An enormous number of GR-based PNCs have been synthesized by this method. For instance, polymethylmethacrylate (PMMA) expanded graphite, polyethylene terephthalate (PET) LDH polystyrene sulfonate (PSS) - GR, etc.^{355,356}

Solution blending method. This is another important method for PNCs synthesis, but this is not as popular as *in-situ* polymerization and melts compounding method.^{352,356} In this method, two or more polymers (matrix) and nano-filler are mixed in a suitable solvent at the required temperature and then with the help of stirring mixed homogeneously.^{357,358} This method of PNCs preparation mostly employed for nanocomposite of conducting and insulating polymers.^{359–361} In this process, first both polymers are dissolved in the common solvent and then casted in the form of film. Some Polyaniline (PANI) and GR/CNTs, polypyrrole (PPY)-clay-based nanocomposites are reported.^{351–353}

Melt compounding method. This is the most common method for production of blend nanocomposites.³⁵⁶ It involves the mixing of two or more polymers or mixing of polymer matrix and filler with the help of extruder below the melting point of the mixing components.^{356,361} This method used for the production of polymer blends at industrial scale. Melt compounding method is equally applicable for compatible and non-compatible mixing.^{361,362} A schematic diagram of an extruder is shown in Figure 51.

5.3.2. Some examples of recently reported GR-based PNCs

The number of polymer nanocomposites has been synthesized using GR and their derivatives, some of them are pointed below.

1. A poly (3,4-ethyldioxythiophene)[PEDOT]/sulphonated GR composite synthesized by *in situ* polymerization.^{341,363} The resultant composite showed outstanding transparency, splendid electrical conductivity, excellent flexibility, as well as high thermal stability and was quickly processed in both organic and aqueous solvents.³⁶³ The conductivity of PEDOT/GR film deposited on PMMA is greater than that of deposited on quartz.³⁶³ The PEDOT/GR composites have high thermal stability and show little mass loss below 297°C and 19% loss below 325°C. The PEDOT/GR composite is

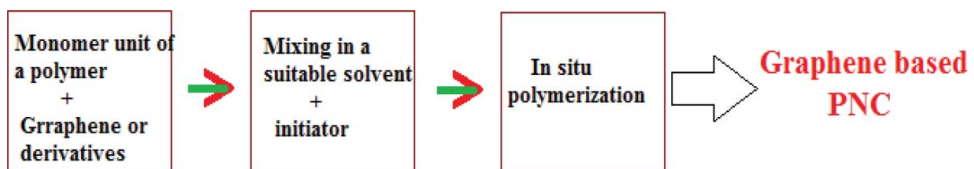


Figure 50. Synthesis outline for the *in-situ* polymerization of graphene-based PNCs.

- thermally more stable than that of PEDOT/PSS composite.^{341,363}
- Epoxy/GR polymer composites were prepared by using *in-situ* polymerization method, and their electromagnetic interference (EMI) shielding was examined.^{16,333} Over the entire frequency range, the EMI shielding effectiveness increased with increasing GR loading.¹⁶ Thus, epoxy/GR composites can be used as practical, lightweight shielding materials for electromagnetic radiation.^{16,334} Graphene oxide (GO) sheet-incorporated epoxy composites were prepared, and thermal expansion was examined by a thermo-mechanical analyzer. The epoxy resin showed poor thermal conductivity, but the inclusion of GR sheets showed a significant improvement. A 5 wt. % GO filled epoxy resin showed four times higher thermal conductivity than that of the neat epoxy resin.³³⁴ Thus, GR composites are promising thermal interface material for heat dissipation.^{334,364}
 - PVA/GR polymer nanocomposites were obtained by incorporating GO as nano filler into the PVA matrix using water as the solvent.^{16,343,365} The mechanical performance of PVA/GR polymer nanocomposite was found much superior to that of pure PVA.^{16,343,365} It is due to the molecular level dispersion of GR sheets in the PVA matrix because of H-bonding between GR and PVA.^{365,366} Zhao

and co-worker prepared thoroughly exfoliated GR nanosheets/PVA nanocomposites using a facial aqueous solution.³⁶⁶ The synthesized nanocomposites showed an improved mechanical behavior and tensile strength after the incorporation of GR nanosheets into the PVA matrix. Wang et al.^{16,365,366} prepared PET/GR polymer nanocomposites using melt compounding method.^{366–368} The electrical conductivity of PET/GR composites increased rapidly with an increase in GR content.^{16,365,366}

- PC/graphite and PC/functionalize GR sheets (FGS) polymer nanocomposites were prepared by melt compounding method.^{369,370} They have found that the tensile modulus of the PC/FGS nano-composites were higher than that of the virgin PC. The electrical conductivity of PC/FGS was superior to that of PC/graphite nanocomposite.³⁷⁰
- PANI/GR composite (GPC) was prepared by the *in-situ* anodic electropolymerization (AEP) of aniline on GR paper.^{16,371} The polymerization was carried out using a three-electrode anodic electro-polymerization cell.^{336,371} In this process, a Pt plate, standard calomel electrode (SCE), and GR paper were used as the counter, reference, and working electrode respectively. 0.05 M aniline and 0.5 M sulphuric acid were used as the electrolyte.^{336,351,371} PANI was electropolymerized via *in-situ* approach

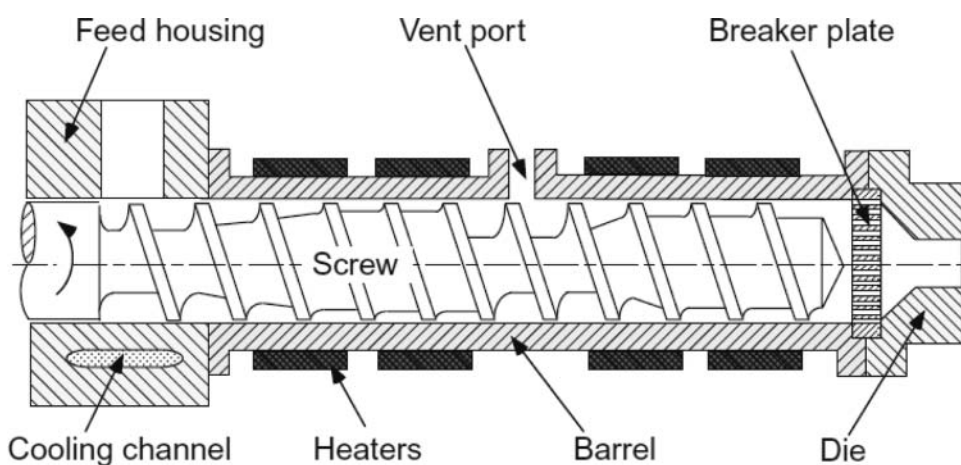


Figure 51. Schematic representation of extruder used in melts compounding method. (© Hanser Publishers. Reproduced with permission from C. Rauwendaal.³⁶² Permission to reuse must be obtained from the rightsholder.)

- on the GR paper at a constant potential of 0.75 V for different periods.^{336,351,371} Wang et al. prepared a high performing GPC electrode using a spin coating method.^{16,372–373} An aqueous dispersion of purified GO film was deposited on a quartz substrate employing a deep coating method accompanied by thermal reduction to obtain GR film. A dark blue solution of PANI in an n-methyl pyrrolidone (NMP) was then spin coated on GR films. The GPC electrode is more suitable for designing electrochromic devices as compared to other materials.^{372,373} The PANI/GR nanosheets/CNTs (PANI/GNS/CNT) nanocomposite was prepared by *in-situ* polymerization.³⁵³ The working electrode was fabricated by mixing electroactive materials, carbon black and polytetrafluoroethylene (PTFE) in ethanol.^{344,353,372} The resulting mixture was then coated onto a nickel substrate with a spatula followed by drying in an oven. The particular capacitance of the PANI/GNS/CNTs composites was much higher than that of pure PANI and PANI/CNTs nanocomposites.^{344,353,372} The long-term cycle stability of the PANI/GNS/CNTs nanocomposites was superior to that of the PANI/CNTs and PANI/GR nanosheet nanocomposites.^{345,353} It was observed that after 100 cycles, the capacitance of the PANI/GNS/CNTs composites lowered by only 6% of the initial capacitance compared to the 52% and 67% reduction observed for the PANI/GR nanosheet and PANI/CNTs composites.^{344–346} Chemically modified GR and PANI nanofiber composites were prepared by *in-situ* polymerization of aniline monomer in the presence of GO in the acidic medium.^{373,374} The resulting PANI/GO composites were reduced to a GR composite by hydrazine monohydrate followed by re-oxidation and re-protonation of the reduced PANI to give PANI/GR nanocomposite.^{344–346,373,374} The conductivity of the PANI/GR nanocomposites (168.7 Sm-1) was slightly lower than that of PANI/GO composites (231.2 Sm-1), reasonably due to a reduction in the level of doping in PANI and a variation in the morphology of the composites during the reduction, re-oxidation, and re-protonation process.^{344–346,373,374}
6. Lee and co-worker synthesized water-borne polyurethane (WPU)/functionalized GR sheet (FGS) nanocomposites by *in-situ* polymerization.³⁷⁵ The electrical conductivity of the nanocomposite was increased 105–106-fold compare to pure WPU due to the homogeneous dispersion of FGS particles in WPU matrix.³⁷⁵ The presence of FGS also increased the melting temperature and heat of

fusion of the soft segment of WPU in the nanocomposites. Liang et al. prepared three types of PNCs by solution mixing process.^{375,376} They used isocyanate modified GR, sulfonated GR, and reduced GR as nano-filler and thermoplastic polyurethane (TPU) as the matrix polymer.³⁷⁷ The extent of thermal degradation of TPU/isocyanate modified GR nano-composite is much higher than that of TPU/sulfonated GR and TPU/reduced GR PNCs.^{16,183,377}

7. PVDF/functionalized GR sheet (FGS) nanocomposites were prepared from GO and expanded graphite (EG) by solution processing and compression molding.^{16,378} The thermal behavior of PVDF/FGS nanocomposite was found to be greater than that of nanocomposite based on PVDF/EG. The mechanical characteristics of both the composites are higher than the pure PVDF.^{16,378}
8. Tris (2, 21-bipyridyl)ruthenium (II) [Ru(bpy)₃]2P/nafion/GR modified electrodes were prepared by the solution mixing of GR and nafion.³⁷⁹ The resulting electrode was immersed in 1 M [Ru(bpy)₃]2P solution to get modified electrode. The modified electrode exhibited excellent sensitivity, selectivity, and stability.³⁷⁹

5.3.3. GR-CNTs hybrid PNCs

CNTs and GR are relatively new allotropes of carbon with 1D and 2D nanostructure (as mentioned above).^{380,381} These have attracted a considerable attention of scientific community over last two decades due to their unique structural and functional properties and have potentially a broad range of applications.³⁸⁰ GR, a monatomic layer of carbon hexagons, can be stacked into graphite or rolled up into cylindrical CNTs. Both are mutually complementary to each other regarding structure and properties and yet share many common properties such as electrical conductivity and ultrahigh mechanical strength but also they have their shortcoming.^{380–383} However, hybrid nanocomposites of CNTs and GR with polymer matrix show excellent stretching ability and flexibility and is supposed to have electrical conductivity and thermal diffusion in all directions uniformly.³⁸⁰ Also to this it is observed that irreversible agglomeration of GR due to Van der Waals interaction is found to be suppressed in the presence of CNTs.^{380,383,384} Shin and coworker fabricated PVA tough fibers based nanocomposite using reduced GO and single-walled CNTs in the solution phase.^{380,383,384} They reported that fabricated fibers exhibit the toughness in the range of 490–970 Jg⁻¹, which indicates excellent mechanical properties.^{384–385} They also explain that such a synergistic toughness enhancement in the

nanocomposite arises due to the optimal combination of reduced GO and SWNTs (ratio 1:1), and no synergistic toughness increase was observed if the ratio of CNTs and GR has changed. It is ultimate because of suitable self-alignment nano-fillers.^{16,334,384}

5.3.4. Distribution, dispersion, and interaction between GR derivatives and polymer

Hybridization and proper coordination between nanomaterials (Fullerenes, GR, CNTs, and GNRs) and polymers has led to the production of composites with excellent electrical and mechanical properties for various newer applications.^{388,389} It happens because of the high surface area, of nano fillers tend to agglomerate and stick to each other, forming micro particles.³⁸⁸ Therefore, distribution and dispersion of these nano filler into individual particles throughout the polymer matrix, mainly the molecular level dispersion, and homogeneous distribution is one of the most important and property determining steps.^{388–390} In this way, aggregation and agglomeration are even more severe for anisotropic nanoparticles mainly for the nano-sheets and nanotubes due to the very high interparticle interaction.³⁸⁸ However, very interestingly, newly discovered graphene and its derivatives as fillers for polymeric materials have opened a new era of nanocomposites.^{388,390–393} Notably, amazing improvements in physical, mechanical properties, and chemical stability of polymer have been reported on a very minute loading of graphene and its derivatives.^{393,394} But due to stacking and restacking process in the case graphene sheets and derivatives similar to other layered nano-fillers (because of the high aspect ratio and strong interparticle interaction), sometimes actual properties of composites hampered.^{388,393,394} To avoid such shortcomings, polymer chemists and materials scientist have selected chemically derived graphene which is available very easily as single layer dispersion in liquids, retaining the single layer state of graphene sheet in polymer media is not easy.³⁹⁵ Such graphene and derivatives is often synthesized by oxidizing graphite powder to graphite oxide using strong oxidizing agents^{173–175} with a highly hydrophilic sheet-like structure, which is then proper exfoliated into the graphene oxide (GO) in a suitable polar solvents, possibly by mechanical shearing.^{388,395} Due the numerous hydrophilic moieties on GO, it is not easily dispersed in nonpolar organic and weakly polar solvents, and polymers matrixes.^{16,388} Several trials have been made by different workers to disperse chemically synthesized graphene in nonpolar organic and weakly polar organic media by specific functionalization of GO.^{395,397,398} However, employing aqueous dispersion of GO to obtain graphene based polymer nanocomposite is more attractive, cheaper, and time efficient. Since GO and functionalization graphene can be easily combined

with the water-soluble polymers and then reduced to rGO without using organic solvents or tedious chemical functionalization.^{16,395,398} In addition to this colloidal polymer, matrixes may be mixed directly with GO to incorporate graphene into water insoluble polymers.^{388,395} Many recent study shows GO, and functionalized graphene can be employed as a surfactant in emulsion polymerization to produce graphene-based nanomaterials.³⁸⁸ Thus, an important strategy for cheaper and environmental friendly experiment, to use an aqueous dispersion of GO and functionalized graphene to synthesis different kind of graphene- and derivatives-based nanocomposites. Recently, some workers have used the epoxy-functionalized GO to address the various challenges of well dispersing graphene sheets in a thermoset resin and show the success of the proposed strategy.^{388,395} Fabrication of epoxy composites with graphene, GO, and functionalized graphene is mostly performed via two pathways.^{395,398} First, stepwise chemical functionalization of graphene and its derivatives, then the removal of solvent from the mixture of epoxy and graphite. Second, dispersion of graphene sheet with non-solvents such as ethanol and acetone.^{388,395}

Direct mixing of reduced graphene powder in the different epoxy compounds mostly gives in poor dispersion and heterogeneous distribution of nano-fillers.^{388,395} It is reported that even on strong ultrasonication of graphene sheets in a non-polar solvent for an extended period it does not guarantee a good distribution especially in the case higher loading of graphene sheets.^{16,388,395} In contrast, chemically derived GO nanosheets easily restock during drying or on heating above the room temperature. And result formation of a layered material consisting of GO sheets that are very strongly bonded together by hydrogen bonding.^{15–17,388} Moreover, it has also been reported that for the good dispersion, we need to ensure good GO-matrix bonding, consequently superior mechanical properties.^{15–17,388,395} Similarly, a novel and single-step method to functionalize and disperse GOES nanosheets in epoxy and obtain high-performance nanocomposites by achieving a high degree of dispersion and good bonding to the matrix.^{15–17,388,395} Although graphite oxide was synthesized long ago, its exact molecular structure is not well known.^{15–17,388,395} Such betterment in dispersion of GO and functionalized GR is due to the presence of epoxy groups because as they facilitate the GO and functionalization GR, compared to other groups such as the carboxyl group which needs activation in the absence of water.^{15–17,395} In the many cases, amines and derivatives have exclusively been used for the functionalization GR and GO and molecular interaction, as

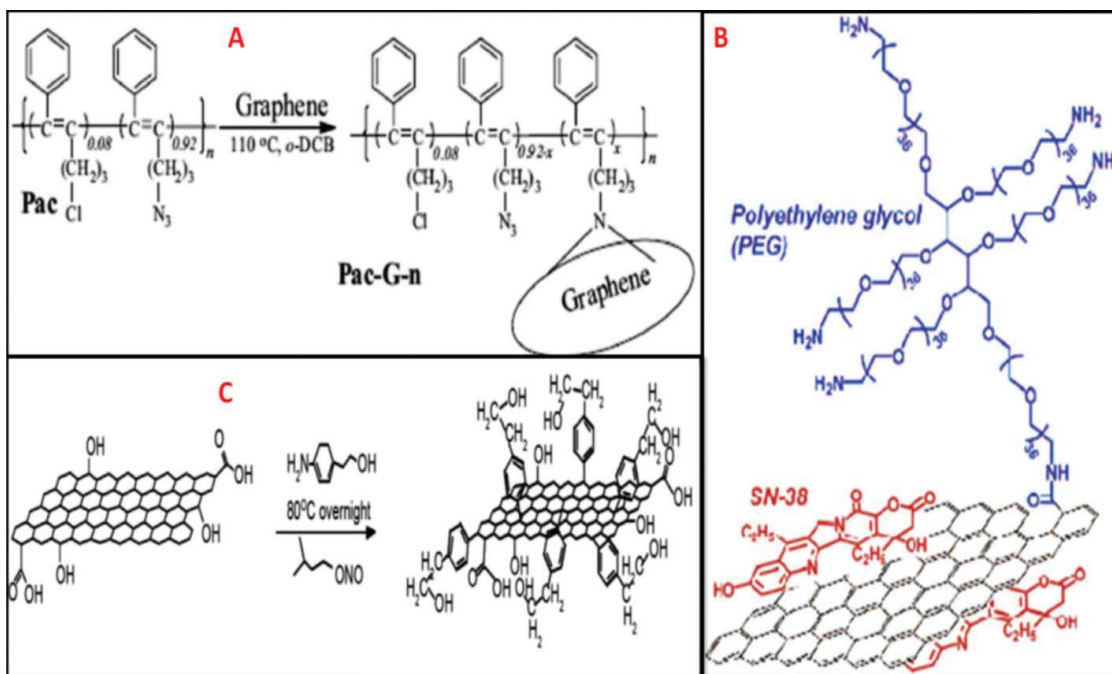


Figure 52. (A) Synthetic route of polyacetylene-graphene composites using nitrene as activator for the proper dispersion. (B) Schematic presentation of interactions between polyethylene glycol and activated graphene sheet (using SN-38). (C) Activation step for good dispersion of graphene nanosheets for polystyrene functionalized graphene nanosheets. (© Elsevier. Reproduced with permission from R. K. Layek and A. K. Nandi³⁸⁸ Permission to reuse must be obtained from the rightsholder.)

shown in Figure 52. Such reaction to produce graphene-based PNCs is mostly carried out in aqueous media or polar and the ambient atmosphere without using any catalyst. These reactions are relatively fast and highly productive, due to the high reactivity of amine and epoxy functional groups.^{16,388,395} These experimental conditions for the reaction serve for the two simultaneous purposes of accommodating graphene sheets at the molecular level and furnishing the interfacial bonding with the matrix that are highly desirable. Higher dispersion and proper homogeneous distribution of nano fillers mean larger area per volume and better bonding between the filler and polymer matrix to improve various physical and mechanical properties.^{16,388,395} The most commonly adopted structural modification and activation of graphene and derivatives for its homogeneous distribution and proper dispersion in the polymer matrixes is diagrammatically shown in Figure 52.³⁸⁸

In summary, regarding the proper dispersion of GR and derivatives in the different polymer functionalization method and type (covalent, non-covalent, Pi-Pi interactions hydrogen bonding or other polar interactions) of interaction between polymer and graphene plays very vital role.^{388,396,400} And an important factor in deciding reinforcement quantity and quality of synthesized nanocomposites.

5.3.5. Other GR-based polymer composites

Poly (*e*-caprolactone) (PCL)-GO composite was prepared using *in-situ* polymerization.⁴⁰¹ The resulting nanocomposite shows excellent mechanical properties and robustness under bending. Poly (lactic acid) (PLA)/GR PNCs were prepared using a response surface method that showed that GR loading had a significant effect on tensile strength.^{402–403} Liu and co-worker fabricated GO reinforced epoxy resin nanocomposite by transferring GO from water to acetone.⁴⁰³ Incorporation of “1 wt% of GO showed a significant improvement in flexural strength, flexural modulus, impact strength and storage modulus.^{404–407} Many groups have synthesized excellent nanocomposites using polymethyl methacrylate (PMMA) and with other polymers with graphene and its derivatives as nanofiller (with different percentage GR and derivatives) by *in-situ* polymerization. Liang and coworker fabricated polydiacetylene/GR nanocomposite by solution processing route and reported that nanocomposite showed excellent actuation character with controllable motion, fast response rate, and high-frequency resonance.^{404–407} Polyphenylene sulfide (PPS)/GR composite was prepared by spraying method. The resulting nanocomposite had seven times higher wear life than that of neat PPS.⁴⁰⁸ Along the same line, Pan and co-worker prepared polyamide/GR coatings by spraying method.^{408,409} They observed that the wear life of the composite coating was higher than that of neat

polyamide 11 coating.^{16,388} Pang and his co-workers reported a novel conductive ultrahigh-molecular-weight polyethylene composite with a segregated and double percolated structure containing high-density polyethylene (HDPE) as carrier polymer for GNS.⁴¹⁰

5.4. Applications and importance of GR-based polymer nanocomposites

Because of GR's unique physical properties, it is treated as one of the most promising candidates for filling agent for nanocomposite applications in comparison to conventional nanofillers.^{16,388} GR/derivatives based nanocomposites show extensive enhancements in their properties, compared to conventional composites.^{388,410–415} GR as nanofiller not only makes the material lighter with very simple processing, but it also makes the composites too much stronger for desired multifunctional applications. Some very interesting statistical data regarding the GR-based PNCs graphically represented in Figures 53–55 (on the basis of Scopus database, analysis result generated on 10/09/015 and Google Scholar).^{410–418}

As we know, the unique properties of GR are responsible for improving the physicochemical qualities of the matrix material upon distribution.^{3,16,388,395} This helps in strengthening and increasing the interfacial interaction between the layers of GR (filler) and matrix (host), i.e., bonding between filler and matrix responsible for reinforcement in the properties of nanocomposites.^{3,16,388,395,414–422} It is important to add that computational calculations, and theoretical

analysis of nanocomposite plays a crucial role in understanding molecular interactions, mechanisms of filler distribution, physical properties and their potential applications.⁴¹⁷ Some simulation software's were developed to provide a cumulative or specific result for the nanocomposites.⁴¹⁷ Since the discovery of GR much excellent research article and review on GR-based PNCs have been published.^{415–422} For instance, Hansama co-worker successfully prepared a stable, low density, lightweight and damage resistance GR-based nanocomposites.⁴²³ Mack and colleagues synthesized nanocomposites of polyacrylonitrile [PAN] nanofibers strengthened by GNP, in which they have proved improved mechanical qualities.^{414,423} Ramanaathan and members reported an exceptional shift in the glass transition temperature of a PNCs with functionalized GR as nano-filler and they observed that, on the addition of functionalized GR 1 wt% to the Polyacrylonitrile (PAN), of the composite material increased by 40°C, but in the case of 0.5 wt% to polymethyl methacrylate (PMMA), they observed a 30°C rise.^{343,388} Das and coworker have fabricated PVA, PMMA nanocomposite using nanoindentation technology, and they reported a notable improvement in crystallinity, elastic modulus, and hardness due to the addition of only 0.06 wt% of GR.^{16,388,424} They suggested that the dramatic reinforcement was due to the suitable interaction between the matrix and the layers of nano-filler.^{420–424} In 2007, Yu research group reported that epoxy-based FLG nanocomposites show fantastic utilizable properties for the electronics industry, which was related to the development of

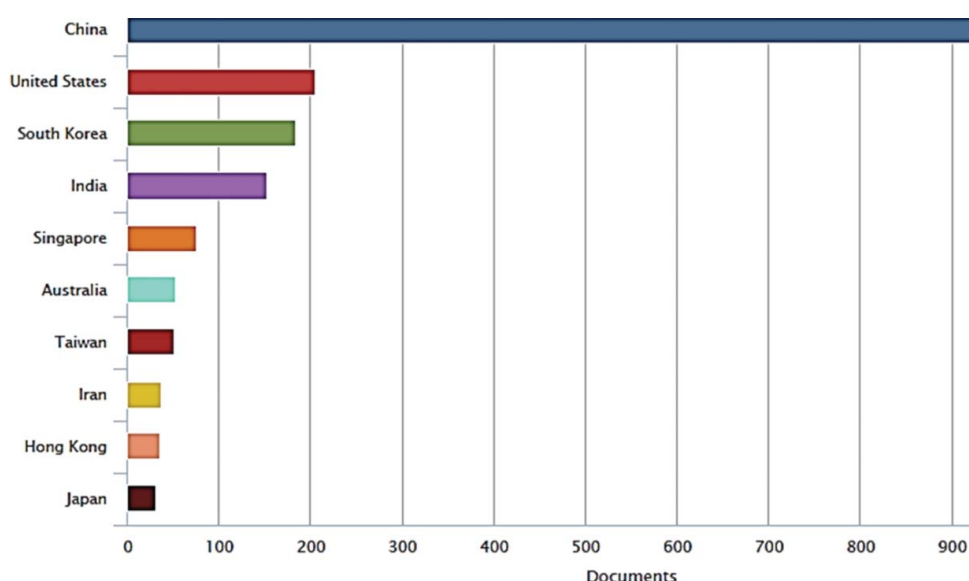


Figure 53. The total number of documents published in Scopus index from 2004–2015 related to graphene-based polymer nanocomposites and contribution of top ten countries (total articles 1842: on the basis of Scopus database, analysis result generated 10/09/15).

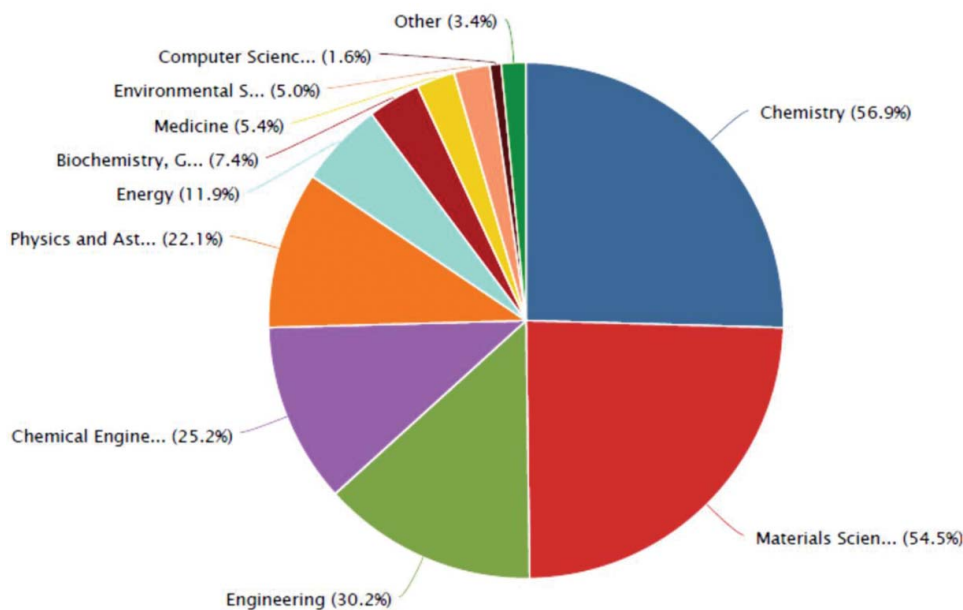


Figure 54. Types of articles published in Scopus index related to graphene-based nanocomposites and its utility in the different subject (on the basis of Scopus database, analysis result generated 10/09/15).

thermal-interface-based materials.³⁴⁶ Both research group successfully prepared from robust 100 μm thick macroscopic GR membranes that can bear massive loads.^{16,388,417–424} The introduction of metal nanoparticles of the matrix along with GR has attracted a lot of researchers due to the advantage it provides by facilitating an improved inter-particle contact shown schematically in Figure 56.^{16,388,417–424}

In 2008, Chen's research group fabricated GR-based electrically conducting paper, along with high mechanical strength and biocompatible.^{373,425–428} They uniformly dispersed GR in a solution using vacuum filtration followed by the thermal annealing and

then they prepared carbon-coated SnO₂-GR sheet composites via the single-pot hydrothermal route.^{336,351,371–373} They utilized synthesized GR-based PNCs as an anode material for Li-ion rechargeable battery, and it exhibited magnificent storage capacity and improved cyclic performance.^{371–373} In 2013, following similar guidelines, Perera's research group prepared V₂O₅ nanowire-GR nanocomposite as an electrode material and they reported that composite electrode exhibited an equilibrated electric double layer energy density of 38.8 Wh kg⁻¹, and pseudocapacitance at a power density of 455 W kg⁻¹, high specific capacitance of 80 F g⁻¹.^{336,351} These results transparently indicate that the composite electrode was capable of sufficient storage and deliverance of charges toward high energy applications especially for ultra-capacitors. Water-dispersed GR/tryptophan/PVA composite material synthesized by Guo research group in 2011 to improve tensile strength, modulus, and thermal stability. And they observed near about 23% increase in tensile strength when a slight loading of GR (0.2 wt %) was introduced in the PVA matrix. Such extensive application and property-oriented huge possibilities suggest that future research and prospects for GR-based PNCs are likely to expand tremendously in all areas of science and technology with some surprises.^{336,351} Thus, it is clear that a large number of GR-based PNCs have been developed and been examined for a range of applications in diverse fields of science and technology such as electronic devices, energy storage, sensors, ESD, and EMI

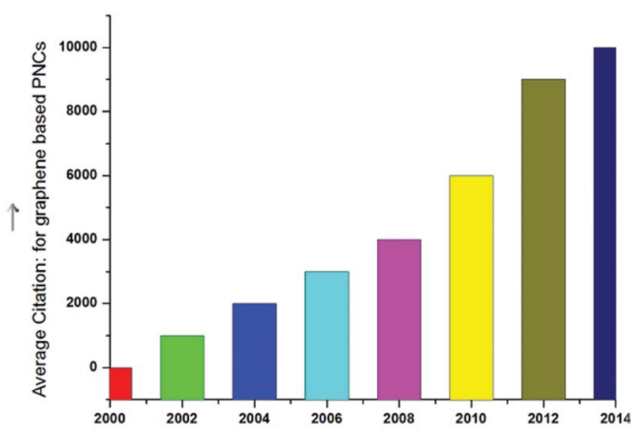


Figure 55. An approximate number of citations related to graphene-based nanocomposites from 2000–2014 (on the basis of Scopus database).

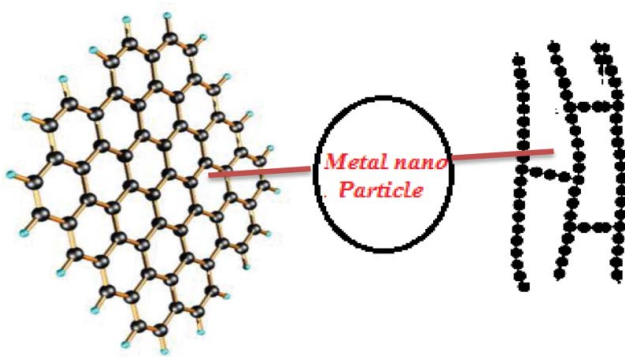


Figure 56. Schematic representation of the sandwich type interaction of the metal particle with two different fillers.

shielding and biomedical applications. A few selected applications of GR-based PNCs are discussed briefly in the sections that follow.^{16,388}

5.5. Ceramic-GR nanocomposites

Recently, it has been reported that incorporation of ceramic materials in FLG result in the formation of unique composite which possesses exceptional electrochemical performance with high charge carrier properties such excellent composites may be a boon to the energy industries.^{326–328,424} Numerous ceramic-GR nanocomposites viz. Al₂O₃-GR, Si₃N₄-GR, SiC-GR, ZrO-Al₂O₃-graphene, ZrB₂-GR etc. are well known which frequently used to increase electrical, thermal conductivity, refractory, mechanical, antifriction, anticorrosive, and biocompatibility properties for diverse applications.^{436,437} The use of GR with ceramics substantially decreases the brittle nature and increases the toughness.^{436,437} The utilization of ZrB₂-GR composite (ultrahigh temperature nanocomposites) is presently known to be used in aerospace industry as a high-temperature barrier for spacecraft during the re-entry event.^{438,439} These nanocomposites are consistently used as the fundamental infrastructure for the nose caps in the military ballistic equipment and space shuttles. It has been observed that carbides and borides of Ta, Zr, Hf, and Nb have similar thermal properties, but they not offer identical mechanical resistance like ceramic GR composites. Recently, Kim and Hong reported that Ti-N-GR composite has shown promising results as a selectively permeable membrane for hydrogen and this PNCs synthesized by Kim et al. via hot press process.^{436,437} The results obtained showed that the hydrogen permeability of TiN-GR membrane was much better than the Pd-Ag amorphous layer at 1.67, 2.09, and 2.83×10^{-7} mol/msPa^{1/2} at 673 K under 0.3 MPa, respectively. Various authors reported swift heavy ions induced modification of fullerene-based systems.

5.6. Biological applications of graphene and GR-based nanocomposite

GR and derivatives have shown potential applications in the biomedical science mainly related to toxicity.^{427–430} Hu and co-worker demonstrated the antibacterial activity of two types of water dispersible GR against E. coli with minimum cytotoxic effects on the human participants.^{428,429} They concluded that GO paper can be used in such environmental and biological application. Liao and co-worker demonstrated the cytotoxic effect of GO and G under the controlled physicochemical parameters.^{428–431} They found that GO was severely hemolytic than G and showed very high activity under tiny size.^{429–431} They proved that, when chitosan was thoroughly coated on GO, the hemolytic activity disappeared altogether, indicating the biocompatibility of the nanocomposite for erythrocytes. In addition to this they also concluded that biological or toxicological responses of the material were dependent on the nature of particle viz. size, quality, and state, the surface charge, and the oxygen threshold.^{428–431} Along the same line, the Liu research group compared four different derivatives of GR materials (graphite, graphite oxide, GO and reduced GO) against E. Coli to observe the toxicity effects and their results showed that GO was the most severely toxic, among the three.^{431–433} Recently, GR-poly-N-vinyl carbazole (PVK) nanocomposites have been employed for antimicrobial application and resulted in 80–85% microbial inhibition and toxicity toward a broad array of bacteria.^{433–435} They also reported that the PVK-GO nanocomposite significantly neutral toward the fibroblast cells, indicating a tremendous potential of this material in biomedical and industrial applications.^{429–437} In 2013, Liu and worker prepared hydroxyapatite-GO nanocomposite as biocompatible prosthetic group and they reported that the (300) and (002) plane of hydroxyapatite nanorods in the GR matrix played a significant role in maintaining mechanical properties of the nanocomposites such material may be backbone of bioengineering in the future.^{429–437}

5.7. In field of sustainable energy

Recent years have witnessed two major problems in the form of waste management and limited energy resources.⁴⁴⁰ At present, waste materials are a potential threat to the environment and the limited energy resources creates a havoc situation worldwide. As a result, extensive research is going on to resolve both of these problems. Among various solid wastes, print media, packaging, and

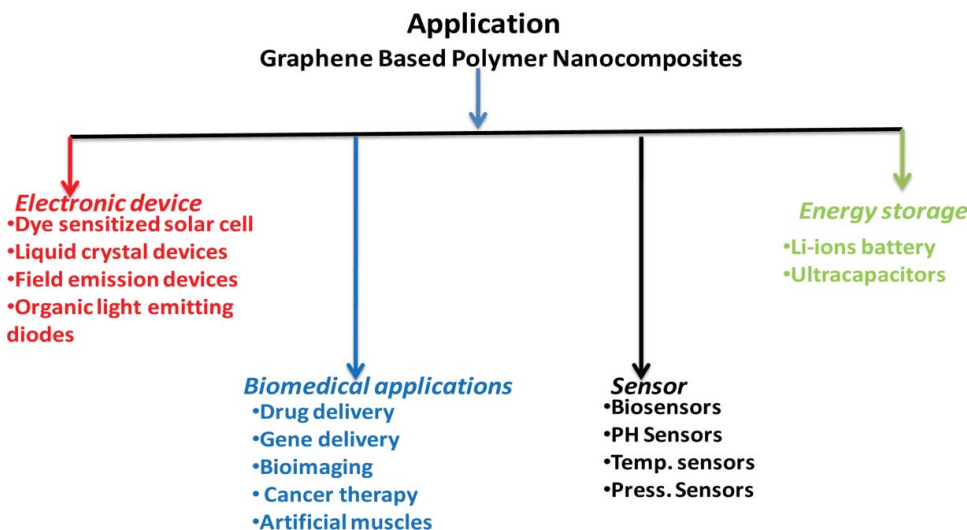


Figure 57. Applications of graphene-based polymer nanocomposites.

educational sectors are the primary producers of paper wastes.^{185,188,440,441} The papers used for printing newspapers, magazines, official works, packaging, and examination purposes are either thrown out or burned with a very few percentage being recycled.^{185–188} According to the report submitted by Indian Agro and Recycled paper mill association (IARPMA), about 14.6 million tons of waste papers are produced in India per year out of which only 26% is recycled, which is much higher as far as the environmental factor is concerned.^{185,188,442–444} Waste papers cause air, water, and soil pollution releasing hazardous and carcinogenic organo-halides thereby disturbing the ecological balance.¹⁸⁵ Cellulose, a major component of paper, can be extracted from these waste papers and utilized for bio-composites and energy storage applications. Cellulose fibers with a porous structure and electrolyte absorption properties are supposed to be a useful substrate for the deposition of energy material for energy storage devices.^{185,442–444} In case of cellulose fibers, there is a huge possibility to tune the physical and chemical properties according to need.¹⁸⁵ Due to its film forming ability and fibrous nature, cellulose fibers can enhance the mechanical stability of cellulose-based nanocomposite. Renewable energy sources have become quintessential for the scientific community and increasing by leaps and bounds day by day. Recently extensive research on SCs aimed at utilization of the environment-friendly materials for SCs applications.^{185,442–444} SCs or electrochemical capacitors, also known as the ultracapacitors, are devices with high specific capacitance and power density, average energy density, long cycle life, low maintenance and fast dynamic for charge propagation.^{185,440–445} These electrochemical capacitors are the emerging energy storage machines filling the fissure between the conventional capacitors and batteries.^{185–188}

The capacitance value of an electrochemical capacitor is determined by two storage principles: double layer capacitance and pseudo capacitance. Both of these contribute to the total capacitance value of the SCs. These electrochemical capacitors usually contain highly porous electrode materials with a high surface area like carbon-based materials which includes CNTs, activated carbon, and GR, which contributes to the double layer capacitance.^{446–447} The specific surface area and pore size of the electrodes plays a significant and important role for the performance of electrochemical capacitors.^{487–488} The pseudo-capacitive material presently investigated includes metal oxides (e.g. RuO₂, SnO₂, MnO₂, etc.) and conducting polymers (e.g. PANI, PPy, PEDOT, etc.) RuO₂/GR sheets nanocomposites have been studied which resulted in a particular capacitance value of 570 F/g.^{185–188,447,449} Uniform nanostructure of Ni(OH)₂ of 7.4 nm thickness showed a specific capacitance of 1715 F/g at scan rate 5mV/s, thus by fabricating this with highly conducting GR high-performance SCs electrodes can be obtained. Other composites based on SnO₂ have also been prepared which reported a specific capacitance of 616F/g and 523F/g.^{450,451} Few works are also stressed on composites based on wood fibers, cellulose fibers and carbon fiber which also exhibited highly specific capacitances.^{185–188} One of the frontline options for the carbon-based materials used for EDLC's is GR. The two-dimensional, transparent, parent of all graphitic forms, GR has been the best choice for the SCs application (Figure 57).^{450,451} GR has recently attracted much attention due to its magnificent features, such as high electrical conductivity (2000 Scm^{-1}), high surface area ($2630 \text{ m}^2\text{g}^{-1}$), transparency, flexibility with Young's modulus of 10 TPa, high electronic carrier mobility ($200,000 \text{ cm}^2 \text{ V}^{-1}\text{s}^{-1}$), and stretch ability. GR, a single

sheet material, has the highest specific capacitance of 550F/g accompanied by the high intensive quantum capacitance of $21 \mu\text{F cm}^{-2}$. This wonder material of the present era has opened way to the material and electronic world and by preparing composites with conducting polymers a full compass of application for memory backup in SRAMs (static random-access memory), power electronics and in many other fields have been studied. Some other most prominent areas where GR-based nanocomposites have been employed. Some of the miscellaneous work on the carbon-based materials and their composites have also been reviewed.^{16,185–188,440–445,451}

6. Conclusions and future prospects

In this article, we tried to incorporate all the fundamental scientific information about the GR, GNRs, CNTs, fullerenes, and GR-based PNCs including brief historical development, method of preparations, structural properties, and prominent scientific applications. CVD, arc method, and laser ablation techniques for CNTs were discussed briefly with technical simplicity. Nearly 12 recently reported GR-based PNCs have been presented with their applications and preparation methods. Intense attention has paid to the recent applications of CNTs, GR, GNRs-based PNCs, and QHE in the case of GR, especially the utilization of these materials in the field of FETs devices, transparent electrodes, sensors, photodetectors, energy storage devices, solar cells, polymer composites, and nanocomposites. Biological application of GR-based PNCs and their applications in the creation of new ceramic materials have also been drawn from the scientific literature.

As mentioned in the previous sections, GR, GNRs, and GR-based PNCs possess several outstanding properties which can be fabricated according to the requirement. Due to such tunable nature of these materials the entire scientific fraternity has shown their great interest for its more and more applications in day to day life, this is why within the 5–6 years these materials have attained a very strong tenability scientists and industrialist both. Novel properties of these materials (CNTs, GR and GNRs) such as room temperature QHE, highest charge transport properties, exceptional thermal conductivity etc., makes these materials a promising candidate as filling agent for polymer composite applications. It is well known that the use of silicon-based materials overcomes the technological barrier as it holds the future for micro to nanoscale electronics. The further modification in the inherent semi-metallic nature of silicon-based materials has been obsolete for FETs application. As a result, GNRs and bilayer GR came into existence with a

suitable band gap, and it seems these materials will be an ideal alternative to silicon-based technology shortly. But it is notable that the GR, GNRs, and GR-based materials still faces so many problems ranging from synthesis and characterization to final device fabrication. However, extensive research going on around the globe on GR and GR-based materials to resolve all these issues. At present, the main obstacle in the GR-based technology is its ultrapure scalable synthesis because only defect-free GR exhibits reported exceptional properties. In this line, some very useful methods have been developed such as ECE of graphite, CVD, etc., however research is continuing for improvement. A number of publications and patents are available for the laboratory scale application and device fabrications using GR and GR-based materials. So it can be assumed that shortly these materials will be the backbone of flexible transparent electrodes, GR/polymer composites for mechanical parts, energy storage, sensors, and organic electronics devices-based industries. GR-based polymer composites have showed the lowest percolation threshold for electrical conductivity and highly improved mechanical, thermal, and gas barrier properties. However, further investigation is still very important for the better understanding of dispersion and interface between the nano-filler and matrix. Therefore, in order to obtain critical successes in device fabrication and common technological application of GR-based PNCs more intense investigation and investment on GR research are required. Recently, atomic scale systematical research and geometrical microscopic studies have shown the evidence of tunable band gap through varying oxidation level and reduction process. Such advance investigations will be a milestone in the path of real time application of GR and GO-based devices in place metal oxide and semiconductor circuits. According to Geim and Novoselov,³ GR is “an ultimate incarnation of all surface.” It has given the exotic and exciting array of the application in all field of science ranging from engineering to biomedical. It has been extensively used for thermally and electrically conducting reinforced nanocomposite, electronic circuits, sensors and transparent and flexible electrodes for display and solar cells, etc. GR as nano filler is superior to conventional nano filler like (Na-MMT, LDH, CNT, CNF, EG, etc.) because of unique characteristics features like very high surface area, aspect ratio, thermal, and electrical conductivity even at room temperature and many more. All these prominently make GR the best carbon nano filler among traditional fillers available. Even there are a broad range of possible applications of GR, it is not compatible with various organic polymers. The dispensability of GR among polymer matrix and GR polymer interaction is still the big issue to solve.

This can be achieved only by surface modification of GR using various organic modifying agents. As reports suggest, the nucleophiles addition of organic molecule to the GR surface is the best way to achieve the bulk production of surface modified GR. In general, surface modification of GR assists the dispensability of GR in different organic media in the fabrication of GR-based nanocomposite. A vast number of GR-based PNCs have been reported which were found to be superior over polymer-based matrix. It has been found that GR-based PNCs exhibit superior mechanical properties compared to other conventional silicon- and graphite-based nanocomposite. There were significant improvements in mechanical properties of GR-based nanocomposites attributed to its very high aspect ratio. The remarkably high thermal stability of GR fabricates thermally stable nanocomposites. Also, a many fold increase in electrical conductivity of nanocomposite was observed which is due to the formation of conducting a network of GR sheets with the polymer matrix.

Acknowledgments

The authors are very grateful to all the authors cited directly or indirectly in the article, along with Dr. Suprabha Nayar (Scientist-F, NML, India) Mr. S. P. Tiwari (Dept. of Physics), Mr. J. P. Tiwari (Dept. of Mechanical Engineering), and Mr. P. K. Gautama (Dept. of Mining Engineering) at ISM Dhanbad for their constant support, discussions, and valuable suggestions.

Funding

Financial support from Department of Science and Technology (DST Project No. SB/FT/CS-085/2012), India and Indian School of Mines (ISM) Dhanbad is greatly acknowledged.

References

- R. E. Smalley, Discovering the fullerenes, *Rev. Mod. Phys.* **69**, 723 (1997).
- B. S. Kademan, V. L. Kalyane, and V. Kumar, Scientometric portrait of Nobel laureate Harold W. Kroto, *SRELS J. Info. Mana.* **39** (2002).
- A. K. Geim and K. S. Novoselov, The rise of graphene, *Nat. Mater.* **6**, 183 (2007).
- S. Ahmad, Carbon nanostructures fullerenes and carbon nanotubes, *Iete Techn. Rev.* **16**, 297 (1999).
- M. S. Dresselhaus, G. Dresselhaus, and R. Saito, *Nanotechnology in Carbon Materials*, Springer, New York (1999).
- I. M. Afanasov, V. A. Morozov, S. G. Ionov, A. N. Seleznev, and G. V. Tendeloo, Preparation, electrical and thermal properties of new exfoliated graphite-based composites, *Carbon* **4**, 263 (2009).
- L. C. Qin, X. Zhao, K. Hirahara, Y. Miyamoto, Y. Ando, and S. Iijima, Materials science: The smallest carbon nanotube, *Nature* **408**, 50 (2000).
- S. Berber, Y. K. Kwon, and D. Tomanek, Unusually high thermal conductivity of carbon nanotubes, *Phys. Rev. Lett.* **84**, 4613 (2000).
- M. S. Dresselhaus, G. Dresselhaus, and P.C. Eklund, *Science of Fullerenes and Carbon Nanotubes: Their Properties and Applications*, Academic Press, New York (1996).
- L. Chen, Y. Hernandez, X. Feng, and K. Mullen, From nanographene and graphene nanoribbons to graphene sheets: chemical synthesis, *Angew. Chem. Int. Ed.* **51**, 7640 (2012).
- V. Singh, D. Joung, L. Zhai, S. Das, S. I. Khondaker, and S. Seal, Graphene based materials: past, present and future, *Prog. Mater. Sci.* **56**, 1178 (2011).
- S. Stankovich, D. A. Dikin, G. H. Domke, K. M. Kohlhaas, E. J. Zimney, E. A. Stach, and R. S. Ruoff, Graphene based composite materials, *Nature* **442**, 7100 (2008).
- A. Tiwari, Fascinating world of immersing graphene technologies, *Adv. Mat. Lett.* **3**, 173 (2012).
- B. N. Patil, S. A. Acharya, Preparation of ZnS-graphene nanocomposite and its photocatalytic behavior for dye degradation, *Adv. Mat. Lett.* **5**, 116 (2014).
- C. He, N. Zhao, C. Shi, E. Liu, J. Li, Fabrication of nano-carbon composites using in situ chemical vapor deposition and their applications, *Adv. Mater.* **27**, 5431 (2015).
- T. K. Das and Smita Prusty, Graphene-based polymer composites and their applications, *Polym. Plast. Technol. Eng.* **52**, 331 (2013).
- P. S. Shivakumar Gouda, Raghavendra Kulkarni, S. N. Kurabet, and Dayananda Jawali, Effects of multi walled carbon nanotubes and graphene on the mechanical properties of hybrid polymer composites, *Adv. Mat. Lett.* **4**, 270 (2013).
- C. Schonenberger and L. Forro, Multiwall carbon nano tubes, *Phys. World* **13**, 37 (2000).
- R. Singhal, D. C. Agarwal, S. Mohapatra, Y. K. Mishra, D. Kabiraj, F. Singh, D. K. Avasthi, A. K. Chawla, R. Chandra, G. Mattei, and J. C. Pivin, Synthesis and characterizations of silver-fullerene C70 nanocomposite, *Appl. Phys. Lett.* **93**, 103114 (2008).
- V. Georgakilas, J. A. Perman, J. Tucek, and R. Zboril, Classification, chemistry, and applications of fullerenes, carbon dots, nanotubes, graphene, nanodiamonds, and combined superstructures, *Chem. Rev.* **115**, 4822 (2015).
- Y.A. Chen, A. Star, and S. Vidal, Sweet carbon nanostructures: carbohydrate conjugates with carbon nanotubes and graphene and their applications, *Chem. Soc. Rev.* **42**, 4542 (2013).
- M. Fujita, K. Wakabayashi, K. Nakada, and K. Kusakabe, Peculiar localized state at zigzag graphite edge, *J. Phys. Soc. Japan* **65**, 1923 (1996).
- G. V. Dubacheva, C. K. Liang, and D. M. Bassani, Functional monolayers from carbon nanostructures–fullerenes, carbon nanotubes, and graphene—as novel materials for solar energy conversion, *Coordin. Chem. Rev.* **256**, 2639 (2012).
- K. Nakada, M. Fujita, G. Dresselhaus, and M.S. Dresselhaus, Edge state in graphene ribbons: Nanometer size effect and edge shape dependence, *Phys. Rev. B* **54**, 17954 (1996).

25. P. R. Buseck, S. J Tsipursky, and R. Hettich, Fullerenes from the geological environment, *Science* **257**, 215 (1992).
26. K. A. Tohji, L. Paul, R. Moro, D. Malhotra, C. Lorents, and R. S. Ruoff, Selective and high-yield synthesis of higher fullerenes, *J. Phys. Chem.* **99**, 17788. (1995).
27. N. G. Bochkarev, Molecules and their migration in the universe, *Paleontol. J.* **44**, 791 (2010).
28. H. Prinzbach, A. Weiler, P. Landenberger, F. Wahl, J. L. Worth Scott, T. M. Gelmont, D. Olevano, and B. V. Iissen-dorff, Gas-phase production and photoelectron spectroscopy of the smallest fullerene, C₂₀, *Nature* **407**, 60 (2000).
29. A. Goel, J. B. Howard, and J. B. Vander Sande, Size analysis of single fullerene molecules by electron microscopy, *Carbon* **42** 1915 (2004).
30. A. K. Choudhary, Fullerene chemistry an overview, *Ind. J. Res.* **6**, 72 (2012).
31. D. L. D. Caspar, Delta-hedral views of fullerene polymorphism, *Science* **343**, 133 (1993).
32. Y. Z. Tan, S. Y. Xie, R. B. Huang, and L. S. Zheng, The stabilization of fused-pentagon fullerene molecules, *Nat. Chem.* **1**, 450, (2009).
33. K. Choho, W. Langenaeker, G. Van de Woude, and P. Geerlings, Reactivity of fullerenes. Quantum-chemical descriptors versus curvature, *J. Mol. Struc.* **8**, 293 (1995).
34. M. Sola, J. Mestres, and M. Duran, Molecular size and pyramidalization: two keys for understanding the reactivity of fullerenes, *J. Phys. Chem.* **99**, 10752 (1995).
35. F. Wudl, Fullerene materials, *J. Mater. Chem.* **12**, 1959 (2002).
36. S. Muhammad, H. L. R.L. Xu, Zhong, Z. M. Su, A. G. Al-Sehemi, and A. Irfan, Quantum chemical design of non-linear optical materials by sp 2-hybridized carbon nano-materials: issues and opportunities, *J. Mater. Chem. C* **1**, 5449 (2013)
37. L. Chiang, Y. Ravi, B. Upasani, and J. W. Swirczewski, Versatile nitronium chemistry for C₆₀ fullerene functionalization, *JACS*, **114**, 10157(1992)
38. R. C. Haddon, Chemistry of the fullerenes: The manifestation of strain in a class of continuous aromatic molecules, *Science* **261**, 1545 (1993).
39. Z. Chen and R. Bruce King, Spherical aromaticity: recent work on fullerenes, polyhedral boranes, and related structures, *Chem. Rev.* **105**, 3613 (2005).
40. N. C. Miller, E. Cho, R. Gysel, C. Risko, V. Coropceanu, and C. E. Miller, Factors governing intercalation of fullerenes and other small molecules between the side chains of semiconducting polymers used in solar cells, *Adv. Eng. Mater.* **2**, 1208 (2012).
41. F. Diederich and R. L. Whetten, Beyond C₆₀: The higher fullerenes, *Acc. Chem. Res.* **25**, 119 (1992).
42. F. Diederich, R. Ettl, Y. Rubin, R. L. Whetten, R. Beck, M. Alvarez, and A. Koch, The higher fullerenes: isolation and characterization of C₇₆, C₈₄, C₉₀, C₉₄, and C₇₀₀, an oxide of D_{5h}-C₇₀, *Science* **252**, 548 (1991).
43. K. V. Reddy, *Symmetry and Spectroscopy of Molecules*, New Age International, New Delhi, India (1998).
44. J. Osterodt, A. Zett, and F. Vogtle, Fullerenes by pyrolysis of hydrocarbons and synthesis of isomeric methanofullerenes, *Tetrahedron* **52**, 4949 (1996).
45. K. Kikuchi, N. Nakahara, T. Wakabayashi, S. Suzuki, H. Shiromaru, Y. Miyake, and Y. Achiba, NMR characterization of isomers of C₇₈, C₈₂ and C₈₄ fullerenes, *Nature* **45**, 142 (1992).
46. D. Bakowies, M. Buehl, and W. Thiel, Can large fullerenes be spherical?, *J. Amer. Chem. Soc.* **117**, 10113 (1995).
47. <http://homepage.hispeed.ch/bakowies/>
48. M. Endo, M. S. Strano, and P. M. Ajayan, Potential applications of carbon nanotubes, In *Carbon Nanotubes* (pp. 13–62). Springer, Berlin Heidelberg (2007).
49. M. Monthoux and V. L. Kuznetsov, Who should be given the credit for the discovery of carbon nanotubes, *Carbon* **44**, 1621 (2006).
50. G. Nicole, Carbon nanotubes-becoming clean, *Mater. Today* **10**, 28 (2007).
51. A. Oberlin, M. Endo, and T. Koyama, Filamentous growth of carbon through benzene decomposition, *J. Cryst. Growth* **32**, 335 (1976).
52. S. Iijima, Helical microtubules of graphitic carbon, *Nature* **354**, 58 (1991).
53. T. Kuila, S. Bose, A. K. Mishra, P. Khanra, N. H. Kim, and J. H. Lee, Chemical functionalization of graphene and its applications, *Prog. Mater. Sci.* **57**, 1061 (2012).
54. J. L. Delgado, M. Á. Herranz, and N. Martin, The nano-forms of carbon, *J. Mater. Chem.* **18**, 1426 (2008).
55. J. P. Salvetat, G. A. D. Briggs, J. M. Bonard, R. R. Bacsa, A. J. Kulik, T. N. Stockli, A. Burnham, and L. Forro, Elastic and shear moduli of single-walled carbon nanotube ropes, *Phys. Rev. Lett.* **82**, 944 (1999).
56. J. Hu, T. W. Odom, and C. M. Lieber, Chemistry and physics in one dimension: synthesis and properties of nanowires and nanotubes, *Acc. Chem. Res.* **32**, 435 (1999).
57. M. Damnjanović, I. Milošević T. Vuković, and R. Sredanović, Full symmetry, optical activity, and potentials of single-wall and multiwall nanotubes, *Phys. Rev. B* **60**, 2728 (1999).
58. M. Terrones, N. Grobert, J. Olivares, J. P Zhang, H. Terrones, K. Kordatos, W. K. Hsu, J. P. Hare, P. D. Townsend, K. Pras-sides, and A. K. Cheetham, Controlled production of aligned-nanotube bundles, *Nature* **388** 6637 (1997).
59. D. V. Kosynkin, A. L. Higginbotham, A. Sinitskii, J. R. Lomeda, A. Dimiev, B. K. Price, and J. M. Tour, Longitudinal unzipping of carbon nanotubes to form graphene nanoribbons, *Nature* **458**, 872 (2009).
60. M. S. Dresselhaus, G. Dresselhaus, and Ph. Avouris (Eds.), *Carbon nanotubes*, *Topics Appl. Phys.* **80**, Springer-Verlag, Berlin Heidelberg 173–211 (2001).
61. H. Omachi, T. Nakayama, E. Takahashi, Y. Segawa, and K. Itami, Initiation of carbon nanotube growth by well-defined carbon nanorings. *Nature chemistry* **5**, 572 (2013)
62. T. W. Odom, J. L. Huang, P. Kim, and C. M. Lieber, Atomic structure and electronic properties of single-walled carbon nanotubes, *Nature* **391**, 62 (1998).
63. Y. Matsuo, K. Tahara, and E. Nakamura, Theoretical studies on structures and aromaticity of finite-length armchair carbon nanotubes, *Organ. Lett.* **5**, 3181 (2003).
64. M. S. Dresselhaus, G. Dresselhaus, and R. Saito, Carbon fibers based on C₆₀ and their symmetry, *Phys. Rev.* **45**, 6234 (1992).
65. E. B. Barros, A. Jorio, G. G. Samsonidze, R. B. Capaz, A. G. S. Filho, J. M. Filho, G. Dresselhaus, and M. S. Dresselhaus, Review on the symmetry-related properties of carbon nanotubes, *Phys. Rep.* **431**, 261 (2006).

66. M. Zheng and E. D. Semke, Enrichment of single chirality carbon nanotubes, *J. Am. Ceram. Soc.* **129**, 6085 (2007).
67. Q. Zhao, M. B. Nardelli, and J. Bernholc, Ultimate strength of carbon nanotubes: a theoretical study, *Phys. Rev.* **65**, 144105 (2002).
68. R. H. Baughman, A. A. Zakhidov, and W. A. de Heer, Carbon nanotubes—the route toward applications, *Science* **297**, 787 (2002).
69. P. Eklund, P. Ajayan, and R. Blackmon, *International Assessment of Research and Development on Carbon Nanotubes: Manufacturing and Applications*, World Technology Evaluation Center, Inc., Baltimore, Maryland (2007).
70. M. R. Loos, L. A. F. Coelho, S. H. Pezzin, and S. C. Amico, Effect of carbon nanotubes addition on the mechanical and thermal properties of epoxy matrices, *Mater. Res.* **11**, 347 (2008).
71. M. Su, B. Zheng, and J. Liu, A scalable CVD method for the synthesis of single-walled carbon nanotubes with high catalyst productivity, *Chem. Rev. Lett.* **322**, 321 (2000).
72. M. Terrones, Science and technology of the twenty-first century: synthesis, properties, and applications of carbon nanotubes, *Ann. Rev. Mater. Res.* **33**, 419 (2003).
73. G. D. Nessim, Properties, synthesis, and growth mechanisms of carbon nanotubes with special focus on thermal chemical vapor deposition, *Nanoscale* **2**, 1306 (2010).
74. C. E. Baddour, and C. Briens, Carbon nanotube synthesis: a review, *Int. J. Chem. React. Eng.* **3**, 1 (2005).
75. M. Ahlskog, E. Seynavee, R. J. M. Vullers, and C. Van Haesendonck, A microdeposition technique for carbon nanotubes based on electron beam lithography, *J. Appl. Phys.* **85**, 8432 (1999).
76. R. L. Vander Wal, G. M. Berger, and T. M. Ticich, Carbon nanotube synthesis in a flame using laser ablation for in situ catalyst generation, *Appl. Phys. A* **77**, 889 (2003).
77. L. Ding, A. Tselev, J. Wang, D. Yuan, H. Chu, T. P. McNicholas, J. Liu, Selective growth of well-aligned semiconducting single-walled carbon nanotubes, *Nano Lett.* **9**, 805 (2009).
78. Y. Zhang, A. Chang, J. Cao, Q. Wang, W. Kim, Y. Li, and H. Dai, Electric-field-directed growth of aligned single-walled carbon nanotubes, *App. Phys. Lett.* **79**, 3155–3157 (2001).
79. N. J. Sano, T. Nakano, and A. Kanki, Synthesis of single walled carbon nanotubes with nanohorns by arc in liquid nitrogen, *Carbon* **42**, 688 (2004).
80. Z. Shi, Y. Lian, F. H. Liao, X. Z. Zhou, Y. Gu, S. Zhang, H. Iijima, K. Li, and S. L. Zhang, Large scale synthesis of single wall carbon nanotubes by arc-discharge method, *J. Phys. Chem. Solids* **61**, 1031 (2000).
81. D. H. Parker, P. Wurz, K. Chatterjee, K. R. Lykke, J. E. Hunt, M. J. Pellin, J. C. Hemminger, D. M. Gruen, and L. M. Stock, High-yield synthesis, separation, and mass spectrometric characterization of fullerenes C₆₀ to C₂₆₆, *JACS* **113**, 7499 (1991).
82. D. S. Bethune, C. H. Kiang, M. S. de Vries, G. R. Gorman, J. Vazquez, and R. Beyers, Cobalt-catalysed growth of carbon nanotubes with single-atomic-layer walls, *Nature* **363**, 605 (1993).
83. A. Thess, R. Lee, P. Nikolaev, H. J. Dai, P. Petit, J. Robert, C. H. Xu, Y. H. Lee, S. G. Kim, A. G. D. Rinzler, T. Colbert, G. E. Scuseria, D. Tomanek, J. E. Fischer, and R.E. Smalley, Crystalline ropes of metallic carbon nanotubes, *Science* **273**, 483 (1996).
84. M. Yudasaka, R. Yamada, N. Sensui, T. Wilkins, T. Ichihashi, and S. Iijima, Mechanism of the effect of NiCo, Ni and Co catalysts on the yield of single-wall carbon nanotubes formed by pulsed Nd:YAG laser ablation, *J. Phys. Chem. B* **103**, 6224 (1999).
85. T. Guo, P. Nikolaev, A. Thess, D. T. Colbert, and R. E. Smalley, Catalytic growth of single-walled nanotubes by laser vaporization, *Chem. Phys. Lett.* **243**, 49 (1995).
86. W. K. Maser, E. Munoz, A. M. Benito, M. T. Martinez, G. F. de la Fuente, Y. Maniette, E. Anglaret, and J. L. Sauvajol, Production of high-density single-walled nanotube material by a simple laser-ablation method, *Chem. Phys. Lett.* **292**, 587 (1998).
87. C. D. Scott, S. Areppalli, P. Nikolaev, and R. E. Smalley, Growth mechanisms for single-wall carbon nanotubes in a laser-ablation process, *Appl. Phys. A Mater. Sci. Process* **72**, 573 (2001).
88. C. D. Scott, S. Areppalli, P. Nikolaev, and R. E. Smalley, Growth mechanisms for single-wall carbon nanotubes in a laser-ablation process, *Appl. Phys. A* **72**, 573 (2001).
89. P. C. Eklund, B. K. Pradhan, U. J. Kim, Q. Xiong, J. E. Fischer, A. D. Friedman, B. C. Holloway, K. Jordan, and M. W. Smith, Large-scale production of single-walled carbon nanotubes using ultrafast pulses from a free electron laser, *Nano Lett.* **2**, 561 (2002).
90. Y. Homma, Y. Kobayashi, T. Ogino, D. Takagi, R. Ito, Y. J. Jung, and P. M. Ajayan, Role of transition metal catalysts in single-walled carbon nanotube growth in chemical vapor deposition, *J. Phys. Chem. B* **107**, 12161 (2003).
91. W. J. Daughton and F. L. Givens, An investigation of the thickness variation of spun-on thin films commonly associated with the semiconductor industry, *J. Electrochem. Soc.* **129**, 173 (1982).
92. M. Kumar, and Y. Ando, Chemical vapor deposition of carbon nanotubes: a review on growth mechanism and mass production, *J. Nanosci. Nanotech.* **10**, 3739 (2010).
93. M. Jos_e-Yacam_an, M. Miki-Yoshida, L. Rend_on, and J. G. Santiesteban, Catalytic growth of carbon microtubes 3250 bules with fullerene structure, *Appl. Phys. Lett.* **62**, 657 (1993).
94. S. P. Umotoy, S. H. Chiao, A. N. Nguyen, V. Vo, J. Huston, J. J. Chen, and C. L. Lei, High temperature chemical vapor deposition chamber, U.S. Patent US6364954 B2 (2002).
95. H. Yu, Q. Zhang, Q. Wang, G. Ning, G. Luo, and F. Wei, Effect of the reaction atmosphere on the diameter of single-walled carbon nanotubes produced by chemical vapor deposition, *Carbon* **44**, 1706 (2006).
96. L. Qingwen, Y. Hao, C. Yan, Z. Jin, and L. Zhongfan, A scalable CVD synthesis of high-purity single-walled carbon nanotubes with porous MgO as support material, *J. Mater. Chem.* **12**, 1179 (2002).
97. H. Ago, S. Imamura, T. Okazaki, T. Saito, M. Yumura, and M. Tsuji, CVD growth of single-walled carbon nanotubes with narrow diameter distribution over Fe/MgO catalyst and their fluorescence spectroscopy, *J. Phys. Chem. B* **109**, 10035 (2005).

98. A. Eftekhari, P. Jafarkhani, and F. Moztarzadeh, High yield synthesis of carbon nanotubes using a water-soluble catalyst support in catalytic chemical vapor deposition, *Carbon* **44**, 1343 (2006).
99. Z. F. Ren, Z. P. Huang, J. W. Xu, J. H. Wang, P. Bush, M. P. Siegal, and P. N. Provencio, Synthesis of large arrays of well-aligned carbon nanotubes on glass, *Science* **282**, 1105 (1998).
100. S. Neupane, M. Lastres, M. Chiarella, W. Z. Li, Q. Su, and G. H. Du, Synthesis and field emission properties of vertically aligned carbon nanotube arrays on copper, *Carbon*, **50**, 2641 (2012).
101. A. V. Melechko, V. I. Merkulov, T. E. McKnight, M. A. Guillorn, K. L. Klein, D. H. Lowndes, and M. L. Simpson, Vertically aligned carbon nanofibers and related structures: controlled synthesis and directed assembly, *J. Appl. Phys.* **97**, 041301 (2005).
102. R. E. Smalley, Y. Li, V. C. Moore, B. K. Price, R. Colorado, H. K. Schmidt, R. H. Hauge, and A. R. Barron, 2006 single wall carbon nanotube amplification: en route to a type-specific growth mechanism, *JACS* **128**, 15824 (2006).
103. P. M. Ajayan, O. Z. Zhou, Carbon nanotubes, *Nature* **80**, 391 (2001).
104. S. Neupane, M. Lastres, M. Chiarella, W. Z. Li, Q. Su, G. and H. Du, Synthesis and field emission properties of vertically aligned carbon nanotube arrays on copper, *Carbon* **50**, 2641 (2012).
105. S. Banerjee, N. Sayangdev, and I. K. Puri, Molecular simulation of the carbon nanotube growth mode during catalytic synthesis, *Appl. Phys. Lett.* **92**, 233121(2008).
106. S. Naha and I. K. Puri, A model for catalytic growth of carbon nanotubes, *J. Phys.* **41**, 065304 (2008).
107. N. M. Inami, A. Mohamed, E. Shikoh, and A. Fujiwara, Synthesis-condition dependence of carbon nanotube growth by alcohol catalytic chemical vapor deposition method, *Sci. Technol. Adv. Mater.* **32**, 3456 (2007).
108. D. Yuan, L. Ding, H. Chu, Y. Feng, T. P. McNicholas, and J. Liu, Horizontally aligned single-walled carbon nanotube on quartz from a large variety of metal catalysts, *Nano Lett.* **8**, 2579 (2008).
109. N. Ishigami, H. Ago, K. Imamoto, M. Tsuji, K. Iakoubovskii, and N. Minami, Crystal plane dependent growth of aligned single-walled carbon nanotubes on sapphire, *JACS* **32**, 3409 (2008).
110. J. Tersoff and R. S. Ruoff, Structural properties of a carbon nanotube crystal, *Phys. Rev. Lett.* **73**, 676. (1994).
111. L. V. Radushkevich, The structure of carbon formed by the thermal decomposition of carbon monoxide on the iron touch, *J. Phys. Chem.* **26**, 88 (1952).
112. Y. Xu, Z. Li, E. Dervishi, V. Saini, J. Cui, A. R. Biris, and A. S. Biris, Surface area and thermal stability effect of the MgO supported catalysts for the synthesis of carbon nanotubes, *J. Mater. Chem.* **18**, 5738 (2008).
113. S. Maghsoudi, A. Khodadadi, and Y. Mortazavi, A novel continuous process for synthesis of carbon nanotubes using iron floating catalyst and MgO particles for CVD of methane in a fluidized bed reactor, *Appl. Surf. Sci.* **25**, 2769 (2010).
114. M. Ritschel, A. Leonhardt, D. Elefant, S. Oswald, and B. Buchner, Rhenium-catalyzed growth carbon nanotubes, *J. Mater. Chem. C* **111**, 8414 (2007).
115. M. Kumar and A. Yoshinori, Carbon nanotubes from 3345 camphor: an environment-friendly nanotechnology, *J. Phys.* **61**, 643 (2007).
116. J. W. Norman, R. Kenneth, L. Kormanyos, A. Nicholas, and P. H. Reiter, Atmospheric pressure chemical vapor deposition, U.S. Patent No. 7, 674, 713(2010).
117. N. Franklin and H. Dai, An enhanced CVD approach to extensive nanotube networks with directionality, *Adv. Mater.* **12**, 890 (2000).
118. X. Wang, Q. X. J. Li, Z. Jin, J. Wang, Y. Li, K. Jiang, and S. Fan, Fabrication of ultralong and electrically uniform single-walled carbon nanotubes on clean substrates, *Nano Lett.* **9**, 3137 (2009).
119. B. I. Yakobson and R. E. Smalley, Fullerene nanotubes: C1,000,000 and beyond: Some unusual new molecules-long, hollow fibers with tantalizing electronic and mechanical properties-have joined diamonds and graphite in the carbon family, *Amer. Scientist* **67**, 324 (1997).
120. J. Prasek, J. Drbohlavova, J. Chomoucka, J. Hubalek, O. Jasek, V. Adam, and R. Kizek, Methods for carbon nanotubes synthesis, review, *J. Mater. Chem.* **21**, 15872 (2011).
121. M. Lin, J. P. Ying Tan, C. Boothroyd, K. P. Loh, E. S. Tok, and Y. L. Foo, Direct observation of single-walled carbon nanotube growth at the atomistic scale, *Nano Lett.* **6**, 449 3355 (2006).
122. J. P. Tessonner, D. Rosenthal, T. W. Hansen, C. Hess, M. E. Schuster, R. Blume, and R. Schlogl, Analysis of the structure and chemical properties of some commercial carbon nanostructures, *Carbon* **47**, 1779 (2009).
123. L. C. Palmer and S. I. Stupp, Molecular self-assembly into one-dimensional nanostructures, *Acc. Chem. Res.* **41**, 1674 (2008).
124. H. J. Dai, C. Kong, N. Zhou, T. Franklin, A. Tombler, S. Cassell, and M. Chapline, Controlled chemical routes to nanotube architectures, physics, and devices, *J. Phys. Chem B* **103**, 11246 (1999).
125. Y. Aviga and R. Kalish, Growth of aligned carbon nanotubes by biasing during growth, *Appl. Phys. Lett.* **78**, 2291 (2001).
126. P. M. Ajayan and T. W Ebbesen, Nanometre-size tubes of carbon, *Rep. Prog. Phys.* **60**, 1025 (1997).
127. M. Endo, H. Muramatsu, T. Hayashi, Y. Kim, M. Terrones, and M. S. Dresselhaus, Nanotechnology: Buckypaper' from coaxial nanotubes, *Nature* **433**, 476 (2005).
128. M. Endo, K. Takeuchi, S. Igarashi, K. Kobori, M. Shirai, and H. W. Kroto, The production and structure of pyrolytic carbon nanotubes (PCNTs), *J. Phys. Chem. Solids* **54**, 184 (1993).
129. V. N. Popov, Carbon nanotubes: properties and application, *Mater. Sci. Eng. R* **43**, 61 (2004).
130. J. J. Gooding, Nanostructuring electrodes with carbon nanotubes: A review on electrochemistry and applications for sensing, *Electrochim. Acta* **50**, 3049 (2005).
131. M. F. L. De, S. H. Volder, R. H. Tawfick, A. Baughman, and J. Hart, CNTs: Present and future commercial applications, *Science* **339**, 535 (2013).
132. P. H. Avouris, R. Martel, T. Hertel, and R. Sandstrom, 3395 AFM-tip-induced and current-induced local oxidation of silicon and metals, *Appl. Phys. A Mater. Sci. Process* **66**, 659 (1998).

133. P. M. Ajayan and O. Z. Zhou, Applications of carbon nanotubes. In *Carbon Nanotubes*, Springer Berlin Heidelberg, pp. 391–425 (2001).
134. I. Thomas, and C. Masamichi, Yoshimura, Fabrication of carbon nanotubes for high-performance scanning probe microscopy, In *Electronic Properties of Carbon Nanotubes*, Jose Mauricio Marulanda, ed., INTECH Open Access Publisher, Rijeka, Croatia (2011).
135. A. Merkoçci, M. Pumera, X. Llopis, B. Perez, M. del Valle, and S. Alegret, New materials for electrochemical sensing VI: carbon nanotubes, TrAC, *Trends Anal. Chem.* **24**, 826 (2005).
136. M. E. Roberts, M. C. Le Mieux, and Z. Bao, Sorted and aligned single-walled carbon nanotube networks for transistor-based aqueous chemical sensors, *Acs Nano* **3**, 3287 (2009).
137. P. Avouris, Molecular electronics with carbon nanotubes, *Acc. Chem. Res.* **35**, 1026 (2002).
138. F. Kreupl, Electronics: carbon nanotubes finally deliver, *Nature* **484**, 321 (2012).
139. J. Deng, and H. S. Wong. A compact SPICE model for carbon-nanotube field-effect transistors including no idealities and its application—Part II: Full device model and circuit performance benchmarking, *Electron Dev. IEEE Trans.* **54**, 3195 (2007).
140. R. A. Martel, T. Schmidt, H. R. Shea, T. Herte, and P. Avouris, Single-and multi-wall carbon nanotube field effect transistors, *Appl. Phys. Lett.* **73**, 2447 (1998).
141. J. E. Fischer, H. Dai, A. Thess, R. Lee, N. M. Hanjani, D. L. Dehaas, and R. E. Smalley, Metallic resistivity in crystalline ropes of single-wall carbon nanotubes, *Phys. Rev. B* **55**, R 4921 (1997).
142. S. Fan, M. G. Chapline, N. R. Franklin, T. W. Tombler, A. M. Cassell, and H. Dai, Self-oriented regular arrays of carbon nanotubes and their field emission properties, *Science* **283**, 514 (1999).
143. G. Pirio, P. Legagneux, D. Pribat, B. K. Teo, M. Chhowalla, G. A. J. Amaralunga, and W. I. Milne. Fabrication and electrical characteristics of carbon nanotube field emission microcathodes with an integrated gate electrode, *Nanotechnology* **13**, 1 (2002).
144. M. H. Yang, B. K. Teo, W. I. Milne, and D. G. Hasko, Carbon nanotube Schottky diode and directionally dependent field-effect transistor using asymmetrical contacts, *Appl. Phys. Lett.* **87**, 253116 (2005).
145. M. H. Yang, B. K. Teo, W. I. Milne, and D. G. Hasko, Carbon nanotube Schottky diode and directionally dependent field-effect transistor using asymmetrical contacts, *Appl. Phys.* **87**, 253116 (2005).
146. C. T. White, and W. M. John, Fundamental properties of single-wall carbon nanotubes, *J. Phys. Chem. B* **109**, 65 (2005).
147. B. Thanveer. Carbon nanotubes as electron sources in display devices. <https://electronicsmail.wordpress.com/>
148. Y. Wang, Z. Shi, Y. Huang, Y. Ma, C. Wang, M. Chen, and Y. Chen, Supercapacitor devices based on graphene materials, *J. Phys. Chem. C* **113**, 13103 (2009).
149. M. Winter, and R. J. Brodd, What are batteries, fuel cells, and supercapacitors?, *Chem. Rev.* **104**, 4245 (2004).
150. P. Xu, T. Gu, Z. Cao, B. Wei, J. Yu, F. Li, J. H. Byun, W. Lu, Q. Li, and T. W. Chou, Carbon nanotube fiber based stretchable wireshaped supercapacitors, *Adv. Energ. Mater.* **3**, 4 (2014).
151. P. Simon, and Y. Gogotsi, Materials for electrochemical capacitors, *Nat. Mater.* **7**, 854 (2008).
152. M. Notarianni, J. Liu, F. Mirri, M. Pasquali, and N. Motta, Graphene-based supercapacitor with carbon nanotube film as highly efficient current collector, *Nanotechnology*, **25**, 405 (2014).
153. T. Kar, J. Pattanayak, and S. Scheiner, Insertion of lithium ions into carbon nanotubes: an ability study, *J. Phys. Chem. A* **105**, 10397 (2001).
154. D. Fauteux, and R. Koksbang, Rechargeable lithium battery anodes: alternatives to metallic lithium, *J. Appl. Electrochem.* **23**, 1 (1993).
155. J. M. Tarascon and M. Armand, Issues and challenges facing rechargeable lithium batteries, *Nature* **414**, 359 (2001).
156. X. Wang, H. Liu, Y. Jin, and C. Chen, Polymer-functionalized multiwalled carbon nanotubes as lithium intercalation hosts, *J. Phys. Chem. B* **110**, 10236 (2006).
157. A. G. Cano-Márquez, F. J. Rodríguez-Macías, J. Campos-Delgado, C. G. Espinosa-González, F. Tristán-López, D. Ramírez-González, D. A. Cullen, D. J. Smith, M. Terrones, and Y. I. Vega-Cantú. Ex-MWNTs: graphene sheets and ribbons produced by lithium intercalation and exfoliation of carbon nanotubes, *Nano Lett.* **9**, 1533 (2009).
158. C. de las Casas and W. Li, A review of application of carbon nanotubes for lithium ion battery anode material, *J. 3480 Power Sour.* **208**, 74 (2012).
159. A. L. M. Reddy, M. M. Shajumon, S. R. Gowda, and P. M. Ajayan, Coaxial MnO₂/carbon nanotube array electrodes for high-performance lithium batteries, *Nano Lett.* **9**, 1002 (2009).
160. C. Liu, Y. Y. Fan, M. Liu, H. T. Cong, H. M. Cheng, and M. S. Dresselhaus, Hydrogen storage in single-walled carbon nanotubes at room temperature, *Science* **286**, 1127 (1999).
161. L. Schlapbach and A. Zuttel, Hydrogen-storage materials for mobile applications, *Nature* **414**, 353 (2001).
162. A. D. K. Jones and T. A. Bekkedahl, Storage of hydrogen in single-walled carbon nanotubes, *Nature* **386**, 377 (1997).
163. W. X. Chen, J. P. Tu, L. Y. Wang, H. Y. Gan, Z. D. Xu, and X. B. Zhang, Tribological application of carbon nanotubes in a metal-based composite coating and composites, *Carbon* **41**, 215 (2003).
164. H. M. Cheng, Q. H. Yang, and C. Liu, Hydrogen storage in carbon nanotubes, *Carbon* **39**, 1447 (2001).
165. C. Tang, C. Man, Y. Chen, F. Yang, L. Luo, Z. F. Liu, and K. W. Wong, Realizing the storage of pressurized hydrogen in carbon nanotubes sealed with aqueous valves, *Energy Technol.* **1**, 309 (2013).
166. Z. Cao and B. B. Wei, A perspective: carbon nanotube macro-films for energy storage, *Ener. Environ. Sci.* **6**, 3183 (2013).
167. Hanaei, Hengameh, M. Khalaji Assadi, and R. Saidur, “Highly efficient antireflective and self-cleaning coatings that incorporate carbon nanotubes (CNTs) into solar cells: A review, *Renew. Sustain. Engy. Rev.* **59**.620 (2016).
168. Y. P. Sun, K. Fu, Y. Lin, and W. Huang, Functionalized carbon nanotubes: properties and applications, *Acc. Chem. Res.* **35**, 1096 (2002).

169. A. M. Kolpak and J. C. Grossman, Azobenzene-functionalized carbon nanotubes as high-energy density solar thermal fuels, *Nano Lett.* **11**, 3162 (2011).
170. N. G. Sahoo, S. Rana, J. W. Cho, L. Li, and S. H. Chan, Polymer nanocomposites based on functionalized carbon nanotubes, *Prog. Polym. Sci.* **35**, 837 (2010).
171. J. N. Coleman, U. Y. Khan, and K. Gun'ko, Mechanical reinforcement of polymers using carbon nanotubes, *Adv. Mater.* **18**, 689 (2006).
172. S. Kazaoui, B. Minami, Y. Nalini, N. Kim, T. Takada, and K. Hara, Near-infrared electroluminescent devices using single-wall carbon nanotubes thin films, *Appl. Phys. Lett.* **87**, 211914 (2005).
173. A. B. Dalton, S. Collins, E. Munoz, J. M. Razal, V. H. Ebron, J. P. Ferraris, and R. H. Baughman, Super-tough carbon-nanotube fibres, *Nature* **423**, 703 (2003).
174. N. M. Pugno, Mimicking nacre with super-nanotubes for producing optimized super-composites, *Nanotechnology* **17**, 5480 (2006).
175. J. H. Du, J. Bai, and H. M. Cheng, The present status and key problems of carbon nanotube based polymer composites, *Express Polym. Lett.* **1**, 253 (2007).
176. D. Rosa, I. Maria, F. Sarasini, M. Sabrina Sarto, and A. Tamburro, EMC impact of advanced carbon fiber/carbon nanotube reinforced composites for next-generation aerospace applications, *Electromagn. Compatibil. IEEE Trans.* **50**, 3, 556 (2008).
177. D. Bello, B. L. Wardle, N. Yamamoto, R. E. J. Guzman deVilloriaGarcia, A. J. Hart, K. Ahn, M. J. Ellenbecker, and M. Hallock, Exposure to nanoscale particles and fibers during machining of hybrid advanced composites containing carbon nanotubes, *J. Nanopart. Reser.* **11**, 249 (2009).
178. H. Qian, E. S. Greenhalgh, M. S. Shaffer, and A. Bismarck, Carbon nanotube-based hierarchical composites: a review, *J. Mater. Chem.* **20**, 4751 (2010).
179. L. K. Jain and Y. W. Mai, On the effect of stitching on mode I delamination toughness of laminated composites, *Composit. Sci. Technol.* **51**, 331 (1994).
180. V. K. Thakur, M. K. Thakur, and R. K. Gupta, Review: raw natural fiber-based polymer composites, *Int. J. Polym. Anal. Characteriz.* **19**, 271 (2014).
181. A. Y. Sham and S. M. Notley, A review of fundamental properties and applications of polymer-graphene hybrid materials, *Soft Matter* **9**, 6653. (2013).
182. Q. H. Wang, K. Kalantar-Zadeh, A. Kis, J. N. Coleman, and M. S. Strano, Electronics and optoelectronics of two dimensional transition metal dichalcogenides, *Nat. Nanotechnol.* **7**, 699 (2012).
183. D. Li, and R. B. Kaner, Graphene-based materials, *Nat. Nanotechnol.* **3**, 101 (2008).
184. R. R Nair, P. Blake, A. N. Grigorenko, K. S. Novoselov, T. J. Booth, T. Stauber, and A.K. Geim, Fine structure constant defines visual transparency of graphene, *Science* **320**, 1308 (2008).
185. R. Oraon, A. De Adhikari, S. K. Tiwari, and G. C. Nayak, Nanoclay based graphene polyaniline hybrid nanocomposites: promising electrode materials for supercapacitors, *RSC Adv.* **5**, 68344 (2015).
186. P. Mukhopadhyay and R. K. Gupta, *Graphite, Graphene, and Their Polymer Nanocomposites*, CRC Press, London, pp. 2–55 (2012).
187. G. P. Kar, S. Biswas, and S. Bose, Tailoring the interface of an immiscible polymer blend by a mutually miscible homopolymer grafted onto graphene oxide: outstanding mechanical properties, *Phys. Chem. Chem. Phys.* **17**, 1821 (2015).
188. A. De Adhikari, R. Oraon, S. K. Tiwari, J. H. Lee, and G. C. Nayak, Effect of waste cellulose fibres on the charge storage capacity of polypyrrole and graphene/polypyrrole electrodes for supercapacitor application, *RSC Adv.* **5**, 27355 (2015).
189. M. Huang, H. Yan, C. Chen, D. Song, T. F. Heinz, and J. Hone, Phonon softening and crystallographic orientation of strained graphene studied by Raman spectroscopy, *Proc. National Academy of Sciences* **106**, 18, 7308 (2009).
190. S. J. Kim, K. Choi, B. Lee, Y. Kim, and B. H. Hong, Materials for flexible, stretchable electronics: Graphene and 2D materials, *Ann. Rev. Mater. Res.* **45**, 84. (2015).
191. M. D. Stoller, S. Park, Y. Zhu, J. An, and R. S. Ruoff, Graphene-based ultracapacitors, *Nano Lett.* **8**, 3498 (2008).
192. X. Li, W. Cai, J. An, S. Kim, J. Nah, D. Yang, and R. S. Ruoff, Large-area synthesis of high-quality and uniform graphene films on copper foils, *Science* **324**, 1312 (2009).
193. D. R. Dreyer, S. Park, C. W. Bielawski, and R. S. Ruoff, The chemistry of graphene oxide, *Chem. Soc. Rev.* **39**, 240. (2010).
194. P. Mukhopadhyay and R. K. Gupta, Eds., *Graphite, Graphene, and Their Polymer Nanocomposites*, CRC Press, London (2012).
195. C. L. Kane and E. J. Mele, Quantum spin Hall effect in graphene, *Phys. Rev. Lett.* **95**, 268012005.
196. http://www.nobelprize.org/nobel_prizes/physics/laurates/2010/geim-photo.html
197. V. M. Pereira, A. C. H. Neto, and N. M. R. Peres, Tight binding approach to uniaxial strain in graphene, *Phys. Rev. B* **80**, 045401 (2009).
198. S. Konschuh, M. Gmitra, and J. Fabian, Tight-binding theory of the spin-orbit coupling in graphene, *Phys. Rev. B* **82**, 245412 (2010).
199. Y. J. Dappe, R. Oszwaldowski, P. Pou, J. Ortega, R. Pérez, and F. Flores, Local-orbital occupancy formulation of density functional theory: Application to Si, C, and graphene, *Phys. Rev. B* **73**, 235124, (2006).
200. H. Min, J. E. Hill, N. A. Sinitsyn, B. R. Sahu, L. Kleinman, and A. H. MacDonald, Intrinsic and Rashba spin-orbit interactions in graphene sheets, *Phys. Rev. B* **74**, 165310. (2006).
201. G. Giovannetti, P. A. Khomyakov, G. Brocks, P. J. Kelly, and J. Brink, Substrate-induced band gap in graphene on hexagonal boron nitride: Ab initio density functional calculations, *Phys. Rev B* **76**, 073103 (2007).
202. M. F. Craciun, S. Russo, M. Yamamoto, J. B. Oostinga, A. F. Morpurgo, and S. Tarucha, Trilayer graphene is a semimetal with a gate-tunable band overlap, *Nat. Nanotechnol.* **4**, 383 (2009).
203. K. K. Gomes, W. W. Mar, F. Guinea, and H. C. Manoharan, Designer Dirac fermions and topological phases in molecular graphene, *Nature* **483**, 306 (2012).
204. A. C. Neto, F. Guinea, N. M. R. Peres, K. S. Novoselov, A. K. Geim, The electronic properties of graphene, *Rev. Moder. Phys.* **81**, 109 (2009).
205. M. Klintenberg, S. Lebegue, M. I. Katsnelson, and O. Eriksson, Theoretical analysis of the chemical bonding and



- electronic structure of graphene interacting with Group IA and Group VIIA elements, *Phys. Rev. B* **81**, 085433 (2010).
206. J. Jung and A. H. MacDonald, Theory of the magnetic-field-induced insulator in neutral graphene sheets, *Phys. Rev. B* **80**, 235417 (2009).
 207. A. F. Morpurgo and F. Guinea, Intervalley scattering, long-range disorder, and effective time-reversal symmetry breaking in graphene, *Phys. Rev. Lett.* **97**, 196804, (2006).
 208. E. Andrei, G. Li, and X. Du, Electronic properties of graphene: a perspective from scanning tunneling microscopy and magneto-transport, *Rep. Progr. Phys.* **75**, 4532 (2012).
 209. S. Sahoo, Quantum Hall effect in graphene: Status and prospects, *Ind. J. Pure Appl. Phys.* **49**, 367 (2011).
 210. J. R. Williams, L. DiCarlo, and C. M. Marcus, Quantum Hall effect in a gate-controlled p-n junction of graphene, *Science* **317**, 638 (2007).
 211. A. Wschalom, and D. D. Flatte, Challenges for semiconductor spintronics, *Nat. Phys.* **3**, 153 (2007).
 212. M. T. Koshino and T. Ando, Orbital diamagnetism in multilayer graphenes: Systematic study with the effective mass approximation, *Phys. Rev. B* **76**, 085425 (2007).
 213. Y. Z. Li, P. Zhou, and Z. Chen, Spin gapless semiconductor metal-half-metal properties in nitrogen-doped zigzag graphene nanoribbons, *ACS Nano.* **3**, 1952 (2009).
 214. Z. Jiang, Y. Zhang, Y. W. Tan, H. L. Stormer, and P. Kim, Quantum Hall effect in graphene, *Sol. Stat. Commun.* **143**, 14 (2007).
 215. V. P. Gusynin, S. G. Sharapov, and J. P. Carbotte, AC conductivity of graphene: from tight-binding model to 2+ 1-dimensional quantum electrodynamics, *Inter. J. Mod. Phys. B* **21**, 4611 (2007).
 216. R. S. Deacon, K. C. Chuang, R. J. Nicholas, K. S. Novoselov, and A. K. Geim, Cyclotron resonance study of the electron and hole velocity in graphene monolayers, *Phys. Rev. B* **76**, 081406. (2007).
 217. K. S. Novoselov, A. K. Geim, S. V. Morozov, D. M. Jiang, I. Katsnelson, I. V. Grigorieva, S.V. Dubonos, and A. A. Firsov, Two-dimensional gas of massless Dirac fermions in graphene, *Nature* **438**, 197 (2005).
 218. E. H. Hwang, S. Adam, S. Das, and D. Sarma, Carrier transport in two-dimensional graphene layers, *Phys. Rev. Lett.* **98**, 186806 (2007).
 219. M. I. Katsnelson, K. S. Novoselov, and A. K. Geim, Chiral tunnelling and the Klein paradox in graphene, *Nat. Phys.* **2**, 620 (2006).
 220. M. F. Craciun, S. Russo, M. J. Yamamoto, B. A. Oostinga, F. Morpurgo, and S. Tarucha, Trilayer graphene is a semimetal with a gate-tunable band overlap, *Nat. Nanotechnol.* **4**, 383 (2009).
 221. F. Guinea, M. I. Katsnelson, and A. K. Geim, Energy gaps and a zero-field quantum Hall effect in graphene by strain engineering, *Nat. Phys.* **6**, 33 (2009).
 222. K. I. Bolotin, F. Ghahari, M. D. Shulman, H. L. Stormer, and P. Kim, Observation of the fractional quantum Hall effect in graphene, *Nature* **462**, 199 (2009).
 223. V. P. Gusynin and S. G. Sharapov, Unconventional integer quantum Hall effect in graphene, *Phys. Rev. Lett.* **95**, 146801 (2005).
 224. K. S. Novoselov, E. McCann, S. V. Morozov, V. I. Fal'ko, M. I. Katsnelson, U. Zeitler, D. Jiang, F. Schedin, and A. K. Geim, Unconventional quantum Hall effect and Berry's phase of 2p in bilayer graphene, *Nat. Phys.* **2**, 180 (2006).
 225. Y. Zhang, Z. Jiang, J. P. Small, M. S. Purewal, Y. W. Tan, M. Fazlollahi, J. D. Chudow, J. A. Jaszcak, H. L. Stormer, and P. Kim, Landau-level splitting in graphene in high magnetic fields, *Phys. Rev. Lett.* **96**, 136806 (2006).
 226. K. Nomura and A. H. MacDonal, Quantum Hall ferromagnetism in graphene, *Phys. Rev. Lett.* **96**, 256602 (2006).
 227. K. S. Novoselov, Z. Jiang, Y. Zhang, S. V. Morozov, H. L. Stormer, U. Zeitler, J. C. Maan, G. S. Boebinger, P. Kim, and A. K. Geim, Room-temperature quantum Hall effect in graphene, *Science* **315**, 1379 (2007).
 228. X. Du, I. Skachko, F. Duerr, A. Luican, and E. Y. Andrei, Fractional quantum Hall effect and insulating phase of Dirac electrons in graphene, *Nature* **462**, 195 (2009).
 229. V. P. Gusynin, S. G. Sharapov, and J. P. Carbotte, Sum rules for the optical and Hall conductivity in graphene, *Phys. Rev. B* **75**, 165407 (2007).
 230. J. H. Ho, Y. H. Lai, Y. H. Chiu, and M. Lin, Landau levels in graphene, *Physica E Low-dimen. Syst. Nanostruct.* **40**, 1725 (2008).
 231. C. Berger, Z. Song, X. Li, X. Wu, N. Brown, C. Naud, and D. Mayou, Electronic confinement and coherence in patterned epitaxial graphene, *Science* **312**, 1196 (2006).
 232. N. M. R. Peres, A. H. Castro Neto, and F. Guinea, Conductance quantization in mesoscopic graphene, *Phys. Rev. B* **73**, 195411 (2006).
 233. M. Ezawa, Supersymmetric structure of quantum Hall effects in graphene, *Phys. Lett. A* **72**, 929 (2008).
 234. J. Moser, A Barreiro, and A. Bachtold, Current-induced cleaning of graphene, *Appl. Phys. Lett.* **91**, 163513 (2007).
 235. M. Polini, R. Asgari, Y. Barlas, T. Pereg-Barnea, and A. H. MacDonald, A pseudochiral Fermi liquid, *Solid State Commun. Graphene* **143**, 62 (2007).
 236. J. Liu, B. W. Li, Y. Z. Tan, A. Giannakopoulos, C. Sanchez-Sanchez, D. Beljonne, P. Ruffieux, R. Fasel, X. Feng, and K. Müllen, Toward cove-edged low band gap graphene nanoribbons, *JACS* **137**, 6103 (2015).
 237. R. R. Cloke, T. Marangoni, G. D. Nguyen, T. Joshi, D. J. Rizzo, C. Bronner, T. Cao, S. G. Louie, M. F. Crommie, and F. R. Fischer, Site-specific substitutional boron doping of semiconducting armchair graphene nanoribbons, *JACS* **137** 8875 (2015).
 238. A. Das, B. Chakraborty, S. Piscanec, S. Pisana, A. K. Sood, and A. C. Ferrari, Phonon renormalization in doped bilayer graphene, *Phys. Rev. B* **79**, 155417 (2009).
 239. H.U. Özdemir, A. Altuntaş, and A. D. Güçlü, Magnetic phases of graphene nanoribbons under potential fluctuations, *Phys. Rev. B*, **93** 014415 (2016).
 240. C. Casiraghi, A. Hartschuh, H. Qian, S. Piscanec, C. Georgi, A. Fasoli, K. S. Novoselov, D. M. Basko, and A. C. Ferrari, Raman spectroscopy of graphene edges, *Nano Lett.* **9**, 1441 (2009).
 241. H. Hsu and L. E. Reichl, Selection rule for the optical absorption of graphene nanoribbons, *Phys. Rev. B* **76**, 045418. (2007).
 242. K. A. Ritter and J. W. Lyding, The influence of edge structure on the electronic properties of graphene quantum dots and nanoribbons, *Nat. Mater.* **8**, 242 (2009).
 243. X. Jia, J. Campos-Delgado, M. Terrones, V. Meunier, and M. S. Dresselhaus, Graphene edges: a review of their fabrication and characterization, *Nanoscale* **3**, 86–95 (2011).
 244. N. Mohanty, D. Moore, Z. Xu, T. S. Sreeprasad, A. Nagaraja, A. A. Rodriguez, and V. Berry, Nanotomy

- based production of transferable and dispersible graphene nanostructures of controlled shape and size, *Nat. Commun.* **3**, 844 (2012).
245. L. Tapaszto, G. Dobrik, P. Lambin, and L. P. Biro, Tailoring the atomic structure of graphene nanoribbons by scanning tunnelling microscope lithography, *Nat. Nanotechnol.* **3**, 401 (2008).
 246. P. Gallagher, K. Todd, and D. G. Gordon, Disorder induced gap behavior in graphene nanoribbons, *Phys. Rev. B* **81**, 115409 (2010).
 247. A. Geim, P. Kim, K. Novoselov, Z. Jiang, H. Stormer, Y. Zhang, S. Morozov, and U. Zeitler, Room temperature Quantum Hall effect in graphene, *APS Meeting Abstracts* (2007).
 248. E. McCann, Asymmetry gap in the electronic band structure of bilayer graphene, *Phys. Rev. B* **74**, 161403 (2006).
 249. S. Bae, H. Kim, Y. Lee, X. Xu, J. S. Park, Y. Zheng, J. Balakrishnan, T. Lei, H. R. Kim, Y. I. Song, and Y. J. Kim, Roll-to-roll production of 30-inch graphene films for transparent electrodes, *Nat. Nanotech.* **5**, 578 (2010).
 250. I. W. Frank, D. M. Tanenbaum, A. M. Van der Zande, and P. L. McEuen, Mechanical properties of suspended graphene sheets, *J. Vac. Sci. Technol.* **25**, 2561 (2007).
 251. C. Lee, X. Wei, J. W. Kysar, and J. Hone, Measurement of the elastic properties and intrinsic strength of monolayer graphene, *Science* **321**, 388 (2008).
 252. M. Mecklenburg, A. Schuchardt, Y. K. Mishra, S. Kaps, R. Adelung, A. Lotnyk, L. Kienle, and K. Schulte, Aerographe: ultra lightweight, flexible nanowall, carbon microtube material with outstanding mechanical performance, *Adv. Mater.* **24**, 3490 (2012).
 253. L. A. Falkovsky, Optical properties of graphene, *J. Phys.* **129**, 1, 012004 (2008).
 254. Z. Z. Zhang, K. Chang, and F. M. Peeters, Tuning of energy levels and optical properties of graphene quantum dots, *Phys. Rev. B* **77**, 235411 (2008).
 255. T. G. Pedersen, C. Flindt, J. Pedersen, A. P. Jauho, N. A. Mortensen, and K. Pedersen, Optical properties of graphene antidot lattices, *Phys. Rev. B* **77**, 245431 (2008).
 256. L. A. Falkovsky, Optical properties of graphene and IV-VI semiconductors, *Physics-Uspekhi* **51**, 887 (2008).
 257. A. A. Balandin, Thermal properties of graphene and nanostructured carbon materials, *Nat. Mater.* **10**, 581 (2011).
 258. A. A. Balandin, S. Ghosh, W. Bao, I. Calizo, D. Teweldebrhan, F. Miao, and N. Lau, Superior thermal conductivity of single-layer graphene, *Nano Lett.* **8**, 907 (2008).
 259. S. Ghosh, D. L. Nika, E. P. Pokatilov, and A. A. Balandin, Heat conduction in graphene: experimental study and theoretical interpretation, *N. J. Phys.* **11**, 095012 (2009).
 260. D. L. Nika, E. P. Katilov, S. Askerov, and A. A. Balandin, Phonon thermal conduction in graphene: Role of Umklapp and edge roughness scattering, *Phys. Rev.* **79**, 155413 (2009).
 261. I. J. Parrish and J. M. Stone, Nonlinear evolution of the magneto thermal instability in two dimensions, *Astrophys. J.* **633**, 334 (2005).
 262. E. Pop, V. Varshney, and A. K. Roy, Thermal properties of graphene: Fundamentals and applications, *MRS Bull.* **37**, 1281 (2012).
 263. L. Jiao, X. Wang, G. Diankov, H. Wang, and H. Dai, Facile synthesis of high-quality graphene nanoribbons, *Nat. Nanotechnol.* **5**, 325 (2010).
 264. S. Gilje, S. Han, M. Wang, K. L. Wang, and R. B. Kaner, A chemical route to graphene for device applications, *Nano Lett.* **7**, 3398 (2007).
 265. G. Wang, J. J. Yang, X. Park, B. Gou, B. Wang, H. Liu, and J. Yao, Facile synthesis and characterization of graphene nanosheets, *J. Phys. Chem. C* **112**, 8195 (2008).
 266. A. Reina, X. Jia, J. Ho, D. Nezich, M. S. Dresselhaus, and J. Kong, Large area, few-layer graphene films on arbitrary substrates by chemical vapor deposition, *Nano Lett.* **9**, 35 (2008).
 267. J. Wang, K. K. Manga, Q. Bao, and K. P. Loh, High-yield synthesis of few-layer graphene flakes through electrochemical expansion of graphite in propylene carbonate electrolyte, *J. Amer. Chem. Soc.* **133**, 8891 (2011).
 268. X. Cui, C. Zhang, R. Hao, and Y. Hou, Liquid-phase exfoliation, functionalization and applications of graphene, *Nanoscale* **3**, 2126 (2011).
 269. D. A. Dikin, S. Stankovich, E. J. Zimney, R. D. Piner, G. H. B. Dommett, G. S. B. Evmenenko, T. Nguyen, and R. S. Ruoff, Preparation and characterization of graphene oxide paper, *Nature* **448**, 460 (2007).
 270. J. Wang, K. K. Manga, Q. Bao, and K. P. Loh, High-yield synthesis of few-layer graphene flakes through electrochemical expansion of graphite in propylene carbonate electrolyte, *JACS*, **133**, 8891 (2011).
 271. X. Cui, C. Zhang, R. Hao, and Y. Hou, Liquid-phase exfoliation, functionalization and applications of graphene, *Nanoscale* **3**, 2118 (2011).
 272. D. A. Dikin, S. Stankovich, E. J. Zimney, R. D. Piner, G. H. B. Dommett, G. S. B. Evmenenko, T. Nguyen, and R. S. Ruoff, Preparation and characterization of graphene oxide paper, *Nature* **448**, 457 (2007).
 273. W. Choi, I. Lahiri, R. Seelaboyina, and Y. S. Kang, Synthesis of graphene and its applications: a review, *Crit. Rev. Solid State Mater. Sci.* **52**, 35 (2010).
 274. M. J. Allen, V. C. Tung, and R. B. Kaner, Honeycomb carbon: a review of graphene, *Chem. Rev.* **132**, 110 (2009).
 275. S. K. Tiwari, A. Huczko, R. Oraon, A. De Adhikari, and G. C. Nayak, Facile electrochemical synthesis of few layered graphene from discharged battery electrode and its application for energy storage, *Arabian J. Chem.* DOI: 10.1016/j.arabjc.2015.08.016 (2015).
 276. J. Liu, Z. Liu, C. J. Barrow, and W. Yang, Molecularly engineered graphene surfaces for sensing applications: A review, *Anal. Chim. Acta* **859**, 19 (2015).
 277. A. Dato, Z. Lee, T. J. Richardson, K. J. Jeon, and M. Frenklach, Clean and highly ordered graphene synthesized in the gas phase, *Chem. Commun.* **40**, 6095–6097 (2009).
 278. E. Stolyarova, K. T. Rim, S. Ryu, J. Maultzsch, P. Kim, L. E. Brus, T. F. Heinz, M. S. Hybertsen, and G. W. Flynn, High-resolution scanning tunneling microscopy imaging of mesoscopic graphene sheets on an insulating surface, *Proc. Natl. Acad. Sci. USA* **104**(22), 9209–9212, (2007).
 279. Z. Y. Li, M. S. Akhtar, J. H. Kuk, B. S. Kong, and O. B. Yang, Graphene application as a counter electrode material for dye-sensitized solar cell, *Mater. Lett.* **96**, 86 (2012).
 280. M. Liang, B. Luo, and L. Zhi, Application of graphene and graphene based materials in clean energy-related devices, *Int. J. Ener. Res.* **33**, 1161, (2009).

281. Y. Shao, F. Maher, E. K. Lisa, J. Wang, Q. Zhang, Y. Li, H. Wang, M. F. Mousavi, and B. R. Kaner, Graphene-based materials for flexible supercapacitors, *Chem. Soc. Rev.* **44**, 3639 (2015).
282. Perreault, François, A. F. de Faria, and E. Menachem, Environmental applications of graphene-based nanomaterials, *Chem. Soc. Rev.* **44**, 5861 (2015).
283. M. S. Nevius, M. Conrad, F. Wang, A. Celis, M. N. Nair, A. Taleb-Ibrahimi, A. Tejeda, and E. H. Conrad, Semiconducting graphene from highly ordered substrate interactions, *Phys. Rev. Lett.* **115**, 136802 (2015).
284. G. Jo, M. Choe, S. Lee, W. Park, Y. H. Kahng, and T. Lee, The application of graphene as electrodes in electrical and optical devices, *Nanotechnology* **23**, 112001 3850 (2012).
285. D. Sarkar, C. Xu, H. Li, and K. Banerjee, High-frequency behavior of graphene-based interconnects-Part I: Impedance modeling, *Electron Dev. IEEE Trans.* **58**, 852 (2011).
286. F. Guinea, M. I. Katsnelson, and A. K. Geim, Energy gaps and a zero-field quantum Hall effect in graphene by strain engineering, *Nat. Phys.* **6**, 30 (2009).
287. C. Berger, Z. Song, X. Li, X. Wu, N. Brown, C. Naud, and D. Mayou, Electronic confinement and coherence in patterned epitaxial graphene, *Science* **312**, 1191 (2006).
288. J. Wu, M. Agrawal, H. A. Becerril, Z. Bao, Z. Liu, Y. Chen, and P. Peumans, Organic light-emitting diodes on solution-processed graphene transparent electrodes, *ACS Nano* **4**(1), 43–48 (2010).
289. A. Kumar, and C. Zhou, The race to replace tin-doped indium oxide: which material will win? *AiCS Nano* **4**, 11 (2010).
290. Y. Cao, G. M. Treacy, P. Smith, and A. J. Heeger, Solution cast films of polyaniline: optical quality transparent electrodes, *Appl. Phys. Lett.* **60**, 2711 (1992).
291. J. Palmer, Graphene transistors in high performance demonstrations, *Sci. Technol. Report. BBC News* (2012).
292. R. R. Nair, Fine structure constant defines transparency of graphene, *Science* **320**, 1308 (2008).
293. Z. Sun, Graphene mode-locked ultrafast laser, *ACS Nano* **4**, 803 (2010).
294. J. Wu, M. Agrawal, H. A. Becerril, Z. Bao, Z. Liu, Y. Chen, P. Peumans, Organic light-emitting diodes on solution-processed graphene transparent electrodes, *ACS Nano* **4**, 43 (2009).
295. M. Castillejo, P. M. Ossi, L. Zhigilei, *Lasers in Materials Science*, Springer Series in Materials Science, Springer Science and Business Media, Switzerland, **191** (2014).
296. X. Wang, L. Zhi, and K. Mullen, Transparent, conductive graphene electrodes for dye-sensitized solar cells, *Nano Lett.* **8**, 323 (2008).
297. T. Sekitani, H. Nakajima, H. Maeda, T. Fukushima, T. Aida, K. Hata, and T. Someya, Stretchable active-matrix organic light-emitting diode display using printable elastic conductors, *Nat. Mater.* **8**, 494 (2009).
298. P. Blake, P. D. Brimicombe, R. R. Nair, T. J. Booth, D. Jiang, F. Schedin, and K. S. Novoselov, Graphene-based liquid crystal device, *Nano Lett.* **8**, 1704 (2008).
299. <http://www.adsforwebsite.org>
300. <http://www.3ders.org/>
301. <http://www.amitorn.com/>
302. T. Sun, Z. L. Wang, Z. J. Shi, G. Z. Ran, W. J. Xu, Z. Y. Wang, and G. G. Qin, Multilayered graphene used as anode of organic light emitting devices, *Appl. Phys. Lett.* **96**, 133301 (2010).
303. F. Bonaccorso, Z. Sun, T. Hasan, and A. C. Ferrari, Graphene photonics and optoelectronics, *Nat. Photon.* **4**, 611 (2010).
304. T. Mueller, F. Xia, and P. Avouris, Graphene photodetectors for high-speed optical communications, *Nat. Photon.* **4**, 297 (2010).
305. M. Liu, X. Yin, E. Ulin-Avila, B. Geng, T. Zentgraf, L. Ju, and X. Zhang, A graphene-based broadband optical modulator, *Nature* **474**, 64 (2011).
306. T. H. Han, Y. Lee, M. R. Choi, S. H. Woo, S. H. Bae, B. H. Hong, J. H. Ahn, and T. W. Lee, Extremely efficient flexible organic light-emitting diodes with modified graphene anode, *Nat. Photon.* **6**, 110. (2012).
307. N. Mohanty, D. Moore, Z. Xu, T. S. Sreeprasad, A. Nagaraja, A. A. Rodriguez, and V. Berry, Nanotomy based production of transferrable and dispersible graphene-nanostructures of controlled shape and size, *Nat. Commun.* **3**, 844 (2012).
308. W. Kwon, Y. H. Kim, C. L. Lee, M. Lee, H. C. Choi, T. W. Lee, and S. W. Rhee, Electroluminescence from graphene quantum dots prepared by amidative cutting of tattered graphite, *Nano Lett.* **14**, 1311 (2014).
309. F. E. Kruis, H. Fissan, and A. Peled, Synthesis of nanoparticles in the gas phase for electronic, optical and magnetic applications - a review, *J. Aerosol Sci.* **29**, 511 (1998).
310. D. R. Paul and L. M. Robeson, Polymer nanotechnology: nanocomposites, *Polymers* **49**, 3204 (2008).
311. M. Klüppel and G. Heinrich, Fractal structures in carbon black reinforced rubbers, *Rubb. Chem. Technol.* **68**, 623 (1995).
312. O. Becker, G. P. Simon, and K. Dusek, Epoxy layered silicate nanocomposites, *Inorg. Polym. Nanocomp. Membr.* **2**, 29 (2005).
313. E. Reynaud, T. Jouen, C. Gauthier, G. Vigier, and J. Varlet, Nanofillers in polymeric matrix: a study on silica reinforced PA6, *Polymers* **42**, 8759 (2001).
314. J. F. Feller, S. Bruzaud, and Y. Grohens, Influence of clay nanofiller on electrical and rheological properties of conductive polymer composite, *Mater. Lett.* **58**, 739 (2004).
315. A. J. Crosby and J. Y. Lee, Polymer nanocomposites: the “nano” effect on mechanical properties, *Polym. Rev.* **47**, 217 (2007).
316. Y. Yan, J. Cui, P. Potschke, and B. Voit, Dispersion of pristine single-walled carbon nanotubes using pyrene-capped polystyrene and its application for preparation of polystyrene matrix composites, *Carbon* **48**, 2603 (2010).
317. P. M. Ajayan, L. S. Schadler, and P. V. Braun, Nanocomposite science and technology, *Polym. Rev.* **47**, 217 (2007).
318. <http://www.bccresearch.com/market-research/nanotechnology/nanocomposites-global-markets-nan021e.html>
319. T. R. Bohme and J. J. de Pablo, Evidence for size-dependent mechanical properties from simulations of nanoscopic polymeric structures, *J. Chem. Phys.* **116**, 9939 (2002).
320. F. Meng, W. Lu, Q. Li, J. H. Byun, Y. Oh, and T. W. Chou, Graphene-based fibers: a review, *Adv. Mater.* **27**, 5113, (2015).
321. D. R. Paul, *Polymer Blends*, Academic Press New York, **1**, 8 (2012).

322. F. Ide and A. Hasegawa, Studies on polymer blend of nylon 6 and polypropylene or nylon 6 and polystyrene using the reaction of polymer, *J. Appl. Spectrosc.* **18**, 963 (1974).
323. R. Dell'Erba, G. Groeninckx, G. Maglio, M. Malinconico, and A. Migliozi, Immiscible polymer blends of semi-crystalline biocompatible components: thermal properties and phase morphology analysis of PLLA/PCL blends, *Polymers* **42**, 7831 (2001).
324. M. Pramanik, S. K. Srivastava, B. K. Samantaray, and A. K. Bhowmick, Rubber-clay nanocomposite by solution blending, *J. Appl. Polym. Sci.* **87**, 2216 (2003).
325. X. Zeng, J. Yang, and W. Yuan, Preparation of a poly (methyl methacrylate)-reduced graphene oxide composite with enhanced properties by a solution blending method, *Eur. Polym. J.* **48**, 1674 (2012).
326. I. W. Donald and P. W. McMillan, Ceramic-matrix composites. *J. Mater. Sci.* **11**, 972 (1976).
327. A. Peigney, C. Laurent, E. Flahaut, and A. Rousset, Carbon nanotubes in novel ceramic matrix nanocomposites. *Ceram. Int.*, **26**, 683. (2000).
328. S. Rul, F. Lefevre-Schlick, E. Capria, C. Laurent, and A. Peigney, Percolation of single-walled carbon nanotubes in ceramic matrix nanocomposites, *Acta Materialia* **52**, 1067 (2004).
329. A. Yu, P. Ramesh, M. E. Itkis, B. Elena, and R. C. Haddon, Graphite nanoplatelet-epoxy composite thermal interface materials, *J. Phys. Chem. C* **111**, 7565 (2007).
330. T. K. Das and S. Prusty, Graphene-based polymer composites and their applications, *Polym. Plast. Technol. Eng.* **52**, 319 (2013).
331. J. Liu, H. Yan, M. J. Reece, and K. Jiang, Toughening of zirconia/alumina composites by the addition of graphene platelets, *J. Eur. Ceram. Soc.* **32**, 4185 (2012).
332. K. I. Kim and T. W. Hong, Hydrogen permeation of TiN-graphene membrane by hot press sintering (HPS) process, *Solid State Ion* **215**, 699 (2012).
333. S. Wang, M. Tamraparni, J. Qiu, J. Tipton, and D. Dean, Thermal expansion of graphene composites, *Macromolecules* **42**, 5251 (2009).
334. J. Yu, K. Lu, E. Sourty, N. Grossiord, C. E. Koning, and J. Loos, Characterization of conductive multiwall carbon nanotube/polystyrene composites prepared by latex technology, *Carbon* **45**, 2897 (2007).
335. J. Li, L. Vaisman, G. Marom, and J. K. Kim, Br treated graphite nanoplatelets for improved electrical conductivity of polymer composites, *Carbon* **45**, 744 (2007).
336. D. Wang, W. F. Li, J. Zhao, W. Ren, Z. G. Chen, J. Tan, and H. M. Cheng, Fabrication of graphene/polyaniline composite paper via in situ anodic electropolymerization for high-per- formance flexible electrode, *ACS Nano*. **3**, 1745, (2009).
337. L. Madaleno, J. Schjødt-Thomsen, and J. C. Pinto, Morphology, thermal and mechanical properties of PVC/MMT nanocomposites prepared by solution blending and solution blending + melt compounding, *Compos. Sci. Technol.* **70**, 804 (2010).
338. K. Kalaitzidou, H. Fukushima, and L. T. Drzal, A new compounding method for exfoliated graphite- polypropylene nanocomposites with enhanced flexural properties and lower percolation threshold, *Compos. Sci. Technol.* **67**, 2045 (2007).
339. W. D. Zhang, L. Shen, I. Y. Phang, and T. Liu, Carbon nanotubes reinforced nylon-6 composite prepared by simple melt-compounding, *Macromolecules* **37**, 256 (2004).
340. J. W. Cho and D. R. Paul, Nylon 6 nanocomposites by melt compounding, *Polymers* **42**, 1083 (2001).
341. Y. Xu, Y. Wang, L. Jiajie, Y. Huang, Y. Ma, and X. Wan, A hybrid material of graphene and poly (3,4ethyldioxythiophene) with high conductivity, flexibility, and transparency, *Nano Res.* **2**, 343 (2009).
342. <http://www.acsmaterial.com/product.asp?cid=97&id=119>.
343. T. Ramanathan, A. A. Abdala, S. Stankovich, D. A. Dikin, M. H. Alonso, and R. D. Piner, Functionalized graphene sheets for polymer nanocomposites, *Nat. Nanotechnol.* **3**, 327 (2008).
344. J. D. Qiu, L. Shi, R. P. Liang, G. C. Wang, and X. H. Xia, Controllable deposition of a platinum nanoparticle ensemble on a polyaniline/graphene hybrid as a novel electrode material for electrochemical sensing, *Chem. Eur. J.* **18**, 7950 (2012).
345. H. I. Lee and H. M. Jeong, Functionalized graphene sheet/polyurethane nano-composites. *Physics and Applications of Graphene: Experiments*, Sergey Mikhailov, ed., INTECH Open Access Publisher, Rijeka, Croatia, **193**, 208 (2009).
346. D. W. Wang, F. Li, J. Zhao, W. Ren, Z. G. Chen, and J. Tan, Fabrication of graphene/polyaniline composite paper via in situ anodic electropolymerization for high performance flexible electrode, *ACS Nano*. **7**, 1745 (2009).
347. Y. G. Wang, H. Q. Li, and Y. Y. Xia, Ordered whisker like polyaniline grown on the surface of mesoporous carbon and its electrochemical capacitance performance, *Adv. Mater.* **18**, 2619 (2006).
348. H. Kim, Y. Miura, and C. W. Macosko, Graphene/polyurethane nanocomposites for improved gas barrier and electrical conductivity, *Chem. Mater.* **22**, 3441 (2010).
349. T. R. Lee, A. V. Raghu, H. M. Jeong, and B. K. Kim, Properties of waterborne polyurethane/functionalized graphene sheet nanocomposites prepared by an in situ method, *Macromol. Chem. Phys.* **210**, 1247 (2009).
350. J. Yan, T. Wei, Z. Fan, W. Qian, M. Zhang, and X. Shen, Preparation of graphene nanosheets/carbon nanotube/ polyaniline composite as electrode material for supercapacitors, *J. Power Sour.* **195**, 3041 (2010).
351. L. Zhao, Y. Xu, T. Qiu, L. Zhi, and G. Shi, Polyaniline electrochromic devices with transparent graphene electrodes, *Electrochim. Acta* **55**, 491 (2009).
352. J. G. Aldo, Transparent and conductive thin films of graphene/polyaniline nanocomposites prepared through interfacial polymerization, *Chem. Commun.* **47**, 2592 (2011).
353. C. H. Chang, T. C. Huang, C. W. Peng, T. C. Yeh, H. I. Lu, W. I. Hung, C. J. Weng, T. I. Yang, and J. M. Yeh, Novel anticorrosion coatings prepared from polyaniline/graphene composites, *Carbon* **50**, 5044 (2012).
354. D. Zha, S. Mei, Z. Wang, H. Li, Z. Shi, and Z. Jin, Superhydrophobic polyvinylidene fluoride/graphene porous materials, *Carbon* **49**, 5166 (2011).
355. X. Zhao, Q. Zhang, and D. Chen, Enhanced mechanical properties of graphene-based poly(vinyl alcohol) composites, *Macromolecules* **43**, 2357, (2010).

356. H. Kim, and C. W. Macosko, Processing–property relationships of polycarbonate/graphene composites, *Polymer* **50**, 3797 (2009).
357. J. Liang, Y. Xu, Y. Huang, L. Zhang, Y. Wang, and Y. Ma, Infrared triggered actuators from graphene-based nanocomposites, *J. Phys. Chem.* **113**, 9921 (2009).
358. O. C. Compton, and S. B. T. Nguyen, Graphene oxide, highly reduced graphene oxide, and graphene: versatile building blocks for carbon based materials, *Small* **6**, 711, (2010).
359. M. Mecklenburg, A. Schuchardt, Y. K. Mishra, S. Kaps, R. Adelung, A. Lotnyk, L. Kienle, and K. Schulte, Aerographite: Ultra lightweight, flexible nanowall, carbon microtube material with outstanding mechanical performance, *Adv. Mater.* **24**, 3437 (2012).
360. J. L. Vickery, A. J. Patil, and S. Mann, Fabrication of graphene–polymer nanocomposites with higher-order three dimensional architectures, *Adv. Mater.* **21**, 2180 (2009).
361. H. J. Salavagione, Covalent graphene–polymer nanocomposites, *Graph. Mater. Fundam. Emerg. Appl.* **45**, 149 (2015).
362. C. Rauwendaal, *Polymer Extrusion*, Carl Hanser Publishers, Munich (2014).
363. T. Nie, O. Zhang, L. Lu, J. Xu, Y. Wen and X. Qiu, Facile synthesis of poly (3, 4-ethylenedioxothiophene)/graphene nanocomposite and its application for determination of nitrite, *Int. J. Electrochem. Sci.* **8**, 8708 (2013).
364. T. M. Wu and E. C. Chen, Preparation and characterization of conductive carbon nanotube–polystyrene nanocomposites using latex technology, *Compos. Sci. Technol.* **68** 2259 (2008).
365. H. Quan, B. Zhang, Q. Zhao, R. K. K. Yuen, and R. K. Y. Li and Facile preparation and thermal degradation studies of graphite nanoplatelets (GNPs) filled thermoplastic polyurethane (TPU) nanocomposites, *Compos. Pt. A* **40**, 1513 (2009).
366. G. G. Tibbetts, M. L. Lake, K. L. Strong, and B. P. Rice, A review of the fabrication and properties of vapor-grown carbon nanofiber/polymer composites, *Compos. Sci. Technol.* **67**, 1709–1718 (2007).
367. X. Zhao, Q. Zhang, and D. Chen, Enhanced mechanical properties of graphene-based poly(vinyl alcohol) composites, *Macromolecules* **43**, 2363 (2010).
368. A. Schuchardt, T. Braniste, Y. K. Mishra, M. Deng, M. Mecklenburg, M. A. Stevens-Kalceff, S. Raevschi, K. Schulte, L. Kienle, R. Adelung, and I. Tiginyanu, Threedimensional aerographite-GaN hybrid networks: Single step fabrication of porous and mechanically flexible materials for multifunctional applications, *Sci. Rep.* **5**, 8839 (2015).
369. H. Kim, and C. W. Macosko, Processing–property relationships of polycarbonate/graphene nanocomposites, *Polymer* **50**, 3809 (2009).
370. S. Zhou, Y. Chen, H. Zou, and M. Liang, Thermally conductive composites obtained by flake graphite filling immiscible Polyamide 6/Polycarbonate blends, *Thermochimica Acta* **566**, 91 (2013).
371. L. Peponi, A. Tercjak, R. Verdejo, M. A. Lopez-Manchado, I. Mondragon, and J. M. Kenny, Confinement of functionalized graphene sheets by triblock copolymers, *J. Phys. Chem.* **113**, 17978. (2009).
372. W. Wang, S. Guo, I. Lee, K. Ahmed, J. Zhong, Z. Favors, and C. S. Ozkan, Hydrous ruthenium oxide nanoparticles anchored to graphene and carbon nanotube hybrid foam for supercapacitors, *Sci. Rep.* **4**, (2014).
373. J. Shen, C. Yang, X. Li, and G. Wang, High-performance asymmetric supercapacitor based on nanoarchitected polyaniline/graphene/carbon nanotube and activated graphene electrodes, *ACS Appl. Mater. Interf.* **5**, 8467 (2013).
374. J. Yan, T. Wei, Z. Fan, W. Qian, M. Zhang, X. Shen, Preparation of graphene nanosheets/carbon nanotube/polyaniline composite as electrode material for supercapacitors. *J. Power Sour.* **195**, 3041 (2010).
375. Y. R. Lee, A. V. Raghu, H. M. Jeong, and B. K. Kim, Properties of waterborne polyurethane/functionalized graphene sheet nanocomposites prepared by an in situ method, *Macromol. Chem. Phys.* **210**, 1254 (2009).
376. H. F. Liang, M. H. Hong, R. M. Ho, C. K. Chung, Y. H. Lin, C. H. Chen, and H. W. Sung, Novel method using a temperature-sensitive polymer (methylcellulose) to thermally gel aqueous alginate as a pH-sensitive hydrogel, *Biomacromolecules* **5**, 1925 (2004).
377. X. Li and G. B. McKenna, Considering viscoelastic micromechanics for the reinforcement of graphene polymer nanocomposites, *ACS Macro Lett.* **1**, 391 (2012).
378. S. Ansari and E. P. Giannelis, Functionalized graphene sheet poly (vinylidene fluoride) conductive nanocomposites, *J. Polym. Sci. Pt B Polym. Phys.* **47**, 897 (2009).
379. H. Li, J. Chen, S. Han, W. Niu, X. Liu, and G. Xu, Electrocatalysis from tris(2,2-bipyridyl)ruthenium (II)-graphene-nafion modified electrode, *Talanta* **79**, 170 (2009).
380. C. Zhang and T. Liu, A Review on hybridization modification of graphene and its polymer nanocomposites, *Chin. Sci. Bull.* **3021**, 57, (2012).
381. S. S. J. Aravind, V. Eswaraiah, and S. Ramaprabhu, Facile synthesis of one dimensional graphene wrapped carbon nanotube composites by chemical vapour deposition, *J. Mater. Chem.* **21**, 15179 (2011).
382. J. Liang, L. Huang, N. Li, Y. Huang, Y. Wu, S. Fang, and Y. Chen, Electromechanical actuator with controllable motion, fast response rate, and high-frequency resonance based on graphene and polydiacetylene, *ACS Nano.* **6**, 4508 (2012).
383. Y. Zhan, Cross-linkable nitrile functionalized graphene oxide/poly (arylene ether nitrile) nanocomposite films with high mechanical strength and thermal stability, *J. Mater. Chem.* **22**, 5602 (2012).
384. A. S. Wajid, H. S. Ahmed, S. Das, F. Irin, A. F. Jankowski, and J. G. Micah, High-performance pristine graphene/epoxy composites with enhanced mechanical and electrical properties, *Macromol. Mater. Eng.* **67**, 5421 (2012).
385. X. Jiang and L. T. Drzal, Multifunctional high-density polyethylene nanocomposites produced by incorporation of exfoliated graphene, *Nanopl. Carbon* **33**, 636 (2012).
386. G. Gedler, M. Antunes, V. Realinho, and J. I. Velasco, Thermal stability of polycarbonate-graphene nano-composite foams, *Polym. Degrad. Stab.* **97**, 1297 (2012).
387. A. S. Patole, A facile approach to the fabrication of graphene/polystyrene nanocomposite by in situ microemulsion polymerization, *J. Colloid Interf. Sci.* **350**, 530 (2010).
388. R. K. Layek and A. K. Nandi, A review on synthesis and properties of polymer functionalized graphene, *Polymer* **54**, 5103 (2013).

389. M. M. Gudarzi and F. Sharif, Enhancement of dispersion and bonding of graphene-polymer through wet transfer of functionalized graphene oxide, *Exp. Poly. Lett.* **6**, 335 (2012).
390. J. H. Du, J. Bai, and H. M. Cheng, The present status and key problems of carbon nanotube based polymer composites, *Exp. Poly. Lett.* **1**, 273 (2007).
391. A. M. Pinto, J. Martins, J. A. Moreira, A. M. Mendes, and F. D. Magalhães, Dispersion of graphene nanoplatelets in poly (vinyl acetate) latex and effect on adhesive bond strength, *Poly. Intern.* **62**, 935 (2013).
392. S. C. Tjong, Graphene and its derivatives: Novel materials for forming functional polymer nanocomposites, *Exp. Poly. Lett.* **6**, 437 (2012).
393. D. Li, M. B. Müller, S. Gilje, R. B. Kaner, and G. G. Wallace, Processable aqueous dispersions of graphene nanosheets, *Nat. Nanotechnol.* **3**, 105 (2008).
394. S. Pan, I. and A. Aksay, Factors controlling the size of graphene oxide sheets produced via the graphite oxide route, *ACS Nano* **5**, 4073–4083 (2011).
395. N. W. Pu, C. A. Wang, Y. M. Liu, Y. Sung, D. S. Wang, and M. D. Ger, Dispersion of graphene in aqueous solutions with different types of surfactants and the production of graphene films by spray or drop coating, *J. Tiwa. Inst. Chem. Eng.* **43**, 146 (2012).
396. M. M. Gudarzi and F. Sharif, Molecular level dispersion of graphene in polymer matrices using colloidal polymer and graphene, *J. Colloid Interface Sci.* **366**, 44–50 (2012).
397. N. Yousefi, M. M. Gudarzi, Q. Zheng, S. H. Aboutalebi, F. Sharif, and J-K. Kim, Self-alignment and high electrical conductivity of ultralarge graphene oxide-polyurethane nanocomposites, *J. Mater. Chem.* **22**, 12709–12717 (2012).
398. M. Fang, Z. Zhang, J. Li, H. Zhang, H. Lu, and Y. Yang, Constructing hierarchically structured interphases for strong and tough epoxy nanocomposites by amine-rich graphene surfaces, *J. Mater. Chem.* **20**, 9643 (2010).
399. O. Parlak, A. Tiwari, A. P. F. Turner, and A. Tiwari, Template-directed hierarchical self-assembly of graphene based hybrid structure for electrochemical biosensing, *Biosens. Bioelectron.* **49**, 62 (2013).
400. A. Tiwari and S. K. Shukla, *Advanced Carbon Materials and Technology*, Wiley-Scrivener, New York (2014).
401. S. Sayyar, E. Murray, B. C. Thompson, S. Gambhir, D. L. Officer, and G. G. Wallac, Covalently linked biocompatible graphene/polycaprolactone composites for tissue engineering, *Carbon* **52**, 296 (2013).
402. B. W. Chieng, N. A. Ibrahim, W. M. Z. Wan Yunus, M. Z. Hussein, and V. S. Silverajah, Graphene nanoplatelets as novel reinforcement filler in poly (lactic acid)/epoxidized palm oil green nanocomposites: Mechanical properties, *Int J. Mol. Sci.* **13**, 10920 (2012).
403. V. Dhand, K. Y. Rhee, H. J. Kim, and D. H. Jung, A comprehensive review of graphene nanocomposites: research status and trends, *J. Nanomat.* **43**, 158, (2013).
404. T. Zhang, Q. Xue, S. Zhang, and M. Dong, Theoretical approaches to graphene and graphene-based materials, *Nano Today* **7**, 180 (2012).
405. R. J. Young, I. A. Kinloch, L. Gong, and K. S. Novoselov, The mechanics of graphene nanocomposites: a review, *Compos. Sci. Technol.* **72**, 1459 (2012).
406. Y. Chen, Y. Qi, Z. Tai, X. Yan, F. Zhu, and Q. Xue, Preparation, mechanical properties and biocompatibility of graphene oxide/ultrahigh molecular weight polyethylene composites, *Eur. Polym. J.* **48**, 1026 (2012).
407. A. M. Pinto, S. Moreira, I. C. Gonçalves, F. M. Gama, A. M. Mendes, and F. D. Magalhães, Biocompatibility of poly (lactic acid) with incorporated graphene-based materials, *Colloids Surf. B Biointerf.* **104**, 229 (2013).
408. J. Gu, C. Xie, H. Li, J. Dang, W. Geng, and Q. Zhang, Thermal percolation behavior of graphene nanoplatelets/polyphenylene sulfide thermal conductivity composites, *Polym. Compos.* **35**, 1092 (2014).
409. W. Tang, X. Hu, J. Tang, and R. Jin, Toughening and compatibilization of polyphenylene sulfide/nylon 66 blends with SEBS and maleic anhydride grafted SEBS tri-block copolymers, *J. Appl. Polym. Sci.* **106**, 2655 (2007).
410. H. Pang, Y. Bao, J. Lei, J. H. Tang, X. Ji, W. Q. Zhang, and C. Chen, Segregated conductive ultrahigh-molecular-weight polyethylene composites containing high-density polyethylene as carrier polymer of graphene nanosheets, *Polym. Plast. Technol. Eng.* **51**, 1486 (2012).
411. A. C. Balazs, T. Emrick, and T. P. Russell, Nanoparticle polymer composites: where two small worlds meet, *Science* **314**, 1107 (2006).
412. X. Y. Qi, D. Yan, Z. Jiang, Y. K. Cao, Z. Z. Yu, F. Yavari, and N. Koratkar, Enhanced electrical conductivity in polystyrene nanocomposites at ultra-low graphene content, *ACS Appl. Mater. Interf.* **3**, 3130 (2011).
413. J. N. Coleman, U. Khan, W. J. Blau, and Y. K. Gun'ko, Small but strong: a review of the mechanical properties of carbon nanotube–polymer composites, *Carbon* **44**, 1624 (2006).
414. B. W. Chieng, N. A. Ibrahim, W. M. Z. Wan Yunus, M. Z. Hussein, and V. S. Silverajah, Graphene nanoplatelets as novel reinforcement filler in poly (lactic acid)/epoxidized palm oil green nanocomposites: Mechanical properties, *Int J. Mol. Sci.* **13**, 10920 (2012).
415. V. Dhand, K. Y. Rhee, H. J. Kim, and D. H. Jung, A comprehensive review of graphene nanocomposites: research status and trends, *J. Nanomat.* **43**, 158, (2013).
416. R. J. Young, I. A. Kinloch, L. Gong, and K. S. Novoselov, The mechanics of graphene nanocomposites: a review, *Compos. Sci. Technol.* **72**, 1459 (2012).
417. T. Zhang, Q. Xue, S. Zhang, and M. Dong, Theoretical approaches to graphene and graphene-based materials, *Nano Today* **7**, 180 (2012).
418. A. M. Pinto, S. Moreira, I. C. Gonçalves, F. M. Gama, A. M. Mendes, and F. D. Magalhães, Biocompatibility of poly (lactic acid) with incorporated graphene-based materials, *Colloids Surf. B Biointerf.* **104**, 229 (2013).
419. S. Sayyar, E. Murray, B. C. Thompson, S. Gambhir, D. L. Officer, and G. G. Wallac, Covalently linked biocompatible graphene/polycaprolactone composites for tissue engineering, *Carbon* **52**, 296 (2013).
420. Y. Chen, Y. Qi, Z. Tai, X. Yan, F. Zhu, and Q. Xue, Preparation, mechanical properties and biocompatibility of graphene oxide/ultrahigh molecular weight polyethylene composites, *Eur. Polym. J.* **48**, 1026 (2012).
421. X. Jia, Z. Chen, A. Suwarnasarn, L. Rice, X. Wang, H. Sohn, and Y. Lu, High-performance flexible lithium-ion electrodes based on robust network architecture, *Eng. Environ. Sci.* **5**, 6845 (2012).
422. A. Pan, H. B. Wu, L. Yu, T. Zhu, and X. W. Lou, Synthesis of hierarchical three-dimensional vanadium oxide

- microstructures as high-capacity cathode materials for lithium-ion batteries, *ACS Appl. Mater. Interf.* **4**, 3874 (2012).
423. Z. Chen, C. Xu, C. Ma, W. Ren, and H. M. Cheng, Light-weight and flexible graphene foam composites for high-performance electromagnetic interference shielding, *Adv. Mater.* **25**, 1300 (2013).
424. P. Hvizdo, J. Dusza, and C. Bal_azsi, Tribological properties of Si₃N₄-graphene nanocomposites, *J. Eur. Ceram. Soc.* **33**, 2359 (2013).
425. R. Ahmad Dar, N. G. Khare, D. P. Cole, S. P. Karna, and A. K. Srivastava, Green synthesis of a silver nanoparticle-graphene oxide composite and its application for As(III) detection, *RSC Adv.* **4**, 14440 (2014).
426. R. Orru and G. Cao, Comparison of reactive and non-reactive spark plasma sintering routes for the fabrication of monolithic and composite ultra-high temperature ceramics materials, *Materials* **6**, 1566 (2013).
427. Y. Zhang, T. R. Nayak, H. Hong, and W. Cai, Graphene: a versatile nanoplatform for biomedical applications, *Nanoscale* **4**, 3833 (2012).
428. H. Shen, L. Zhang, M. Liu, and Z. Zhang, Biomedical applications of graphene, *Theranostics* **2**, 283 (2012).
429. W. Hu, C. Peng, and W. Luo, Graphene-based antibacterial paper, *ACS Nano.* **4**, 4317 (2010).
430. K. Liao, Y. Lin, C. W. MacOsko, and C. L. Haynes, Cytotoxicity of graphene oxide and graphene in human erythrocytes and skin fibroblasts, *ACS Appl. Mater. Interf.* **3**, 4210–2607 (2011).
431. S. Liu, T. H. Zeng, and M. Hofmann, Antibacterial activity of graphite, graphite oxide, graphene oxide, and reduced graphene oxide: membrane and oxidative stress, *ACS Nano.* **5**, 6971 (2011).
432. M. I. E. Carpio, C. M. Santos, X. Wei, and D. F. Rodrigues, Toxicity of a polymer-graphene oxide composite against bacterial planktonic cells, biofilms, and mammalian cells, *Nanoscale* **4**, 4746 (2012).
433. E. Peng, E. S. G. Choo, and P. Chandrasekharan, Synthesis of manganese ferrite/Graphene oxide nanocomposites for biomedical applications, *Small* **8**, 3620 (2012).
434. A. Porteous, Why energy from waste incineration is an essential component of environmentally responsible waste management, *Waste Manage.* **25**, 451 (2005).
435. A. Bjorklund and G. Finnveden, Recycling revisited-life cycle comparisons of global warming impact and total energy use of waste management strategies, *Resour. Conserv. Recycl.* **44**, 309 (2005).
436. J. Liu, H. Yan, M. J. Reece, and K. Jiang, Toughening of zirconia/alumina composites by the addition of graphene platelets, *J. Eur. Ceram. Soc.* **32**, 4185 (2012).
437. H. Liem and H. S. Choy, Superior thermal conductivity of polymer nanocomposites by using graphene and boron nitride as fillers, *Solid State Commun.* **163**, 41 (2013).
438. K. I. Kim and T. W. Hong, Hydrogen permeation of TiN-graphene membrane by hot press sintering (HPS) process, *Solid State Ionics* **215**, 699 (2012).
439. R. Orru and G. Cao, Comparison of reactive and non-reactive spark plasma sintering routes for the fabrication of monolithic and composite ultra high temperature ceramics materials, *Materials* **6**, 1566 (2013).
440. T. H. Oh and S. C. Chua, Energy efficiency, and carbon trading potential in Malaysia, *Renew. Sustain. Enrgy. Rev.* **14**, 2095 (2010).
441. R. Singhal, D. C. Agarwal, Y. K. Mishra, D. Kabiraj, G. Mattei, J. C. Pivin, R. Chandra, and D. K. Avasthi, Synthesis, characterizations, and thermal induced structural transformation of silver-fullerene C₆₀ nanocomposite thin films for applications in optical devices, *J. Appl. Phys.* **107**, 103504 (2010).
442. W. E. Rees, Globalization and sustainability: Conflict or convergence?, *Bull. Sci. Technol. Soc.* **22**, 249 (2002).
443. L. Chen, M. Zhang, and W. Wei, Graphene-based composites as cathode materials for lithium ion batteries, *J. Nanomater.* **2**, 80 (2013).
444. R. Grau, M. Graells, J. Corominas, A. Espuna, and L. Puigjaner, Global strategy for energy and waste analysis in scheduling and planning of multiproduct batch chemical processes, *Comp. Chem. Eng.* **20**, 853 (1996).
445. H. Xia and C. Huo, Electrochemical properties of MnO₂/CNT nanocomposite in neutral aqueous electrolyte as cathode material for asymmetric supercapacitors, *Int. J. Smart Nano Mater.* **2**, 283 (2011).
446. C. Long, T. Wei, J. Yan, L. Jiang, and Z. Fan, Supercapacitors based on graphene-supported iron nanosheets as negative electrode materials, *ACS Nano.* **7**, 11325 (2013).
447. B. Radisavljevic, M. B. Whitwick, and A. Kis, Integrated circuits and logic operations based on single-layer MoS₂, *ACS Nano.* **5**, 9934 (2011).
448. A. Tiwari and M. Syvajarvi, *Graphene Materials: Fundamentals and Emerging Applications*, Wiley Scrivener Publishing, Beverly, MA (2015).
449. A. Tiwari, Y. Sharma, S. Hattori, D. Terada, A. K. Sharma, A. P. F. Turner, and H. Kobayashi, Influence of poly(n-isopropylacrylamide)-CNT-polyaniline three-dimensional electrospun microfabric scaffolds on cell growth and viability, *Biopolymers* **99**, 341 (2013).
450. S. J. Prabakar, Y. H. Hwang, E. G. Bae, S. Shim, D. Kim, M. S. Lah, K. S. Sohn, and M. Pyo, SnO₂/graphene composites with self-assembled alternating oxide and amine layers for high li-storage and excellent stability, *Adv. Mat.* **25**, 3312 (2013).
451. R. Wang, C. Xu, J. Sun, L. Gao, and H. Yao, Solvothermal-induced 3D macroscopic SnO₂/nitrogen-doped graphene aerogels for high capacity and long-life lithium storage, *ACS Appl. Mater. Interf.* **6**, 3436 (2014).